C01 and PC01

Role of S6 in activation and inactivation of Kv1.4

Q. Zhou[1,2], A. Lis[2], H. Guo[2], M. Liu[2], R.L. Rasmusson[2,1] and G.C. Bett[3,2]

[1]Biomedical Engineering, SUNY, University at Buffalo, Buffalo, NY, USA, [2]Physiology and Biophysics, SUNY, University at Buffalo, Buffalo, NY, USA and [3]Gynecology-Obstetrics, SUNY, University at Buffalo, Buffalo, NY, USA

The "proline hinge", a Proline-Valine-Proline (P-V-P) sequence, is a common structural motif in several voltage-gated ion channels. Kv1.4 is a voltage-gated K+ channel with a proline hinge at the intracellular side of S6. Kv1.4 (KCNA4), is a member of the Shaker-related family of voltage-gated K+ channels. Kv1.4 opens in response to depolarization, but then quickly inactivates to produce a transient outward current. This is thought to be the major molecular basis of I_{to} in the endocardial tissue of several mammalian species. In addition, this channel is thought to underlie an A type current in brain and smooth muscle.

Kv1.4 channels have two distinct inactviation mechanisms: N- and C-type. N-type inactivation is rapid inactivation resulting from occlusion of the pore by the lipophilic N-terminal. C-type inactivation is slower, and involves structural changes on the intracellular and extracellular faces of the pore. We mutated the second proline to glycine or alanine: P558A and P558G. These mutations were studied in the presence and the absence of the N-terminal to separate the effects of the interaction between the proline hinge and N and C-type inactivation.

Mutations were made in Kv1.4 and heterologously expressed in Xenopus oocytes as previously (1). All procedures were in accordance with the IACUC protocols and federal guidelines.

Both the P558A and P558G mutations slowed or removed N- and C-type inactivation, as well as altering recovery from inactivation. P558A was very disruptive: activation was slowed more than an order of magnitude, and no inactivation was observed. The P558G mutation slowed N- and C-type inactivation by nearly an order of magnitude. The P558G mutation was sensitive to extracellular acidosis and intracellular quinidine binding, which suggests that transmembrane communication in N and C-type inactivation was preserved. Activation, studied in the absence of the N-terminal was also slowed and showed no sigmoid delay. Examination of the effects of the mutation using a modification of our previously reported Kv1.4 model (1) required a single rate limiting voltage insensitive step. However, the voltage dependence of activation required a positive shift in the voltage dependent steps of activation. A model with shifted voltage dependence of activation and a slow voltage insensitive preactivated to open transition accounted for the altered activation. This suggests that movement of S6 is energetically linked to early movements of the voltage sensor, as well as a final cooperative opening of the intracellular gate. Inactivation changes induced by the P558G required slowing of N- and C-type inactivation.

These findings are consistent with significant structural rearrangements involving the intracellular side of S6 during C-type inactivation and our hypothesis that the proline hinge plays a significant role in inactivation and recovery.
Bett GC, et al 2011. Biophys J. 100:11-21

This work was funded in part by the NIH

Where applicable, the authors confirm that the experiments described here conform with The Physiological Society ethical requirements.

C02 and PC02

Assessment of magnitude and dispersion of epicardial conduction velocity in Langendorff perfused murine hearts

Y. Zhang[1,2], G.D. Matthews[2], L.A. Black[1], C.L. Huang[2], M. Lei[1] and J. Fraser[2]

[1]Institute of Cardiovascular Sciences, University of Manchester, Manchester, UK and [2]Physiological Laboratory, University of Cambridge, Cambridge, UK

Background: Clinically important arrhythmias including atrial fibrillation, and ventricular tachycardia and fibrillation are thought to result from re-entrant excitation. These could arise from alterations not only in the magnitude but also dispersions in the direction taken by the action potential conduction, that could potentially result from anatomical change. Thus, the increased arrhythmogenicity shown by ageing *Scn5a*+/- hearts correlates with increased fibrosis [1,2]. Similarly, cardiomyocyte-specific deletion of *Pak1* (*Pak1*(cko)) increases the cardiac hypertrophy, also accompanied by tissue fibrosis, during pressure overload [3]. The present report introduces multi-array epicardial measurements of both the magnitude and the dispersion of conduction.
Methods and Results: 32 and 64 multi-electrode array (MEA) measurements were made from ventricles of Langendorff-perfused murine *Scn5a*+/-, *Pak1*(cko) and WT hearts. These were paced at 8 Hz from the endocardial atrioventricular (AV) node; left ventricular (LV) base, LV apex and the middle of the 64 channel arrays. MEA recordings were obtained from the free walls of the right ventricular ouflow tract (RVOT), right ventricle (RV) or LV. Local activation times (LATs) at each individual MEA electrode were obtained from the timings of the maximal negative slopes in their electrophysiological traces. Conduction properties were then assessed from the LAT measurements by two methods. First, mean conduction velocity (CV) over the entire array was determined. The effective epicardial propagation velocity in m $s^{-1}$of the activation pattern was obtained from the gradient of its fitted plane. Second, a local vector analysis obtained velocity and conduction direction measurements over short (300 μm) distances. This provided the dispersion of such directions from their standard deviations. In accord with previous reports implicating the RVOT in arrhythmia [4], the RVOT showed the slowest CVs and greatest dispersions in conduction direction in *Scn5a*+/- compared to WT. Two-way ANOVAs demonstrated that both anatomical region and genotype independently affected

CV magnitude whereas anatomical region alone affected their dispersions during pacing at the atrioventricular node. Preliminary experiments in *Pak1*(cko) mice similarly suggested slower CVs but greater dispersions in conduction direction compared with WT.
Conclusions: Our novel quantitation of the magnitude and dispersion in direction of conduction implicates the RVOT in the increased arrhythmogenecity shown by *Scn5a+/-* hearts in accordance with clinical results. It provides preliminary evidence for similar findings in *Pak1*(cko) hearts. It may accordingly provide a potentially useful means of assessing for the presence and extent of arrhythmic substrate.

Jeevaratnam K et al. (2011) Pflugers Arch 461, 29-44.

Hao X et al. (2011) Circ Arrhythm Electrophysiol 4, 397-406.

Liu W et al. (2011). Circulation 124, 2702-2715.

Meregalli PG et al. (2005). Cardiovasc Res 67, 367-378.

Supported by the BBSRC, MRC, Wellcome Trust, BHF and NSFC.

Where applicable, the authors confirm that the experiments described here conform with The Physiological Society ethical requirements.

C03 and PC03

Novel mutations in *ABCC9* gene: associated with early repolarisation syndrome?

S. Chaigne[4], S. Chatel[3,1], F. Sacher[4], F. Kyndt[5,1], G. Loussouarn[1,2], H. Le Marec[1,3], V. Probst[3,1], I. Baró[1,2], J. Schott[1,2] and M. Haïssaguerre[4]

[1]Inserm UMR1084 - CNRS UMR6291, l'institut du Thorax, Nantes, France, [2]CNRS, UMR6291, l'institut du thorax, Nantes, France, [3]Service de Cardiologie, l'institut du thorax, CHU Nantes, Nantes, France, [4]Hôpital Haut-Lévêque, Université de Bordeaux, Bordeaux, France and [5]Service de Génétique, CHU Nantes, Nantes, France

The early repolarisation syndrome (ERS), a particular electrocardiographic aspect defined as a J-point elevation, notching or slurring of the terminal portion of the R wave (J wave), and tall/symmetric T wave, had been interpreted by electrophysiologists as benign until very recently. Indeed, there are now studies concluding that individuals with ERS in infero-lateral leads are at higher risk of developing ventricular arrhythmia and sudden cardiac death. Therefore, ERS potential malignant nature cannot be neglected anymore (Haïssaguerre *et al.* 2008). ERS phenotype has been correlated to mutations of *KCNJ8*, encoding the predominant cardiac K_{ATP} channel pore-forming subunit, Kir6.1, or of genes coding for the Ca^{2+} channels generating the L-type Ca^{2+} current, or the Na^{+} channel $Na_v1.5$ (Haïssaguerre *et al.* 2008; Medeiros-Domingo A *et al.*, 2010; Burashnikov E *et al.*, 2010; Watanabe H*et al.*, 2011).
The cardiac K_{ATP} channel is an octameric complex of four pore-forming Kir6.1 or Kir6.2 subunits and four regulatory subunits SUR2A (encoded by *ABCC9*).

Little is known about the extent to which K_{ATP} mutations contribute to ERS associated with sudden cardiac death. The purpose of this study was to further explore *ABCC9* as a novel susceptibility gene for ERS.

Direct DNA sequencing of *ABCC9* was performed among 94 probands diagnosed with ERS or idiopathic ventricular fibrillation (VF). Three rare mutations were identified in *ABCC9* (leading to p.A665T, p.V1137I, and pV1319I) and functionally characterized. Mutant SUR2A cDNA-containing plasmids were co-transfected with Kir6.x subunits cDNA-containing plasmids in COS-7 cells. Wild type (WT) and mutants K^+ currents were recorded using the whole-cell configuration of the patch clamp technique at room temperature.

We observed no effect of SUR2A V1137I variant on the K^+ current when compared to WT SUR2A, whatever the co-expressed Kir6.x subunit. However, K_{ATP} current of Kir6.1-SUR2A-A665T was significantly increased only in the presence of 100 μM pinacidil, a K_{ATP} channel activator, compared to Kir6.1-SUR2A WT current (22.7 ± 3.3 pA/pF, n = 29 vs. 63.8 ± 17.3 pA/pF, n = 17, for WT and A665T, respectively; $p < 0.05$, Mann-Whitney rank sum test), but when expressed with Kir6.2, no difference could be detected (71.7 ± 16.8 pA/pF, n = 34 vs. 83.8 ± 26.1 pA/pF, n = 37, for WT and A665T, respectively; p = 0.46, M-W). Inside-out patch clamp recording showed that the ATP sensibility was unchanged for Kir6.2-SUR2A-A665T compared to Kir6.2-SUR2A WT channels.

Function of Kir6.x-SUR2A-V1319I, and expression level and localization of Kir6.1 protein when co-expressed with SUR2A-A665T are currently under investigation.

In this study, we identified *ABCC9* as a novel ERS susceptibility gene and a mutation leading to a marked gain-of-function of the cardiac K_{ATP} Kir 6.1-SUR2A channel complex.

Burashnikov E *et al.* (2010). *Heart Rhythm* **7**, 1872-1882.

Haissaguerre *et al.* (2008). *N Engl J Med* **358**, 2016–2023

Haissaguerre *et al.* (2009). *J Cardiovasc Electrophysiol* **20**, 93-98

Medeiros-Domingo A *et al.* (2010). *Heart Rhythm* **7**, 1466-1471

Watanabe H*et al.* (2011). *Circ Arrhythm Electrophysiol* **4**, 874-881

Where applicable, the authors confirm that the experiments described here conform with The Physiological Society ethical requirements.

C04 and PC04

Age-associated alterations in intracellular calcium handling within the sinoatrial node

F.S. Hatch[1], M.K. Lancaster[2] and S.A. Jones[1]

[1]Biological Sciences, University of Hull, Hull, UK and [2]Faculty of Biological Sciences, University of Leeds, Leeds, UK

The sodium-calcium exchange serves as a major mechanism for intracellular calcium extrusion and has previously been suggested to be essential for normal pacemaking [1]. However, increases in NCX1 expression (e.g. in end-stage heart failure) are also associated with increased susceptibility to arrhythmias. If such changes in calcium regulation are evident with ageing it may similarly underlie the known increased predisposition to arrhythmias in the elderly.

Male Wistar rats at the ages of 6 months (young), 12 months (adult) and 24 months (old) (n=5 per group) were sacrificed by anaesthetic overdose via intraperitoneal injection. The SAN region of the heart was removed and intrinsic pacemaker activity recorded in bicarbonate-buffered saline at 37°C, under control conditions and in the presence of incrementing concentrations of nifedipine (0.1μm, 1μm, 3μm, 10μm and 30μm) to block L-type calcium channels (Cav1.2). Western blot and immunocytochemistry assessed expression of Cav1.2, sodium-calcium exchanger (NCX1) and plasma membrane calcium ATPase pumps (PMCA) within the SAN. Data are mean±SEM percentages relative to the average young control values, compared by ANOVA followed by Students t-test with Bonferroni's adjustment ($p<0.05$).

There was a significant age-associated decline in heart rate from young to old (young 100±3.4% vs. old 78±4.9%), accompanied by a change in sensitivity to nifedipine from young to old. The EC50 for nifedipine did not differ significantly between ages (average 1.31 μM) but the Hill slope changed from -1.1 in the young to -3.1 in the old. For the young a maximum dose of 30μm was required to stop pacemaker activity compared with a maximum dose of 3μm in the old.

Within the SAN protein expression of Cav1.2 and PMCA significantly decreased from young to old (Cav1.2 young 100±14.6% vs. old 61±13.9%: PMCA young 100±5.7% vs. 78±1.7%), whereas NCX1 expression increased in the old heart (young 100±5.3% vs. old 171±13.6%). In contrast in the right atrial muscle we observed similar changes in Cav1.2 (young 100±12.5% vs. old 53±11.8%) and PMCA (young 100±9.2% vs. 64±4.6%) but there was also a significant decrease in NCX1 expression (young 100±15.3% vs. old 51±7.9%).

In conclusion significant alterations in function of the SAN and sensitivity to calcium channel blockade were observed in old age accompanied by changes in the expression of calcium regulatory proteins. The observed changes may be instrumental in rendering the heart more susceptible to arrhythmias.

Sanders L *et al*. (2006) *J Physiol* **571**: 639-49.

Where applicable, the authors confirm that the experiments described here conform with The Physiological Society ethical requirements.

C05 and PC05

The TRIC-A knockout mouse model provides insight into the labile gating nature of TRIC-B channels

E. Venturi[1], S.J. Pitt[1], E. Galfre[1], F. O'Brien[1], M. Nishi[2], H. Takeshima[2] and R. Sitsapesan[1]

[1]School of Physiology and Pharmacology, University of Bristol, Bristol, UK and [2]Graduate School of Pharmaceutical Sciences, Kyoto University, Kyoto, Japan

Trimeric intracellular cation channels (TRIC-A and TRIC-B) are located in the sarcoplasmic reticulum (SR) of most cells and are present in both cardiac and skeletal muscle. Mutant mice lacking both TRIC-A and TRIC-B channels die due to embryonic heart failure demonstrating their essential, but as yet, uncharacterised role in the heart (1). Identifying the distinct biophysical properties of TRIC-A and TRIC-B channels derived from the SR of normal muscle is not possible due to the presence of both types of channel, yet this is crucial for a full understanding of their roles in cardiac excitation-contraction coupling. We have therefore isolated the light SR membrane (LSR) fraction from mouse TRIC-A knockout tissue. LSR vesicles were fused with planar phosphatidylethanolamine lipid bilayers as previously described (2) and single-channel recordings of native TRIC-B channels were obtained under voltage-clamp conditions in symmetrical solutions of 210 mM K-PIPES, pH 7.2. The LSR vesicles incorporated into the bilayers in a fixed orientation such that the *cis* chamber corresponded to the cytosolic side of the channels and the *trans* chamber corresponded with the luminal face of the channels. Using these isolation procedures and experimental recording conditions, we find that the single-channel conductance of TRIC-B channels varies between channels. The maximum (or full) open state that we observe, falls within the approximate range 170-230 pS (n=27). The TRIC-B channels always gate in sub-conductance states and while these are also of a variable nature, predominant sub-conductance levels are found at 158 ± 4 pS (n=17; S.E.M.), 122±1 pS (n=19; S.E.M.), 93 ± 2 pS (n=18; S.E.M.) and 62±2 pS (n=18; S.E.M.). TRIC-B channel gating was voltage-dependent and channels were inhibited at negative holding potentials. For example, open probability was 0.05±0.012 at +30 mV but only 0.005±0.003 at -30 mV (n=5; S.E.M.; student's t-test $^{*}p<0.05$). Application of 300 mM KCl to the cytosolic channel side produced a parallel shift in the current-voltage relationship and a shift in the reversal potential to approximately -20 mV indicating that TRIC-B is not permeable to anions. These results differ from our previous conductance measurements of recombinantly expressed, detergent purified TRIC-B channels which exhibited a maximum single-channel conductance of approximately 140 pS (2). This study demonstrates that the conductance and gating properties of TRIC-B channels are exceptionally labile and may be easily perturbed by detergent purification procedures and/or use of yeast expres-

sion systems. The intrinsic variability of TRIC-B channel gating may be an important regulatory feature which enables flexible physiological control over monovalent cation fluxes across the SR.

Yazawa, M., Ferrante, C., Feng, J., Mio, K., Ogura, T., Zhang, M., Lin, P. H., Pan, Z., Komazaki, S., Kato, K., Nishi, M., Zhao, X., Weisleder, N., Sato, C., Ma, J., and Takeshima, H. (2007). TRIC channels are essential for Ca^{2+} handling in intracellular stores. *Nature.* 448.78-82

Pitt, S.J., Park, K.-H., Nishi, M., Urashima, T., Aoki, S., Yamazaki, D., Ma, J., Takeshima, H. & Sitsapesan, R. (2010). Charade of the SR K^+-channel: Two ion-channels, TRIC-A and TRIC-B, masquerade as a single ion channel. *Biophys.J.* 99, 417-426.

This work was supported by the British Heart Foundation and the Japan Society for the Promotion of Science.

Where applicable, the authors confirm that the experiments described here conform with The Physiological Society ethical requirements.

C06 and PC06

Modulation of the steady state outward K+ current by noradrenaline via β2 αδρενοχεπτορσ ιν ρατ ατριαλ χαρδιομψοχψτεσ

R. Bond, S.C. Choisy, J.M. Hancock, J.C. Hancox and A.F. James

Cardiovascular Research Laboratories, School of Physiology & Pharmacology, University of Bristol, Bristol, UK

Steady state outward K+ currents (IKss) show very rapid activation and relatively slow or no inactivation and therefore contribute outward current throughout phases 1,2 and the early part of phase 3 of the action potential (AP). They are thought to be important in cardiac cell types with abbreviated plateau phases (Choisy et al. 2004). Inwardly rectifying background K+ currents (e.g. IK1) regulate membrane excitability as well as contributing to the late phases of action potential repolarisation. Both these currents have been suggested to be under noradrenergic control (Ravens et al. 1989, Fedida et al. 1991). More recently, noradrenaline (NA) has been shown to have biphasic effects on resting membrane potential in rat left atrial and pulmonary vein preparations (Doisne et al. 2009). At present, however, there are no published data describing the modulation of these currents by NA in rat atrial cardiomyocytes. The present study was designed to investigate noradrenergic modulation of the steady state K+ outward current and inward rectifying current in rat atrial cardiomyocytes. Male Wistar rats (200-320 g) were anaesthetised with an intra-peritoneal injection of sodium pentobarbital (60-100 mg/kg). The heart was then rapidly excised, mounted on a Langendorff apparatus and retrogradely perfused via the aorta with a series of solutions at 37 oC as previously described (Choisy et al. 2004). The left atrium was then removed, finely chopped and triturated in Kraftbrühe (KB) solution. Ionic currents were recorded in whole cell voltage clamp mode using a standard external Tyrode's solution and K+-based pipette solution. Cardiomyocytes were held at a holding potential of -80 mV and

a ramp protocol applied every 3 s: a step to +20 mV for 100 ms was followed by a ramp to -120 mV over 500 ms. IKss was measured as the steady-state outward current at +20 mV and IK1 was measured as the K+-dependent inward current at -120 mV. Current voltage relations were analyzed by repeated measures two way ANOVA with Bonferroni post hoc test ($p<0.05$ was considered significant). NA (1 μM) significantly inhibited the steady state outward current at +20 mV but was without effect on IK1 at -120 mV (n=6). This inhibition was unaffected in the presence of atenolol (1 μM, n=7), prazosin (5 μM, n=7) or atenolol plus prazosin (n= 7). On the other hand, in the presence of propranalol (1 μM) the inhibitory effect of NA on steady state outward K+ current was abolished (n=5). Furthermore the steady state outward K+ current was significantly inhibited by the β2-adrenoceptor-selective agonist, zinterol (1 μM) in the presence of atenolol (1 μM) (n=5).These data suggest that the steady state outward K+ current in rat atrial cardiomyocytes is modulated by NA via the β2 adrenoceptor.

Choisy SC, Hancox JC, Arberry LA, Reynolds M, Shattock MJ and James AF (2004) Evidence for a novel K+ channel modulated by α1A-adrenoceptors in cardiac myocytes. Mol Pharmacol 66:735-748

Doisne N, Maupoil V, Cosnay P and Findlay I (2009) Catecholaminergic automatic activity in the rat pulmonary vein: electrophysiological differences between cardiac muscle in the left atrium and pulmonary vein. Am J Physiol Heart Circ Physiol 297: H102–H108.

Fedida D, Braun AP and Giles WR (1991) α1-adrenoceptors reduce background K+ current in rabbit ventricular myocytes. J Physiol 441: 673-684.

Ravens U, Wang X-L and Wettner E (1989) Alpha adrenoceptor stimulation reduces outward currents in rat ventricular myocytes. J Pharmacol Exp Ther 250: 364-370.

RB was supported by a BHF CRTF Award (FS/10/68).

Where applicable, the authors confirm that the experiments described here conform with The Physiological Society ethical requirements.

C07 and PC07

In cardiac ventricular myocytes correction of severe leak from the sarcoplasmic reticulum increases the amplitude and the rate of decay of the systolic calcium transient

R. Sankaranarayanan, Y. Li, D. Greensmith, A. Trafford, L. Venetucci and D. Eisner

Cardiovascular Research Group, University of Manchester, Manchester, UK

INTRODUCTION: In cardiac muscle the amplitude and duration of the systolic calcium (Ca) transient and thence contraction are modulated by the release and reuptake of Ca from the sarcoplasmic reticulum (SR). In heart failure there is a decrease in both the amplitude and rate constant of decay of the Ca transient. These result in part from decreased sarco/endoplasmic reticulum ATPase activity but also due to increased leak through the SR Ca release channel (Ryanodine Receptor, RyR). The objective of this study was to determine whether the reduction in the ampli-

tude and rate constant of decay of the systolic Ca transient caused by severe SR Ca leak can be corrected by decreasing the opening of the RyR.
METHODS: Experiments were performed on rat ventricular myocytes, voltage-clamped using the perforated patch clamp technique and stimulated at 0.5 Hz with 100 ms duration depolarizing pulses from -40 mV to 0 mV. Cytosolic Ca concentration was measured using the fluorescent indicator Fluo-3 AM. Data are described as mean ±SEM. Tests for statistical significance were performed using one way ANOVA.
RESULTS: The application of 2 mM caffeine to increase leak through the RyR decreased the amplitude of the Ca transient from 769 ± 160 nM to 158 ± 28 nM (n=12, p =0.001). This was accompanied by a decrease in the rate constant of decay of the systolic Ca transient from 13.5±1.6 second^{-1} to 6.8 ± 0.65 second^{-1}(p=0.001). We next investigated the effects of decreasing RyR leak by adding 100 μM tetracaine (in the continued presence of caffeine) to decrease RyR opening. This resulted in an initial decrease in the amplitude of the Ca transient, due to decreased RyR opening. This was, however, followed by an increase of both the amplitude and rate constant to levels greater than those observed in caffeine alone (334±68.6 nM;p=0.026 and 10.8± 1.2 second^{-1} ;p=0.02
CONCLUSIONS: In our experiments, inhibition of RyR with 100μM tetracaine partially restores the changes in Ca transient amplitude and rate of decay produced by severe SR Ca leak induced with 2mM caffeine. These results suggest that inhibition of RyR and reduction of SR Ca leak could represent a viable treatment strategy to improve contractility and relaxation in patients with heart failure.

This work was funded by the British Heart Foundation

Where applicable, the authors confirm that the experiments described here conform with The Physiological Society ethical requirements.

C08 and PC08

The capacity to modulate ryanodine receptor channel gating by FK506-binding proteins is contained within three amino acid residues

E. Galfre, E. Venturi, S.J. Pitt, S. Bellamy, R.B. Sessions and R. Sitsapesan

university of bristol, Bristol, UK

FKBP12 and FKBP12.6 form part of the macromolecular ryanodine receptor (RyR) complex in striated muscle and there is general agreement that dissociation of FKBPs from RyRs is involved in the progression of heart disease and skeletal muscle disorders. There is high structural homology between FKBP12 and FKBP12.6 and evidence suggests that both proteins compete for the same binding sites on the cardiac isoform of RyR (RyR2) (1). However, whereas FKBP12 activates RyR2, FKBP12.6 has negligible ability as an activator of RyR2 and behaves instead as an antagonist of FKBP12 (1). To investigate the structural differences between FKBP12 and FKBP12.6 that are important for conferring the ability to activate RyR2, we

generated a triple mutant of FKBP12 ($FKBP12_{E31Q/D32N/W59F}$), where the amino acids Glu^{31}, Asp^{32} and Trp^{59} were mutated to the corresponding residues in FKBP12.6 (Gln^{31}, Asn^{32} and Phe^{59}). $FKBP12_{E31Q/D32N/W59F}$ was cloned and recombinantly expressed in E.coli. The effects of FKBP12, FKBP12.6 and $FKBP12_{E31Q/D32N/W59F}$ on the gating of single cardiac (RyR2) and skeletal (RyR1) channels incorporated into planar phosphatidylethanolamine bilayers were compared using previously described methods (1).

$FKBP12_{E31Q/D32N/W59F}$ had no effect on RyR2 channel gating (open probability (Po) was 0.206±0.08 before, and 0.223±0.10 after, addition of 1 μM $FKBP12_{E31Q/D32N/W59F}$ (SEM; n=5)). The triple FKBP12 mutant, therefore, lost the ability to activate RyR2 and instead behaved more like FKBP12.6. Further experiments were carried out with RyR1 and we found that FKBP12 significantly inhibited RyR1 whereas both FKBP12.6 and $FKBP12_{E31Q/D32N/W59F}$ were activators (Po was 0.021±0.008 before, and 0.110±0.026 after, 1 μM $FKBP12_{E31Q/D32N/W59F}$ (SEM; n=7; $p<0.01$)).

In summary, our results demonstrate a clear distinction in the regulatory effects of FKBPs on RyR1 and RyR2. We also demonstrate that, following the binding of FKBP12/FKBP12.6 to RyR1 or RyR2, the capacity to functionally regulate channel gating is contained within the amino acid residues Glu^{31}, Asp^{32} and Trp^{59} in FKBP12 and Gln^{31}, Asn^{32} and Phe^{59} in FKBP12.6. These findings are relevant to understanding physiological regulation of sarcoplasmic reticulum Ca^{2+} release and the role of FKBPs in cardiac and skeletal muscle disease.

Galfré, E., Pitt, S. J., Venturi, E., Sitsapesan, M, Zaccai, N.R., Tsaneva-Atanasova, K., O'Neill, S. & Sitsapesan, R. (2012). FKBP12 activates the cardiac ryanodine receptor Ca^{2+}-release channel and is antagonised by FKBP12.6. PLoS ONE, 7, Issue 2, e31956.

This work was supported by the British Heart Foundation.

Where applicable, the authors confirm that the experiments described here conform with The Physiological Society ethical requirements.

C09 and PC09

Popdc1 and Popdc2 deficiency results in an impaired response to β–αδρενεργιχ σιγναλλινγ

S. Simrick[1], C. Terracciano[2] and T. Brand[1]

[1]Developmental Dynamics, HHSC, NHLI, Imperial College London, Harefield, UK and [2]Cell Electrophysiology, HHSC, NHLI, Imperial College London, Harefield, UK

The Popeye domain containing (Popdc) gene family encode membrane proteins with a high-affinity cAMP-binding domain. Single null mutants for *Popdc1* and *Popdc2* display stress-induced bradycardia, implicating *Popdc* genes in the cardiac response to β-adrenergic signalling[1]. Here we report our preliminary telemetric ECG analysis of the *Popdc1/2* double mutants (heterozygous, dHET and homozygous null, dKO) at rest and after swimming exercise, or isoproterenol injection (2mg/kg body

weight was administered intraperitoneally under isoflurane anaesthesia). Telemetry devices were implanted under isoflurane anaesthesia with vetergesic analgesia, a minimum of 10 days prior to stress testing to allow for sufficient recovery.
As previously published, average heart rate for *Popdc1* mutant mice was reduced during forced swimming (6 minutes) and recovery (30 minutes) compared to age matched (5.5 months) wild type (WT) males (*Popdc1KO*: 604±98bpm swim, 632±63bpm recovery vs. WT: 692±53bpm swim, 729±19bpm recovery). Preliminary data indicate that the average heart rate for *Popdc1/2dKO* (631±74bpm swim, 572±68bpm recovery) is similarly reduced compared to age-matched controls. Further analysis of ECG data shows an increased incidence of sinus pauses during forced swimming (*Popdc1/2dKO*: 119 pauses, WT: 49 pauses) and recovery (*Popdc1/2dKO*: 273 pauses vs. WT: 0 pauses). Consistently, the averaged heart rate increase following isoproterenol treatment was decreased in the *Popdc1/2dHET* (3%, n=3) and *Popdc1/2dKO* (-11%, n=1) male mice aged 5.5 to 8 months compared to age matched controls (10%, n=2).
This impaired stress response was also observed in ventricular cardiac myocytes (isolated from 3 month age matched male mice) treated with increasing concentrations of isoproterenol (10^{-10}M to 10^{-4}M). *Popdc1/2dHET* ventricular cardiac myocytes displayed an increase in delayed after depolarisations and spontaneously generated action potentials compared to WT controls (spontaneously generated action potentials at 3Hz, $p<0.05$ at 10-4M). Together these data indicate that deficiency of Popdc1 and Popdc2 results in an impaired response to β-adrenergic signalling. By further analysing the single and double *Popdc1/2* mutants at the organ and cellular level, we aim to define the role of Popdc proteins in cardiac stress response.

Froese A *et al* (2012) *J Clin Invest.* **122**, 1119-30.

Funded by the Medical Research Council MR/J010383/1

Where applicable, the authors confirm that the experiments described here conform with The Physiological Society ethical requirements.

C10 and PC10

Interfering with lysosomal function in atrial and ventricular myocytes reduces the response to isoprenaline

R.A. Bayliss, E.L. Bolton, D. Bloor-Young, G. Churchill, A. Galione and D.A. Terrar

Department of Pharmacology, University of Oxford, Oxford, UK

NAADP is a calcium mobilising compound acting via a two-pool mechanism, with roles for two intracellular Ca2+ stores (the lysosome and the sarcoplasmic reticulum (SR)) (1). In both atrial and ventricular myocytes, NAADP increases cellular Ca2+ transients through enhancement of SR Ca2+ load (2). Our working hypothesis is that actions of NAADP involve Ca2+ release from the lysosome via a two-pore Ca2+ channel and that this in turn leads to additional Ca2+being loaded into

the SR. Tissue levels of NAADP are raised after whole-heart perfusion with isoprenaline, suggesting a role for NAADP in the beta-adrenergic response (2). In sea-urchin eggs actions of NAADP can be suppressed by either bafilomycin (which inhibits a V-type Ca2+ ATP-ase in the lysosomal membrane) (1) or by NED-19 which non-competitively inhibits the action of NAADP at two-pore Ca2+ channels (3). Further, bafilomycin superfusion has been shown to reduce ventricular myocyte Ca2+ transient amplitude (2).

This project aimed to measure the response of cardiac myocytes to NAADP and investigate the relevance of this pathway to beta-adrenergic signalling.

All experiments were carried out using isolated guinea pig myocytes (see (4) for atrial isolations and (2) for ventricular isolations). Cells were loaded with fluo 5F calcium indicator and stimulated to fire action potentials. All data are presented as mean ± SEM. Statistical analyses were carried out using Students t-test or ANOVA with Tukey correction as appropriate. Significance is defined as $p<0.05$.

To investigate the cellular response to NAADP cells were loaded with a 'caged' compound, which is inactive until exposed to UV light. UV photorelease of NAADP elicited a significant increase in cellular Ca2+ transient amplitude in both atrial and ventricular myocytes, significant by 3min and reaching 35±13 and 42±11% respectively after 5min. This response was completely abolished when photorelease was carried out in the presence of NED-19.

Application of bafilomycin to atrial myocytes reduced Ca2+ transient amplitude by 19±5% from control. In the continued presence of bafilomycin, the increase in Ca2+ transient amplitude elicited by isoprenaline was significantly reduced in both atrial and ventricular myocytes (from 63±8 to 36±9% and from 148±6 to 102±12% respectively). Further, in the presence of NED-19, the response of ventricular myocytes to isoprenaline was reduced from 148±6% to 105±6%. Isoprenaline responses in the presence of bafilomycin and NED-19 were not significantly different.

These data support the two-pool model for NAADP actions in cardiac myocytes. It appears from these observations that the NAADP system is constitutively active, and has a physiological role in cardiac signalling that is modulated by beta-adrenoceptor stimulation.

Yamasaki et al. (2005) FEBS J. 272: 4598-606

Macgregor et al. (2007) J Biol Chem. 282: 15302-11

Naylor et al. (2009) Nat Chem Biol. 5: 220-6

Collins et al. (2011) Cell Calcium 50: 449-58

We would like to thank the British Heart Foundation for their support of this work.

Where applicable, the authors confirm that the experiments described here conform with The Physiological Society ethical requirements.

C11 and PC11

The role of cGMP dependent nitric oxide signalling on cardiac repolarisation in adult guinea pig ventricular myocytes

R.E. Caves[1], K.E. Brack[2], A. Ng[2] and J.S. Mitcheson[1]

[1]Cell Physiology and Pharmacology, University of Leicester, Leicester, UK and [2]Cardiovascular Sciences, University of Leicester, Leicester, UK

Nitric oxide (NO) signalling has been linked with the regulation of cardiac repolarisation. Abnormalities in cardiac repolarisation are associated with an increased risk of arrhythmia and sudden cardiac death. Studies from isolated heart preparations with intact innervation have demonstrated a clear antifibrillatory effect following vagus nerve stimulation, which is dependent on neuronally released NO. The cellular and molecular basis for this protective effect is unknown. In this study, NO regulation of repolarisation via activation of cGMP dependent pathways was investigated using a novel NO and haem-independent activator of soluble guanylyl cyclase (sGC) - BAY 60-2770. All experiments were performed on acutely isolated adult ventricular guinea pig myocytes maintained in Tyrode at 35-37 °C. The perforated patch current clamp technique was used to record action potentials (AP) and times to 90% repolarisation (APD_{90}) were determined in cells paced at 2 Hz. Cellular cGMP was quantified by radio-immunoassay and expressed as a fold change relative to basal levels. Data are presented as mean ± SEM. 1 μM BAY 60-2770 increased cellular cGMP by just 2.1 ± 0.2 (n = 5) fold on its own and by 7.9 ± 0.7 (n = 4) fold in the presence of 100 μM IBMX (3-Isobutyl-1-methylxanthine), a non-selective phosphodiesterase (PDE) inhibitor. In-vitro assays on purified sGC have shown that ODQ (1H-[1,2,4]Oxadiazolo[4,3-a]quinoxalin-1-one) potentiates the action of BAY 60-2770, and this was corroborated in our experiments by 1 μM BAY 60-2770 + 10 μM ODQ causing a dramatic 38.7 (n = 2) fold increase of cGMP. Despite these substantial increases in cellular cGMP levels with sGC activation, APD_{90} changes were relatively modest except when PDEs were inhibited. Thus, 1 μM BAY 60-2770 alone resulted in a small, but statistically significant ($p < 0.001$) shortening of APD_{90} from 223.3 ± 8.1 ms (n = 6) in basal conditions to 213.0 ± 7.4 ms (n = 6), and adding ODQ to BAY 60-2770 caused no significant further APD_{90} shortening. In contrast, when cGMP hydrolysis was blocked by IBMX (100 μM) and protein kinase A was inhibited by H89 (3 μM), BAY 60-2770 caused a pronounced lengthening of APD_{90} of 19.5 ± 5.6 ms ($p < 0.01$, n = 8). This lengthening occurred in the late rather than early stages of the AP, supporting our preliminary findings that delayed rectifier potassium currents are modulated by these pathways. Overall, our results demonstrate the complex interplay between cGMP and cAMP mediated effects on the ion channels regulating cardiac repolarisation. The relative lack of effect of BAY 60-2770 + ODQ on APD_{90}, despite large changes in cellular levels of cGMP, provide further evidence that PDEs limit cGMP accumulation close to ion channels in the sarcolemma and demonstrate the functional importance of compartmentalisation of cGMP.

Where applicable, the authors confirm that the experiments described here conform with The Physiological Society ethical requirements.

C12 and PC12

The arrhythmic effect of nifedipine mediated via the low affinity β1–αδρενοχεπτορ

C.L. Sam[1,2], T.B. Bolton[2], I.T. Piper[1] and N.S. Freestone[1]

[1]Faculty of Science, Engineering and Computing, Kingston University, Surrey, UK and [2]Division of Biomedical Sciences, St George's University of London, London, UK

Several β-adrenoceptor blocking drugs at high concentrations cause cardiostimulation.Such non-conventional partial agonists (eg. pindolol) have been contra-indicated in the treatment of heart disease (Podrid and Lown, 1982).Freestone *et al* (1999) have shown that CGP12177, structurally similar to pindolol, causes smaller increases in intracellular calcium concentration, but is 40 times more pro-arrhythmic than isoprenaline (ISO) in mouse ventricular myocytes.Cardiostimulatory effects of CGP12177 are propranolol-insensitive but are blocked by bupranolol.These, and other observations, have led to the designation of a new receptor – the low affinity β1-adrenoceptor separate to the high affinity β1-adrenoceptor.Myocyte contraction is caused by CICR through RyR of the sarcoplasmic reticulum.We determine whether CGP12177 caused the spontaneous release of calcium from the SR thus providing a mechanism for its reported arrhythmogenic effects.Atrial cells were isolated from WKY rats by a method developed in our laboratories (Freestone *et al*, 2000).Images of calcium events were obtained by the Zeiss LSM510 Meta confocal microscope.Cells were perfused with propranolol (200nM) alone, ISO alone (100nM), CGP12177 (1μM) in the presence of propranolol, 2-APB (5μM) and propranolol in the presence of CGP12177 and nifedipine (10μM) and propranolol in the presence of CGP12177 and the frequency of calcium events recorded.When perfused with propranolol there were 0.05 ± 0.03 s^{-1} whole cell calcium waves, 0.4 ± 0.1 s^{-1} large but localised calcium release events (wavelets) and 41 ± 6.7 s^{-1} calcium sparks observed (n =12).CGP12177 in presence of propranolol (200nM) significantly increased the incidence of wavelets to, 0.86 ± 0.17s^{-1} at 1μM CGP12177 ($p < 0.005$; n=12).Addition of ISO resulted in an increase ($p < 0.01$) in spark frequency from 26.7 ± 4.5 s^{-1} to 38.7 ± 7.9 s^{-1} from basal (n=5) but did not increase the frequency of whole cell calcium waves or wavelets.2-APB and propranolol perfusion resulted in 0.4 ± 0.2 wavelets s^{-1} and 30.4 ± 4.3 calcium sparks s^{-1} (n=7 cells from 3 animals).CGP12177 with 2-APB and propranolol increased the incidence of wavelets to 1.9 ± 0.4 wavelets s^{-1} ($p < 0.005$) but did not alter the frequency of calcium sparks.Addition of CGP12177 with nifedipine in the presence of propranolol resulted in an increase in calcium wavelets from 0.6 ± 0.2 to 1.1 ± 0.4 s^{-1} (n=9) but no calcium waves were observed.Nifedipine and CGP12177 in the presence of propranolol caused a decrease in the calcium events in rat atrial myocytes.However, CGP12177 in the presence of propranolol is associated with more potent

arrhythmogenic effects.Experiments with 2-APB show that arrhythmogenic effects coming from low affinity β1-adrenoceptor are not via IP3R calcium release and therefore a different mechanism must exist.

Podrid PJ and Lown B. (1982) *Am Heart J* **104** : 491-6.

Freestone NS *et al*. (1999) *Naunyn-Schmiedeberg's Arch Pharmacol.***360** : 445–456

Freestone *et al*. (2000) *Pflugers Arch.***441** : 78-87

We wish to acknowledge the help of Dr Oleksandr Povstyan

Where applicable, the authors confirm that the experiments described here conform with The Physiological Society ethical requirements.

C13 and PC13

Exploring upstream therapeutic targets for treating cardiac hypertrophy and associated arrhythmias

W. Liu[1], M. Zi[1], R. Naumann[2], R. Xiao[3], L. Neyses[1], J. Solaro[4], Y. Ke[4], H. Zhang[1], E. Cartwright[1], M. Lei[1] and X. Wang[1]

[1]University of Manchester, Manchester, UK, [2]Max Planck Institute of Molecular Cell Biology and Genetics, Dresden, Germany, [3]Institute of Molecular Medicine, Peking University, Beijing, China and [4]Department of Physiology and Biophysics and Centre for Cardiovascular Research, University of Illinois, Chicago, IL, USA

Heart failure is one of the most common causes of morbidity and mortality in the human population. The number of patients suffering from heart failure is estimated to be up to 23 million worldwide. Cardiac hypertrophy is regarded as one of the most critical predisposing risk factors for the onset of heart failure. It has been reported that more than half of deaths from heart failure are caused by hypertrophy-associated ventricular arrhythmias. Yet, despite the enormity of this problem, the identification of the fundamental mechanisms underlying hypertrophy and its associated arrhythmias remain elusive.

Over the past few years using genetically modified mouse models, mathematical simulations and pharmacological agents our group has investigated the roles of a number of intracellular signalling proteins in cardiac hypertrophy and associated ventricular arrhythmias. We recently discovered that p21-activated kinase-1 (Pak-1) and its downstream effecters, mitogen-activated protein kinase kinase 4 (MKK4) and MKK7 are critical for controlling cardiac hypertrophy, and Pak1 activator, FTY-720 (a sphingosine-like analogue) is able to reserve existing hypertrophy through negative regulation of NFAT transcription activity. Furthermore, we have identified a new role for MKK4 in maintaining Cx43 expression/distribution, which are important for preservation of normal cardiac electrical function. Preliminary data from our ongoing projects also suggests that MKK7 likely plays a novel role for preventing ventricular arrhythmias by stabilising microtubule-associated protein and ankryrin,

which are required for anchoring many membrane proteins including the Na+/K+ ATPase, the voltage gated Na+ channel and the Na+/Ca2+ exchanger.
In summary, our research provides new insights into exploring upstream therapeutic targets for treating cardiac hypertrophy and stress-associated ventricular arrhythmias.
Aforementioned experiments were carried out on murine hypertrophic models induced by transverse aortic constriction (TAC). 8-10 week old male mice were subjected to TAC or a sham operation under isoflurane anesthesia and artificial ventilation. 0.1mg/kg buprenorphine was given post operation.

Where applicable, the authors confirm that the experiments described here conform with The Physiological Society ethical requirements.

C14 and PC14

The time course and magnitude of conduction velocity response to raised cyclic adenosine monophosphate in the intact rat heart

A. Campbell, F. Burton, G. Baillie and G.L. Smith

ICAMS, University of Glasgow, Glasgow, UK

Abnormalities in conduction velocity (CV) can lead to the generation of re-entrant arrhythmias, a common precursor of ventricular fibrillation (VF). CV is determined by intercellular gap-junction resistance and is thought to be increased during B-adrenergic stimulation although the mechanism is poorly understood. Studies suggest that increasing intracellular cAMP levels increases gap-junction conductance but effect on CV in intact heart is unclear.
Adult male Wistar rats (300-500g) were euthanised and hearts Langendorff perfused with modified Tyrode's solution. CV was recorded using custom electrodes, consisting of bipolar stimulating electrodes and two sets of bipolar recording electrodes. Channel 1 (Ch1) recording electrodes were positioned 1mm from Channel 2 (Ch2) recording electrodes. These electrodes were placed on the epicardial surface of the left ventricle and rotated to achieve record on the axis of maximal CV. The ventricle was paced continuously at 7HZ and the delay between the AP wavefront reaching Ch1 and Ch2 was recorded at a sampling rate of 10 KHz. From this CV could be calculated. In some experiments, blebbistatin (3-10μM) was perfused onto the heart 25 mins before experimental measurements to minimise movement artefacts in CV measurements. Drugs which raise intracellular cAMP were applied for 5 mins and continuous recordings of CV were made prior to during and on washout.
Under control conditions the average CV was 66.3±5 cm.s-1 .The phosphodiesterase (PDE) inhibitor, 3-isobutyl-1-mthylxanthine (IBMX 100μM) significantly increased CV by 9.7%±1.3 ($p< 0.001$ n=4) compared to DMSO control group. Isoproterenol (Iso, 100nM) significantly increased conduction velocity by 9.0%±1.4 ($p<0.01$ n=4). The time course of the CV response to IBMX was significantly slower than the

chronotropic response ($p<0.05$ n=4), with a half time of 58.7±9.1s for the chronotropic response and a half time of 133.1±20.2s for the CV response. Similar difference in chronotropic and dromotropic responses were also seen in response to iso.
These results suggest that β-adrenergic stimulation may increase ventricular CV via a stimulatory G-protein mediated pathway. Whether it is via activation of protein kinase A (PKA) or exchange protein directly activated by cAMP (EPAC) has yet to be established. If the phase lag between chrontropic and dromotropic responses applies during increased cardiac sympathetic activity it may generate a period where conduction block and re-entry may be more common.

Professor Godfrey Smith,

Dr. George Baillie,

Dr. Francis Burton,

Aileen Rankin,

Michael Dunne,

British Heart Foundation

Where applicable, the authors confirm that the experiments described here conform with The Physiological Society ethical requirements.

C15 and PC15

The Popeye domain containing gene family is required for cardiac conduction system development in zebrafish

K.L. Poon[1], B.C. Kirchmaier[2], T. Schwerte[3], J. Huisken[5], C. Winkler[6], B. Jungblut[7], D. Stainier[5], P. Kohl[4,8], T.A. Quinn[4,8] and T. Brand[1]

[1]Developmental Dynamics, NHLI/Imperial College London, London, UK, [2]Hubrecht Laboratory, Institute for Developmental Biology, Utrecht, Netherlands, [3]Institute of Zoology, Innsbruck, Austria, [4]Cardiac Biophysics and Systems Biology, NHLI/Imperial College London, London, UK, [5]University of California San Francisco, San Francsico, CA, USA, [6]Department of Biological Sciences, University of Singapore, Singapore, Singapore, [7]Max Planck Institute for Heart and Lung Research, Bad Nauheim, Germany and [8]Department of Computer Science, University of Oxford, Oxford, UK

The Popeye domain containing (Popdc) genes encode a family of transmembrane proteins with an evolutionary conserved Popeye domain, which functions as a cAMP-binding domain. Analysis of Popdc1 and Popdc2 null mutants in mice revealed that the Popdc family of genes might play a role in age-related sinus node degeneration that consequently leads to progressive bradyarrythmia phenotypes under stress. To advance our understanding of the role of Popdc genes in the cardiac conduction system (CCS), we performed morpholino-mediated knockdown experiments in zebrafish, capitalising on its fast development and comparable electro-

physiology with humans, among other merits as a model for cardiovascular studies. Upon knockdown of popdc2, aberrant development of heart and skeletal muscle was observed. The morphant hearts were morphologically distorted in addition to massive oedema which confounded analysis of CCS function. A submaximal dose of morpholino that does not affect cardiac morphology was then used, which revealed the morphant cardiac arrhythmia phenotype, characterized by irregular ventricular contractions with a 2:1, or 3:1 atrial/ventricular conduction ratio. A reduction in heart frequency was also observed. Recordings of calcium transients in popdc2 morphants on the background of a transgenic calcium reporter line using high spatial resolution SPIM microscopy further detailed the spectrum of arrhythmic phenotypes. Ongoing analysis of the CCS phenotypes in popdc1 morphant suggests the presence of cardiac conduction disorders in the popdc1 morphant. These data suggest an important and evolutionary conserved role of the Popdc gene family in CCS function.

Where applicable, the authors confirm that the experiments described here conform with The Physiological Society ethical requirements.

C16 and PC16

The molecular and electrophysiological basis of triggered activity arising from the right ventricular outflow tract

H. Schneider, S.J. Logantha, M.R. Boyett, V.S. Mahadevan, O. Monfredi and H. Dobrzynski

Cardiovascular Research Group, University of Manchester, Manchester, UK

In the structurally normal heart, ventricular tachycardia (VT) frequently arises from the right ventricular outflow tract (RVOT). It has been postulated that this is due to triggered activity. We have investigated the molecular phenotype of the RVOT to determine if this could account for its arrhythmogenicity.
Wistar rats (3-months old) were sacrificed according to a Home Office-approved method. Tissue samples for qPCR were taken from the right ventricular apex (RV) the infundibulum (RVOT1) and ventriculo-arterial junction (RVOT2) of the RVOT (n=8). qPCR was performed using TaqMan low density array cards. In total, 96 transcription factors, ion channels, extracellular matrix genes and signalling molecules were analysed. The abundance of transcripts was normalised to 4 different reference genes (18S, αMYH6, NCX1 and the average abundance of 90 transcripts). The results were qualitatively similar using all methods. Statminer software (Integromics) was used to determine significant differences in relative abundance. In addition, intracellular action potential recordings were made using 20-30 MΩ, 3M KCl-filled microelectrodes from the endocardial surface of an open-book preparation of the RVOT (n=3 animals); only data from 1 preparation are presented. Compared to the RV, expression of Tbx3, was significantly increased by ~70% in the RVOT. Expression of $Na_v1.5$, was significantly reduced by ~50% in the RVOT (compared to the RV) and this is expected to result in an action potential with a lower

maximum rate of rise (dV/dtmax) and smaller amplitude. Expression of $K_{ir}2.1$ and $K_{ir}2.2$, was significantly reduced by ~34% and ~10%, respectively, in the RVOT and this is expected to result in a more positive maximum diastolic potential. Other differences are: for example, $K_v1.5$ and KChiP2 were significantly increased by 68% and 98%, and $K_{ir}3.1$, $K_{ir}3.4$, RYR2 and NCX1 were significantly reduced by 55%, 50%, 34% and 32%, in the RVOT (compared to the RV). Recordings of intracellular action potentials were made from 6 RV, 3 RVOT1 and 7 RVOT2 sites (in one preparation). Electrical stimuli of twice threshold strength, 2 ms duration and at 1 Hz evoked action potentials with a maximum rate of rise (dV/dtmax) of 360±18, 299±19 and 210±36 V/s in the RV, RVOT1 and RVOT2 regions, respectively. Corresponding action potential amplitudes were 105±2, 101±3 and 86±2 mV. The maximum diastolic potential was 77.3±1.1, -75.1±2.8 and 74.6±2.2 mV in the RV, RVOT1 and RVOT2 regions, respectively.
The RVOT exhibits various characteristics similar to those of the sinoatrial and atrioventricular nodes. It is known that the RVOT shares the same embryonic origin from 'primary myocardium' as the sinoatrial and atrioventricular nodes and this is likely to be the reason for nodal-like myocytes in the RVOT. This offers a plausible explanation for the arrhythmia burden of the RVOT.

Where applicable, the authors confirm that the experiments described here conform with The Physiological Society ethical requirements.

C17 and PC17

Mismatch between simulations and action potential prolongation in Timothy Syndrome

G. Bett[1,2], S. Fernandez[3], A. Lis[2], Q. Zhou[4] and R.L. Rasmusson[2,4]

[1]Gynecology-Obstetrics, SUNY, University at Buffalo, Buffalo, NY, USA, [2]Physiology, SUNY Buffalo, Buffalo, NY, USA, [3]Medicine, SUNY, University at Buffalo, Buffalo, NY, USA and [4]Biomedical Engineering, SUNY, University at Buffalo, Buffalo, NY, USA

Timothy Syndrome (TS) is a multi-symptom disorder characterized by arrhythmias and sudden cardiac death. TS is also associated with impaired cognitive function, and autism spectrum disorder. TS is the result of a de novo point mutation at the intracellular side of S6 in domain I of the L-type Ca2+ channel (Cav1.2). The G406R mutation is a gain of function mutation which interferes with normal inactivation of this Ca2+ channel. There are two forms of TS, with the identical mutation on two mutually exclusive exons, one on 8 (TS2) and the other on 8a (TS2).
The TS2 mutation is lethal in mice. However, mice with the TS2 mutation and transcriptional interference with from a NEO promotor (TS2-NEO) survive to reproductive age. We crossed TS2-NEO with a mouse carrying a cardiac-specific tamoxifen-inducible CRE to develop a cardiac specific inducible form of TS. Exposure to tamoxifen upregulated expression of the exon with the TS2 mutation, and the CRE-TS2-NEO mouse had a noticeable phenotype compared to the mild phenotype of the TS2-NEO.

Tamoxifen 10mg/mL suspended in corn oil was administered by intraperitoneal injection, 100ul (1mg/day) for 2 consecutive days. Tissue was harvested 4 days following the last injection. Mice were anaesthetized via injection of ketamine-xylazine (0.1ml/10g), and left ventricular myocytes dissociated using the Langendorff technique (1). Cells were voltage clamped or current clamped. Computer simulations were performed using our previously published model (1). All procedures were in accordance with institutional and government guidelines.
In the computer model, complete elimination of both Ca2+ dependent and independent components of inactivation in 20% of L-type Ca2+ channels results in prolongation of the action potential (AP) by less than a millisecond. This was expected since inactivation of the Ca2+ current plays little role in repolarization, due to the short duration of the mouse AP. In contrast, experimental results show that there is a significant prolongation of the AP resulting from exposure to tamoxifen and removal of the NEO cassette. Injection with tamoxifen increased AP duration by 40.9 ± 15.8 ms in CRE-TS2-NEO mice vs. 1.9 ± 3.0 ms in control mice (n=5, $p<0.01$). Single cell measurements showed a similar increase in AP. This discordance between simulation and prolongation of repolarization is not unique to mice. AP simulations of TS in guinea pig models shows AP prolongation, but not the profound clinical AP prolongation associated with TS (2). Single cell Ca2+ currents suggest there is little change in inactivation of the L-type calcium channel. This was most evident at positive potentials where Ca2+ dependent inactivation is minimal. However, the changes in kinetics appeared mild compared to the simulation conditions. These data indicate that although TS arises from a point mutation in the L-type Ca2+ channel, there is substantial electrical remodeling in the heart that produce the extreme AP prolongation observed.

Bondarenko VE et al (2004) Am. J. Physiol 287(3):H1378-403

Splawski I, et al (2004). Cell 119:19-31.

Funded in part by the Simons Foundation, the American Heart Association, and the NIH.

Where applicable, the authors confirm that the experiments described here conform with The Physiological Society ethical requirements.

C18 and PC18

The Effects of the Short QT Syndrome on Electrical and Mechanical Function of the Heart: Insights from Modelling

I. Adeniran[1], J.C. Hancox[2] and H. Zhang[1]

[1]Biological Physics Group, School of Physics and Astronomy, The University of Manchester, Manchester, UK and [2]Department of Physiology and Cardiovascular Research Laboratories, School of Medical Sciences, University of Bristol, Bristol, UK

The Short QT Syndrome (SQTS) is a recently identified genetic cardiac channelopathy. It is characterised by abnormally short QT intervals, an increased inci-

dence of atrial and ventricular arrhythmias and an increased risk of sudden death (1). Currently, five distinct forms affecting different cardiac ion channels have been identified; *KCNH2* (SQT1), *KCNQ1* (SQT2), *KCNH2* (SQT3), *CACNA1C* (SQT4) and *CACNB2b* (SQT5). However, due to the lack of phenotypically accurate animal models of the SQTS, the effects of SQTS on ventricular electro-mechanical dynamics have not been elucidated. The aim of this study was to investigate by computer modelling the functional consequences of the SQTS on ventricular electrical and mechanical behaviour. We developed an electromechanical model of the human ventricular myocyte by coupling a human ventricular myocyte model for electrical activity (2) with the Rice myofilament mechanical model (3). For SQT1, a Markov chain model was developed for simulating the experimentally-observed kinetic properties of the N588K-mutated hERG/I_{Kr} channel. SQT2 was modelled by modifying the I_{Ks} Markov chain model formulation of Silva and Rudy (4) to reproduce the experimentally-observed kinetic properties of the V307L-mutated I_{Ks} channel. For SQT3, we used our Hodgkin-Huxley model (5) to simulate the experimentally-observed kinetic properties of the D172N-mutant $I_{Kir2.1}$. The resulting electromechanical model was used to investigate the electromechanical consequences of SQT1, SQT2 and SQT3 at the single cell, 2D and 3D tissue levels. Our simulation data suggested that all three considered SQTS abbreviated the duration of action potentials (APs), which resulted in reduced amplitude of intracellular Ca^{2+} transient, leading to reduced contractile force by 20-80% for SQT1, SQT2 and SQT3. In conclusion, we have developed a human electromechanical model for ventricular myocytes and used it to investigate the functional consequences of the SQTS on ventricular contraction at single cell, 2D tissue and 3D organ levels. It has been shown that the SQT1-3 mutation compromises the binding of calcium to troponin leading to impaired interaction between actin and myosin and thereby less ventricular contractile force.

Gaita F *et al.* (2003). *Circulation* **108**, 965–70.

ten Tusscher KHWJ & Panfilov AV (2006). *Am J Physiol Heart Circ Physiol* **291**, H1088–1100.

Rice JJ *et al.* (2008). *Biophys J* **95**, 2368–90.

Adeniran *et al.* (2011). *Plos Comput Biol* **7**, e1002313.

Adeniran *et al.* (2012). *Cardiovasc Res* **94**, 66-76.

This work was supported by the British Heart Foundation.

Where applicable, the authors confirm that the experiments described here conform with The Physiological Society ethical requirements.

C19 and PC19

The role of tissue heterogeneity and anisotropy in the genesis and development of atrial fibrillation

T.D. Butters[1], J. Zhao[2], B. Smaill[2] and H. Zhang[1]

[1]University of Manchester, Manchester, UK and [2]Auckland Bioengineering Institute, Auckland, New Zealand

Atrial fibrillation (AF) is the most common sustained arrhythmia in the developed world, affecting approximately 1.5% of its population [1]. Although AF is a common arrhythmia its genesis is not well understood. Biophysically detailed computer models of the atria provide a powerful alternative to experimental animal models that allow for in-depth investigations into the roles of specific elements such as ion channel or structural remodelling in arrhythmogenesis. The aim of this study was to develop a 3D mathematical model for the sheep atria. Based on experimental data from Ehrlich *et al*., Burashnikov *et al*., and Lenaerts *et al*. [3-5], electrophysiologically detailed models were developed for different cell types of the sheep atria – the pectinate muscles (PM), crista terminalis (CT), right atrial appendage (RAA), Bachmann's bundle (BB), the left atrium (LA) and the pulmonary veins (PV). These single cell models were then incorporated into an anatomically detailed reconstruction of a sheep atria, which was segmented into the various cell types and contained detailed fibre orientation information throughout the tissue. Using the developed model, we investigate the genesis of AF, and the importance of electrical heterogeneity and fibre structure on its development. In simulations, fibrillation was induced by rapidly pacing the pulmonary vein region. It was found that AF can be induced when the electrical heterogeneity is modelled, regardless of whether or not the complex fibre structure is considered. However, when the fibre structure was ignored the fibrillatory patterns were very different, with fewer re-entrant wavelets forming and a more homogeneous pattern throughout the atria. When the electrical heterogeneity was ignored it was not possible to induce AF with the same pacing protocol. In conclusion, a biophysically detailed 3D anatomical and electrophysiological model for the sheep atria has been developed, providing a useful tool for studying cardiac arrhythmias such as AF. Our simulation data has shown that the differences in action potential morphology in the atria are key for the genesis of AF, and the complex fibre structure is important for its development.

Lip GYH, Kakar P, Watson T. Atrial fibrillation – the growing epidemic. (2007). Heart. **93(5)**, 542-543.

Tanaka K, Zlochiver S, Vikstrom KL *et al*. Spatial distribution of fibrosis governs fibrillation wave dynamics in the posterior left atrium during heart failure. (2007). Circ. Res. **101(2)**, 839-847.

Ehrlich JR, Cha TJ, Zhang L, *et al*. Cellular electrophysiology of canine pulmonary vein cardiomyocytes: action potential and ionic current properties. (2003). J. Physiol. **551(Pt 3)**, 801-813.

Burashnikov A, MannavaS, Antzelevitch C. Transmembrane action potential heterogeneity in the canine isolated arterially perfused right atrium: effect of IKr and IKur/Ito block.Am. J. Physiol. (2004). Heart Circ. Physiol. **286**, H2393-H2400.

Lenaerts I, Bito V, Heinzel FR, *et al*. Ultrastructural and functional remodelling of the coupling between Ca2+ influx and sarcoplasmic reticulum Ca2+ release in the right atrial myocytes from experimental persistent atrial fibrillation. (2009). Circ. Res. **105**, 876-885.

This work was funded by the Engineering and Physical Sciences Research Council (UK).

Where applicable, the authors confirm that the experiments described here conform with The Physiological Society ethical requirements.

PC20

Which are the most evidence-based and cost-effective strategies for treating patients with heart failure?

J. Creed

University of Leeds, Leeds, UK

Heart failure is a chronic, progressive, clinical syndrome, resulting from ventricular dysfunction. Not only is it the leading cause of hospital admissions in the over 65s but with its increasing incidence and poor prognosis this disease is a significant burden on the healthcare system. It is essential to determine which are the most evidence-based and cost-effective treatments for patients with heart failure. This review aims to establish which treatments have been shown to be effective in prolonging the lives of these patients while also improving their quality of life and functional capability. Moreover, the treatments are scrutinized in terms of expenditure; are the management strategies suggested for use in the current American College of Cardiology guidelines effective in terms of quality of life adjusted years. These questions are considered for a number of treatment options including; pharmacological interventions, device therapy, mechanical circulatory support, surgery and heart transplantation and the new directions that are under investigation.
The treatments established in the guidelines are largely proven to be both clinically and cost effective and thus should be adhered to; however evidence from this review suggests that other pharmacological treatments not considered in the recommendations could be of benefit to patients with heart failure. Furthermore, it is uncertain if the new ideas discussed will be clinically and/or cost effective yet, however the current research shows great promise.

de Giuli et al., 2005

Hunt et al., 2009

Ott et al., 2008

Simon Harrrison, University of Leeds

Where applicable, the authors confirm that the experiments described here conform with The Physiological Society ethical requirements.

PC21

May the transient outward current 4-aminopyridine sensitive contribute to the "plateau" of the action potential in mouse sinoatrial node?

M. Gonotkov, E. Lebedeva and V. Golovko

Institute of Physiology, Syktyvkar, Russian Federation

The transient outward current (I to) has been identified in sinoatrial node of rabbit. However neither its physiological role has yet been clarified (Uese et al.1999; Boyett et al., 2001; Verkerk, van Ginneken, 2001). Very little is known about of the 4-aminopyridine (4-AP) sensitive current in sinoatrial (SA) node of the mouse (Lavrik, Golovko 2007; Kharche et al. 2011).

The goals of the present study is to investigate the characteristics action potential (AP) and I to possible contribution to the action potential (AP) generation in the male albino mouse (two-month-old; Mus domesticus; n strips = 34) spontaneously contractions strips using the microelectrode method.

The mean frequency of AP generation was 312 ± 29 beats per min, bpm (K+ 5.4 mM; Ca2+ 1.8 mM ; 31 C). Aminopyridine (0.5 mM, "Sigma") lengthened the action potential duration at the 20% repolarization (APD20) by 50% in pacemaker cells with upstroke velocity dV/dtmax - 3±1 V/s (mean ± SE, n cells =19) was registered. This was accompanied by decreasing of dV/dtmax 30-50% compared with the control (n=5; $p < 0.01$; fig. 1). It has been also identified that 4-AP does not cause lengthened of the final repolarization phase (phase 3).

Action potential auricle type have been recorded also from subendocardial side SA area and characterized short APD20 - 7±2 ms (n cells =10). 4 –AP (0.1 mM) lengthened the APD20 (really plateau) by 50% (EC50) in auricle cells with dV/dt max - 110±6 V/s was registered. In other words we found that shorter spike AP than was higher 4-AP sensitivity SA area mouse cells.

The received results don't explain the phenomenon of decrease upstroke velocity, which was first time recorded at exposure 4-AP. However some assumptions can be made about the transition from phase 0 to phase 2 ("plateau") at exposure 4-AP. Block of I to current increased [K+]i , which indirectly slowed the conductance of Na channels - seems to us most likely.

Supported by the Ural's Division RAS 11-4-HP-438, 12-P-4-1054, 12-U-4-1022.

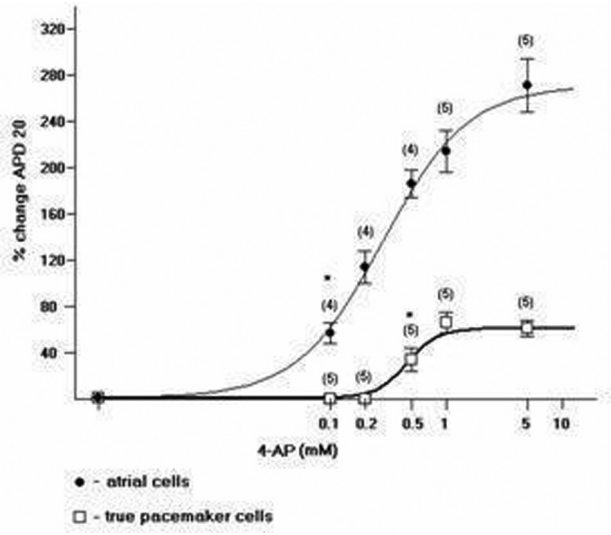

Dose-dependent change of APD20 by 4-AP.

* - $p < 0.01$.

Where applicable, the authors confirm that the experiments described here conform with The Physiological Society ethical requirements.

PC22

Stimulation of I_{Ca} by protein kinase A is facilitated by caveolin-3 in rat cardiac ventricular myocytes

S. Bryant, T. Kimura-Wozniak, C. Orchard and A. James

School of Physiology & Pharmacology, University of Bristol, Bristol, UK

Transverse (t-) tubules are invaginations of the surface membrane of mammalian cardiac ventricular myocytes. The function of many of the key proteins involved in excitation-contraction coupling occurs predominantly at the t-tubules; it has been suggested that this is due, in part, to localised stimulation of ion flux pathways at the t-tubules by protein kinase A (PKA)-induced phosphorylation. Caveolin-3 (Cav-3) has previously been implicated in the localisation of PKA activity. We have, therefore, investigated the role of Cav-3 on the L-type Ca current (I_{Ca}), which flows predominantly across the t-tubule membrane, in rat ventricular myocytes.
Myocytes were isolated from male Wistar rats (250-300 g). Animals were killed either by cervical dislocation or under pentobarbitone (140 mg/kg i.p.) general anaesthesia in accordance with UK legislation. I_{Ca} was recorded using the whole-cell patch clamp technique with 5 mM BAPTA in the pipette solution to inhibit Ca-

dependent inactivation of I_{Ca}. From a holding potential of -80 mV, a 100 ms step depolarisation to -40 mV was used to inactivate I_{Na}, followed by a 500 ms step depolarisation (-50 to +80 mV) to activate I_{Ca} (0.2 Hz at room temperature). Standard immunohistochemical techniques were used in conjunction with confocal microscopy to determine the localisation of Cav-3, L-type Ca channels (LTCC) and phosphorylated LTCC (pLTCC). Incubation with TAT-tagged C3SD peptide (C3SD) was used to disrupt normal protein binding to Cav-3 (MacDougall et al., 2012). Scrambled peptide (Scram) and non incubated cells (Con) were used as controls. β_2-adrenoceptor stimulation was achieved by zinterol (Zint, 1-10 μM) applied to cells pre-exposed to atenolol (10 μM). Data are expressed as mean±SEM (n). Statistical analysis was performed by analysis of variance (1 or 2 way) with the appropriate Bonferroni post hoc test; significance was taken at $p<0.05$.
The amplitude of I_{Ca} at 0 mV was not altered by Scram but was reduced by C3SD (Con -7.6±0.3 (11), Scram -8.0±0.4 (9), C3SD -5.4±0.2 (15) pA/pF, $p<0.0001$ C3SD vs Scram). C3SD had no effect on the distribution of staining of Cav-3 or LTCC but significantly altered the distribution of pLTCC staining.
The PKA inhibitor H-89 decreased the amplitude of I_{Ca} at 0 mV in the absence and presence of C3SD (Con -7.6±0.5 to -3.6±0.5 (5) pA/pF, $p<0.001$; C3SD -5.4±0.4 to -3.7±0.3 (5) pA/pF, $p<0.001$). Peak I_{Ca} was not different between the 2 groups in the presence of H-89. H-89 also decreased staining of pLTCC. The concentration-dependent increase of I_{Ca} caused by Zint was inhibited in cells incubated in C3SD. These data are compatible with the hypothesis that Cav-3 plays an important role in mediating the stimulation of I_{Ca} by PKA-induced phosphorylation under basal conditions, and in response to β_2-adrenoceptor stimulation.

Reference: MacDougall DA, Agarwal S, Stopford E, Chu H, Collins J, Longster A, Colyer J, Harvey R & Calaghan S (2012). J Mol Cell Cardiol 52, 388-400.

This work was supported by the British Heart Foundation

Where applicable, the authors confirm that the experiments described here conform with The Physiological Society ethical requirements.

PC23

Endothelial signalling to vascular smooth muscle exhibits a time-of-day variation

M. Denniff, H. Turrell and G. Rodrigo

Cardiovascular Sciences, Leicester University, Leicester, UK

The circadian rhythm in blood pressure is characterized by a nocturnal “dip” in man, coupled to a decrease in peripheral resistance (Sindrup et al., 1991). Peripheral resistance reflects vascular tone set by the contractile status of vascular smooth muscle (VSM), which is modulated by endothelial production of nitric oxide (NO). Circadian variation in endothelial-dependent relaxation of VSM is suggested from experiments showing that the acetylcholine-induced increase in forearm blood flow in man peaks at 0800 with a trough at 2000 hours, and this difference was reduced

by L-NAME (Shaw et al., 2001). We have therefore looked at the impact of the time-of-day on contractile response of mesenteric resistance vessels to phenylephrine and its modulation by acetylcholine.

Adult male Wistar rats were housed with a 12 hour light/dark cycle and euthanized by stunning and cervical dislocation, three hours into the animals resting (light) or active (dark) period. The mesentery was removed and recordings of contractile force were made from 2–4 mm ring segments of the superior mesenteric artery first-order branches, using a wire-myograph at 37°C. (Data are mean ± S.E.M; n=animals/preparations; compared with t-test or 2-way ANOVA). Dose-response curves of contraction strength to phenylephrine (PHE) show a time-of-day variation in the maximal amplitude of contraction (200μM), which peaked during the resting period at 18.6 ± 1.2 mN (n=5/21) versus 11.8 ± 0.9 mN in the active period (n=4/28; $p<0.001$), with no difference in EC_{50} at 3.3±0.4 versus 4.1±0.7 μM. Inhibition of endothelial nitric oxide synthase (eNOS) with L-NAME (400μM) resulted in a further increase in the maximal PHE-induced contraction, which was significantly greater in active than resting period arteries at 19.5 ± 1.4 mN (n=4/24) in resting versus 17.7 ± 0.8 mN in active period (n=5/31; $p<0.01$). Dose-response curves of the relaxation of the PHE-induced contraction by acetylcholine exhibit strong time-of-day variation, with the dose-response curve shifted to the left during the active period with an EC_{50} of 232 ± 31 nM (n=5/22) during the resting and 58.6 ± 11 nM (n=4/22; $p<0.001$) in the active period. qRT-PCR analysis of mRNA and western blot measurement of protein levels of eNOS in snap frozen vessels show a 3.5-fold increase in eNOS gene expression during the animal's active period, which translated to 2.4-fold increase ($p<0.05$; n=10) in total eNOS protein and 1.5-fold increase of phosphorylated-S1177 eNOS $p<0.01$; n=10). In endothelium denuded vessels, the time-of-day variation in contractile response to PHE was absent.

Our data show the presence of a time-of-day variation in excitation-contraction coupling of VSM, which is endothelial-dependent and appears to involve NO-signalling, This has implications for both vascular contractility and clot formation.

Shaw JA, Chin-Dusting JP, Kingwell BA & Dart AM. (2001). Diurnal variation in endothelium-dependent vasodilatation is not apparent in coronary artery disease. Circulation 103, 806-812.

Sindrup JH, Kastrup J, Christensen H & Jorgensen B. (1991). Nocturnal variations in peripheral blood flow, systemic blood pressure, and heart rate in humans. Am J Physiol 261, H982-988.

HET was supported by the BHF

Where applicable, the authors confirm that the experiments described here conform with The Physiological Society ethical requirements.

PC24

Atrial remodeling causes different cellular Ca^{2+} handling in pigs with hypertension versus atrial fibrillation

G. Jin, F.R. Heinzel, P. Wakula, P. Schoenleiter, S. Radulovic, M. Schwarzl, H. Post, B. Pieske and G. Antoons

Cardiology, Medical University of Graz, Graz, Austria

Atrial remodeling is observed in hypertensive heart disease and also in atrial fibrillation (AF). It often disturbs Ca^{2+} homeostasis, which could contribute to arrhythmogenesis. Common strategies to reduce cardiac remodeling in heart failure have failed to improve the prognosis of AF in large clinical trials, indicating different underlying mechanisms of remodeling. In this study, we investigate if Ca^{2+} handling responds differently to rapid atrial pacing and hypertension as triggers of atrial remodeling.

In 11 anaesthetized, landrace pigs (1 vol% isoflurane, 25 μg/kg/h fentanyl), a custom-made, telemetry-controlled pacemaker was implanted. Rapid atrial pacing (600 bpm) for 6 w induced sustained AF (no detectable SR for > 1h). A group of 8 pigs received a subcutaneous DOCA-depot (100 mg/kg, 90-day release) and a high-lipid/salt diet during 12 w, to induce hypertension (HYP). The left atrial area was assessed by echocardiography during sedation (20 mg/kg ketamine, 0.5 mg/kg midazolam, 0.5 mg/kg azaperone) repetitively. Values of 41 untreated pigs (19-70 kg) served as controls to consider natural growth. In 11 landrace pigs, rapid atrial pacing (600 bpm) for 6 w induced sustained AF (no detectable SR for > 1h). A group of 8 pigs received a subcutaneous DOCA-depot and a high-lipid/salt diet during 12 w, to induce hypertension (HYP). The left atrial area was assessed by echocardiography during sedation repetitively. Values obtained in 41 healty, untreated pigs (19-70 kg) served as controls to consider natural growth. Cells were isolated from left (LA) or right atrium (RA)(N=6 AF, N=3 HYP, N=4 control). Calcium transients (CaT) were measured during field stimulation using Fura-2 AM (0.5 – 2 Hz, 37°C). SR Ca^{2+} content was measured as the peak of caffeine-induced CaT. Western blots were performed on homogenates of 3 RA and 3 LA in each group, and normalized to total protein with Ponceau staining. Data are expressed as mean ± s.e.m.

After 2 w of rapid pacing, left atrial size was larger compared to control and further increased after 6 w of pacing (Fig A). In hypertensive pigs, the systolic blood pressure was 139±11 vs 95±6 mmHg after 12 w treatment ($P<0.05$, tail-cuff-method). The increase in left atrial size was less pronounced (Fig B). In single cells isolated from LA after 6 w pacing, the frequency-dependent Ca^{2+} response was blunted, and CaT amplitude tended to be decreased (0.55±0.03, n=9, vs 0.64±0.04 $F_{340/380}$ in control, n=5, 1 Hz), despite higher SR Ca^{2+} content (1.7±0.15 vs 1.1±0.38 $F_{340/380}$ in control, n=4, $P<0.05$, ANOVA). Fractional release was less efficient. At the molecular level, Na/Ca exchanger was upregulated, while PLB phosphorylation levels were decreased; rate of Ca^{2+} decline was unaltered. Ca^{2+} handling was not different between LA and RA. In HYP, CaT amplitude was decreased in RA

(0.41±0.03$F_{340/F380}$, n=9), but maintained in LA cells (0.58±0.04 $F_{340/380}$, n=9). Compared to RA, Ca^{2+} decline was faster in LA (86±24 ms vs 142±16 ms in RA), which was associated with an increased PLB phosphorylation at Ser16 and Thr17 in LA. SR Ca^{2+} content was not increased.

In conclusion, in hypertensive remodeling, Ca^{2+} handling is better maintained in LA than RA. In AF, in both LA and RA, the Ca^{2+} release process is less efficient. Unlike in hypertension, SR Ca^{2+} load is increased, which heralds a potential risk of Ca^{2+} overload and arrhythmias.

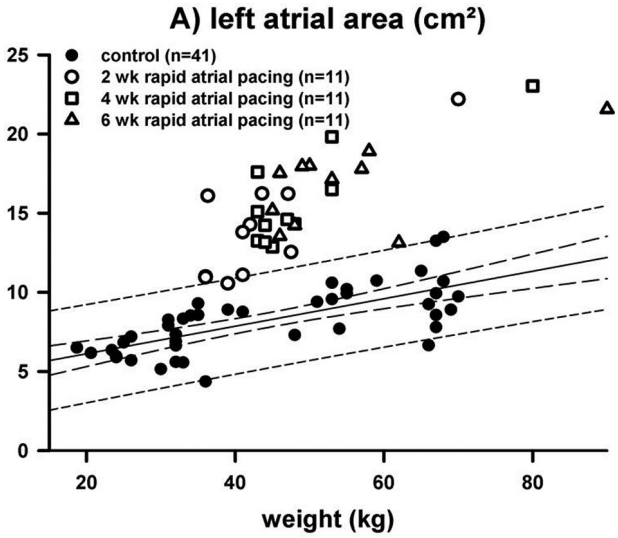

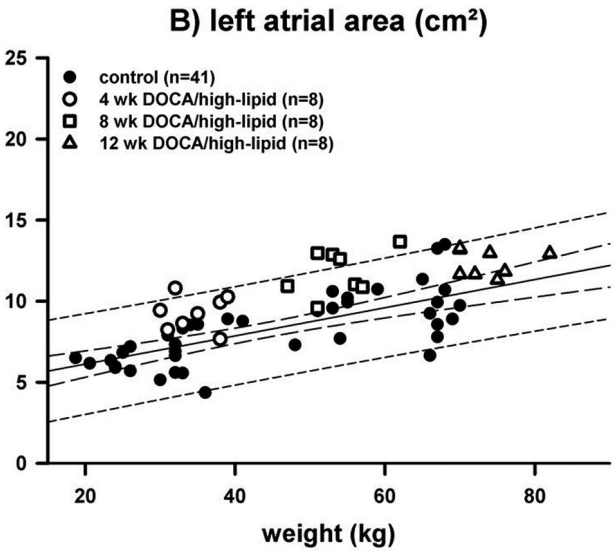

Where applicable, the authors confirm that the experiments described here conform with The Physiological Society ethical requirements.

PC25

Using computational modelling to investigate mechanical ventilation settings in acute respiratory distress syndrome (ARDS)

T. Ali and J.G. Hardman

Division of Anaesthesia and Intensive Care, Univeristy of Nottingham, Nottingham, UK

Acute lung injury (ALI) defined by hypoxemia (PaO2/FiO2 ≤300mmHg) and its severe form acute respiratory distress syndrome (ARDS) (PaO2/FiO2 ≤200mmHg) account for 79 and 59 cases per 100,000 persons respectively [1]. Such patients require mechanical ventilation (MV) and the optimal ventilator settings are often difficult to determine for individual patients and can further induce stretch related lung injury. The ARDSNET trial [2] crucially showed that lowering tidal volume from 12 to 6mL/kg had a significant reduction in mortality and time spent on MV. Following this publication little progress has been made in elucidated the ideal settings for MV such as PEEP and application of recruitment manoeuvres (RM) to further lower mortality which is often difficult to study in the clinical setting. Computational modelling can offer a real alternative to test separate hypothesis in a safe and effective manner and our aim was to simulate ARDS disease patient parameters to directly compare the model predictions with data reported in the ARDSNET trial. The ARDSNET patient database was accessed with permission NHLBI Bio-

logic Specimen and Data Respiratory Information Centre to create virtual ARDS patients and analysed using the Nottingham Physiological simulator (NPS) [3]. The baseline MV parameters including tidal volume, arterial blood gases, PEEP and airway pressures used in the ARDS Network study were computed into the NPS to analyse the outcomes. Previous results have shown that the simulator is capable of providing realistic predictions of ideal MV settings [4] and work is currently underway to increase the number of virtual patients used to compare actual and predicted outcomes from mechanical ventilation. Mathematical models of physiological processes offer a real alternative to expensive and time consuming in vivo experiments as a single variable can be studied in isolation. The development of such tools will offer clinicians a more detailed insight into the disease process to help them determine the best strategy for improving oxygenation. However such models need to be rigorously tested to account for the varying uncertainty in the patient populations. The ARDSNET study contained data from 861 ARDS patients and will prove invaluable in the further development and validation of the NPS.

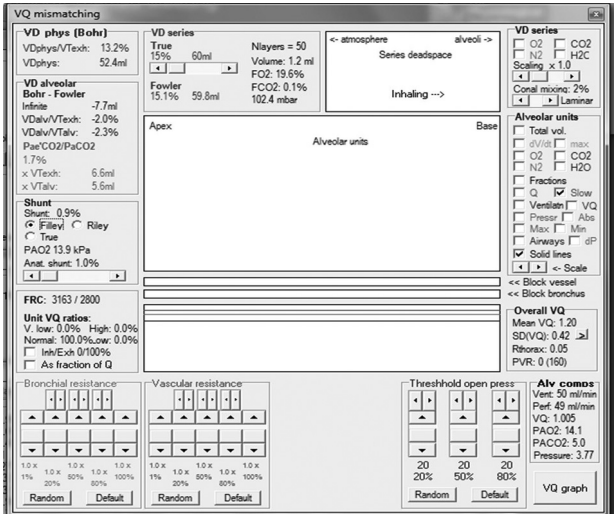

Figure illustrating a simulation being carried out with the NPS.

Fan, E., et al., Recruitment maneuvers for acute lung injury: a systematic review. Am J Respir Crit Care Med, 2008. 178(11): p. 1156-63.

ARDSNET, Ventilation with lower tidal volumes as compared with traditional tidal volumes for acute lung injury and the acute respiratory distress syndrome. The Acute Respiratory Distress Syndrome Network. N Engl J Med, 2000. 342(18): p. 1301-8.

Hardman, J.G., et al., A physiology simulator: validation of its respiratory components and its ability to predict the patient's response to changes in mechanical ventilation. Br J Anaesth, 1998. 81(3): p. 327-32.

Das, A., et al., A systems engineering approach to validation of a pulmonary physiology simulator for clinical applications. J R Soc Interface, 2011. 8(54): p. 44-55.

We would like to acknowledge The National heart, lung and blood institute (NHLBI) Biologic Specimen and Data Respiratory Information Centre for granting access to the ARDSNET study database (2000).

Where applicable, the authors confirm that the experiments described here conform with The Physiological Society ethical requirements.

PC26

Diffusion tensor magnetic resonance imaging of anisotropic and orthotropic architecture of the human foetal ventricular myocardium

E. Pervolaraki[1], R.A. Anderson[2], A.P. Benson[1], B.J. Moore[1], H. Zhang[3] and A.V. Holden[1]

[1]School of Biomedical Sciences, University of Leeds, Leeds, UK, [2]MRC Centre for Reproductive Health, University of Edinburgh, Edinburgh, UK and [3]School of Physics and Astronomy, University of Manchester, Manchester, UK

Myocardial architecture – the orientation and organisation of myocytes, fibrocytes and supporting collagen fibres in the three-dimensional myocardium – determines the spatial pattern of propagation and contraction within the heart. Cardiac diffusion tensor magnetic resonance imaging (DT-MRI) provides a non-destructive measure of the magnitude (eigenvalues λ_1, λ_2, λ_3) and direction (their eigenvectors) of proton (water) diffusion in three dimensions. The eigenvectors have been used to quantify ventricular myofibre orientation and organisation (Gilbert et al., 2011). In an isotropic tissue $\lambda_1 \sim \lambda_2 \sim \lambda_3$ and diffusion from a point source is into a sphere; in a cylindrically anisotropic tissue $\lambda_1 > \lambda_2 \sim \lambda_3$ diffusion is into an ellipsoid; in an anisotropic and orthotropic tissue $\lambda_1 > \lambda_2 > \lambda_3$ and diffusion is into a flattened ellipsoid. The orientation of the ellipsoid long axis is taken as the myofibre orientation, and the flattened ellipsoid may be interpreted as the orientation of cleavage planes between myolamellae. The diffusive spread of voltage leads to anisotropy and orthotropy in propagation velocity.

11 human foetal hearts, 14 to 20 weeks gestational age, with wet weight from 0.26 - 1.41g, were fixed (10% formalin) and imaged (MRI, FLASH, DT-MRI) in fomblin using a 9.4T Bruker Biospin MRI as in Benson et al. (2011), with a spatial resolution of 100 - 200μm, that is fine enough for computational modelling of tissue electrophysiology. $\lambda_1 > \lambda_2 > \lambda_3$, their eigenvectors and derived quantities (angles derived from eigenvectors and fractional anisotropy (FA) derived from eigenvalues) were calculated, $0 \leq FA \leq 1$. The ventricular walls and septum of all the 11 human foetal hearts were anisotropic and orthotropic (Fig. 1), with a ratio of eigenvalues $\lambda_1:\lambda_2:\lambda_3$ of ~ 8:2:1, and with mean FA<0.3. The mean FA of adult rat myocardium is 0.43 (±0.001) and is associated with anisotropy and orthotropy in propagation velocities in the ratio of 4:2:1 (Hooks et al, 2007), that can be simulated by diffusion coefficients in the ratio of 16:4:1.

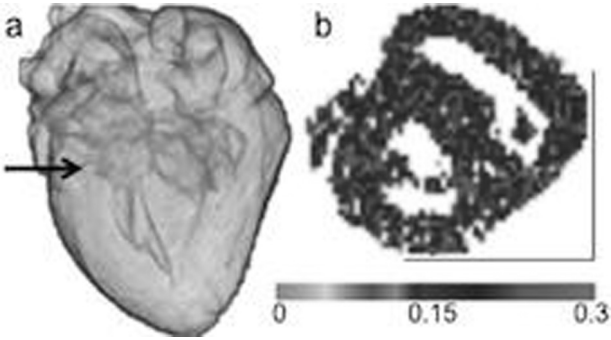

Figure 1. (a) Surface view of 3-D diffusion weighted image of 110 days gestational age foetal human heart and (b) the corresponding fractional anisotropy map of a mid-equatorial short axis slice. Scale bar is 10mm.

Benson A.P. et al., (2011) Interface Focus 1 101-116.

Gilbert S.H. et al. (2011) American J Physiology 302 H287-H298.

Hooks D.A. et al. (2007) Circ.Res. 101 e103-112.

Where applicable, the authors confirm that the experiments described here conform with The Physiological Society ethical requirements.

PC27

Effects of phosphodiesterase type 5 inhibition on intracellular calcium handling and its implications for cardioprotection and antiarrhythmogenesis

D.C. Hutchings, M. Lawless, D.A. Eisner and A.W. Trafford

Cardiac Physiology, University of Manchester, Manchester, UK

Introduction: Phosphodiesterase 5A inhibition with sildenafil (Sil) improves cardiac function and functional indices in heart failure (HF)1. In addition, acute application of Sil in animal models of myocardial infarction has direct cardioprotective and antiarrhythmic effects2. Sildenafil reduces L-type Ca2+ current (ICa,L) 3 and attenuates adrenergically-driven inotropism4, yet effects on myocyte calcium handling are largely undetermined. Our aim was to establish whether sildenafil exerts antiarrhythmic and negatively inotropic effects through alterations in Ca2+ handling.
Methods: Isolated adult rat ventricular myocytes (ARVMs) were voltage clamped using whole-cell or perforated patch techniques, and Ca2+ fluorescence measured using the indicator Fura-2. Cells were paced at 0.5Hz with depolarising steps from -60mV to +10mV. Sarcoplasmic reticulum (SR) content was determined by application of caffeine (10-20mmol/l) and integration of inward NCX current. Rate constants for Ca2+ extrusion from the cell (kcaff) and Ca2+ uptake into the SR (kSERCA) were determined by fitting 1st order exponentials to decay phases of the respec-

tive Ca2+ transients5. Following an initial control protocol, a therapeutically relevant dose of Sil (1μM) applied. Data are presented as normalised to control for n cells. Differences between groups are determined with student's paired t tests.
Results: Sil reduced SR content by 26.5% (n=9, p<0.01). In addition, though to a lesser extent, Sil reduced Ca2+ transient amplitude (by -13.6%, n=9, p<0.05). This was not accompanied by a reduction in calculated SERCA activity (kSERCA -2.3% with Sil, p=0.97, n=5). Peak and integrated ICa,L were also reduced with Sil (-9.1% & -6.0%, respectively, n=9, p<0.05). This effect on ICa,L was also seen in adult dog ventricular myocytes (reducing peak and integrated ICa,L by 15.9% and 26.4% respectively, p<0.05 & p<0.01, n=6, temp 23C). Effect of Sil on integral ICa,L in ARVMs could not be 'washed out' by further application of control solution (washout -9.2%, p<0.05, n=8), and subsequent re-application of Sil reduced integral ICa,L even further (-15.2%, p<0.05, n=8). These effects cannot be attributed to 'run-down' effects.
Conclusions: Sil substantially reduced SR content. Given that there was no significant reduction in kSERCA, this reduction may be mediated through ryanodine receptor modulation. Such reductions in SR content may reduce pro-arrhythmic SR Ca2+ release, and indicate a novel mechanism through which sildenafil exerts an antiarrhythmic effect.
Acute reductions in Ca2+ transient amplitude and ICa,L with Sil indicate acute negative inotropic effects and may contribute to our understanding of its cardioprotective effects in the setting of hyperadrenergic drive in HF.

1. Guazzi M et al. Circ Heart Fail. 2011 Jan;4(1):8-17

2. Nagy O et al. Br J Pharmacol. 2004 Feb;141(4):549-51

3. Chiang C et al. Cardiovasc Res. 2002;55(2):290-9

4. Lee D et al. Basic Res Cardiol. 2010 May;105(3):337-47

5. Dibb K et al. J Mol Cell Card. 2004. 37, 1171–1181

Where applicable, the authors confirm that the experiments described here conform with The Physiological Society ethical requirements.

PC28

Modulation of ryanodine receptor open probability has no maintained effect on the amplitude of systolic calcium release in sheep or dog ventricular myocytes

D.J. Greensmith, A.W. Trafford, K.M. Dibb and D.A. Eisner

Unit of Cardiac Physiology, The University Of Manchester, Manchester, UK

Caffeine is frequently used as an agent to increase the open probability of the Ryanodine receptor (RyR). However, our group has previously demonstrated that in rat, application of 500 μM caffeine has no sustained effect on systolic Ca. Rather, following an initial increase, the intracellular calcium ($[Ca^{2+}]_i$) transient amplitude returns to that of control steady state in around 20 s (Trafford et al., 2000). This

temporary potentiation was due to a concurrent decrease in SR Ca, which was measured at steady state but calculated on a beat by beat basis. Our aim was to determine if the above phenomenon could also be observed in larger mammals. In addition, we measured beat by beat SR Ca in real time using the low affinity Ca indicator Mag-Fura-2.

Young (~18 months) Sheep were killed in accordance with The Home Office Animal (Scientific Procedures) Act 1986 for enzymatic isolation of left ventricular mid myocardial myocytes. Dog ventricular myocytes were kindly provided by Michael Morton (Astra Zeneca). Myocytes were either loaded with Fura-2 for cytoplasmic Ca measurement or co-loaded with Fluo-3 and Mag-Fura-2 for cytoplasmic and SR Ca measurement respectively. Myocytes were current clamped via perforated patch and paced at 0.5 Hz.

Sustained application of 500 μM caffeine in sheep myocytes initially increased the $[Ca^{2+}]_i$ transient amplitude which subsequently returned to control levels. The rate at which the $[Ca^{2+}]_i$ transient amplitude decreased following potentiation was faster when compared to rat, typically occurring within 5 beats. In dog myocytes loaded with Fluo-3 and Mag-Fura-2, sustained application of 500 μM caffeine also resulted in a temporary potentiation of the $[Ca^{2+}]_i$ transient amplitude, which returned to that of control at around the same rate as those in sheep. We also observed an initial increase in the amplitude of SR Ca loss in the presence of 500 μM caffeine, which returned to that of control. The decrease of the $[Ca^{2+}]_i$ transient amplitude and the amplitude of SR Ca loss occurred at the same rate. In the presence of caffeine, SR Ca content was decreased to a lower steady state, agreeing qualitatively with the calculated SR Ca reduction observed in rat.

These data demonstrate that modulation of RyR open probability has no maintained effect on the $[Ca^{2+}]_i$ transient amplitude, even in larger mammals. The direct measurement of SR Ca during these experiments also confirms that SR Ca loss underlies the post potentiation reduction of systolic Ca, compensating for a sustained increase in RyR open probability and allowing the myocyte to maintain a constant inotropy. The rapid rate at which the $[Ca^{2+}]_i$ transient returns to control values in these larger mammals when compared to rat is presumably due to a greater dependence on sodium calcium exchange.

Trafford AW et al. (2000). J physiol 522, 259-270.

Where applicable, the authors confirm that the experiments described here conform with The Physiological Society ethical requirements.

PC29

Wheat germ agglutinin staining of rabbit cardiac myocytes

H.C. Gadeberg, C. Kong, M.B. Cannell and A.F. James

University of Bristol, Bristol, UK

Wheat germ agglutinin (WGA), a member of the lectin family that binds to N-acetyl-D-glucosamine and sialic acid residues found on the surface of cell membranes, has been used extensively to stain surface membranes, including t-tubules in cardiac myocytes (Savio-Galimberti et al. 2008). It has also been used as an indicator of the Golgi apparatus and nuclear core complexes (Iida & Page 1989; Miller et al. 1991). In this study, we have examined the effect of fixation on the staining of rabbit cardiac myocytes with WGA.

Isolated rabbit atrial and ventricular myocytes were stained with an AlexaFluor 488-conjugated WGA. Images were acquired using a Leica SP5 confocal imaging system and excitation wavelengths of 488 nm and 590 nm with the aperture set to 1 Airy unit. Images were analysed using ImageJ: Binary images were calculated by thresholding images and the percentage of bright pixels within the cell including ('%total area') and excluding ('%intracellular area') the cell edge were calculated. Cells were fixed with 4% paraformaldehyde (PFA) for 10 min before incubation with WGA for 10 min, 30 min or 1 hr . The duration of incubation had no significant effect on the percentage total area or the percentage intracellular area stained. However, significant intracellular staining was observed in atrial and ventricular myocytes (atrial cells, 6.2±1.5%, n=13; ventricular cells, 9.0±1.5%, n=13; $P>0.05$, Mann-Whitney test). Visual inspection showed a staining pattern in ventricular cells consistent with t-tubules. On the other hand, the intracellular staining in atrial myocytes suggested binding of the WGA to intracellular organelles, such as the nucleus and Golgi. This suggested that the membranes had been permeabilized during fixation allowing WGA to enter. To investigate this possibility, cells were stained with WGA before fixation. With this technique, atrial myocytes showed significantly less staining inside the cell (0.1±0.04% of intracellular area, n=7), compared to ventricular myocytes (7.7±0.93%, n=9), $p<0.001$, Mann-Whitney test. Cells fixed before staining were compared with cells treated with 0.1% Triton-X to permeabilise the membrane, to assess whether permeabilization during fixation could explain the staining pattern observed. This method produced staining similar to non-permeabilised cells with 6.66±1.81% of the intracellular area stained in atrial cells (n=7), and 9.67±1.38% in ventricular (n=7), $P>0.05$ unpaired t-test.

In summary, WGA is an important tool for staining the cell membranes, however the protocol used for staining must be considered. The current data suggests that fixing cells using PFA results in significant permeabilisation of the cell membrane and subsequent intracellular staining with WGA. Care should therefore be taken in the interpretation of images of cardiac myocytes stained using WGA.

Iida, H. & Page, E., 1989. Localization of wheat-germ agglutinin-binding sites in the Golgi complex of cultured rat atrial myocytes. Cell and Tissue Research, 257(2), pp.325-331.

Miller, M., Park, M.K. & Hanover, J.A., 1991. Nuclear pore complex: structure, function, and regulation. Physiological reviews, 71(3), pp.909-49.

Savio-Galimberti, E. et al., 2008. Novel features of the rabbit transverse tubular system revealed by quantitative analysis of three-dimensional reconstructions from confocal images. Biophysical journal, 95(4), pp.2053-62.

Where applicable, the authors confirm that the experiments described here conform with The Physiological Society ethical requirements.

PC30

Action potential clamp and pharmacological study of the gain-of-function T618I hERG channel pore mutant

A. El Harchi[1], D. Melgari[1], H. Zhang[2] and J. Hancox[1]

[1]School of Physiology and Pharmacology, University of Bristol, Bristol, UK and [2]School of Physics and Astronomy, University of Manchester, Manchester, UK

The rapid delayed rectifier K^+ current (I_{Kr}) is key to normal ventricular repolarization. Mutations to hERG (human Ether-à-go-go-Related gene) can result in either a loss or gain of function of channels responsible for I_{Kr}. The aim of this study was to investigate electrophysiological and pharmacological properties of a recently identified pore-mutation (T618I) associated with variant 1 short QT syndrome (SQTS) (Sun et al, 2011). Whole-cell patch clamp recordings of wild-type (WT) and T618I hERG current (I_{hERG}) were made at 37ºC from hERG-expressing HEK 293 cells, using previously described K^+-based pipette solution and standard extracellular solution (El Harchi et al, 2012). Results are presented as mean ± S.E.M or mean ± 95% confidence interval (C.I). Statistical comparisons were made using unpaired t-tests. Under conventional voltage-clamp, voltage-dependent rectification was evident for both WT and T618I I_{hERG}, though for T618I I_{hERG} maximal current was ~30 mV right-ward voltage-shifted compared to WT I_{hERG}, consistent with a reported alteration to voltage-dependent inactivation for this mutation (Sun et al, 2011). The use of ventricular action potential (AP) voltage-clamp ("AP clamp") revealed marked differences in the profile of WT and T618I I_{hERG} during AP repolarisation. Maximal WT I_{hERG} occurred comparatively late during the AP waveform, at -30.7 ± 1.2 mV (n=14), whilst for T618I hERG peak I_{hERG} occurred significantly earlier during the ventricular AP plateau, at +5.1 ± 2.1 mV (n=19;$P < 0.001$ versus WT). The Class Ia antiarrhythmic drug disopyramide inhibited WT I_{hERG} with a half-maximal inhibitory concentration (IC_{50}) of 7.68 μM (C.I. 6.1 μM to 9.6 μM) and T618I I_{hERG} with an IC_{50} of 16.8 μM (C.I 8.6 to 33.1 μM). The reported clinical concentration range of disopyramide lies between ~6-8 μM (Zema, 1984) and therefore disopyramide may be predicted to retain some I_{hERG} inhibitory activity in the setting of T618I-linked variant 1 SQTS. The occurrence of greater I_{hERG}, earlier in the ventricular AP plateau is anticipated to lead to accelerated repolarization and hence AP and QT interval abbreviation.

El Harchi A, Zhang YH, Hussein L, Dempsey CE, Hancox JC (2012) Molecular determinants of hERG potassium channel inhibition by disopyramide. J Mol Cell Cardiol 52: 185-195.

Sun Y, Quan XQ, Fromme S, Cox RH, Zhang P, Zhang L, Guo D, Guo J, Patel C, Kowey PR, Yan GX (2011) A novel mutation in the KCNH2 gene associated with short QT syndrome. J Mol Cell Cardiol 50: 433-441.

Zema MJ (1984) Serum drug concentration and adverse effects in cardiac patients after administration of a new controlled-release disopyramide preparation. Ther Drug Monit 6: 192-198.

This work was funded by the British Heart Foundation (PG/10/96).

Where applicable, the authors confirm that the experiments described here conform with The Physiological Society ethical requirements.

PC31

Remote ischaemic conditioning attenuates endothelin-1 induced hypertrophic response in rat cardiomyoblasts

A.P. Vanezis, S.A. Edroos, N.J. Samani and G.C. Rodrigo

Cardiovascular Sciences, University of Leicester, Leicester, UK

Introduction: Repeated remote ischaemic conditioning (RIC) significantly reduces the inflammatory response following a myocardial infarction (MI), and this improves left ventricular remodelling (Wei et al., 2011). However, it is unclear whether this is mediated directly by the reduction in the pro-inflammatory response or direct signalling to the myocardium by a blood borne agent. As the cardioprotective effect of acute RIC results from a blood borne agent, we hypothesised that RIC generates a blood borne signal capable of reducing the hypertrophic response by modulating gene expression associated with remodelling.
Methods: Superfusate was collected from Langendorff perfused Wistar rat hearts during the reperfusion phase of conditioning ischaemia (RIC-superfusate). Blood was taken from healthy volunteers after 3 cycles of 5 minutes of upper arm conditioning by cuff inflation/deflation (RIC-serum). The RIC-superfusate/serum was applied to H9c2 cardiomyoblasts in culture treated with endothelin-1 (ET-1) to stimulate hypertrophy. Cell surface area was determined from fluorescence images of phalloidin-FITC/Hoechst stained cells. Expression of four genes: a marker of hypertrophy (BNP), the foetal genes (α-actin and βMHC) and the cardiac stress-related gene (ms-1), were determined using qRT-PCR. Response to RIC-superfusate/serum was compared to saline/serum collected immediately prior to RIC.
Results:ET-1 (100ng/mL) caused a significant degree of cellular hypertrophy after 48 hours to $22.8\pm1.1\times10^{-3}$ mm^2 versus $16.4\pm0.7\times10^{-3}$ mm^2 in untreated cells (n=10 experiments/300 cells, $p<0.01$). Pre-treatment with either RIC-superfusate or RIC-serum significantly reduced the ET-1 induced hypertrophic response from $19.8\pm0.8\times10^{-3}$ mm^2 to $14.7\pm0.6\times10^{-3}$ mm^2 and $23.6\pm1.5\times10^{-3}$ mm^2 to $16.1\pm1.1\times10^{-3}$ mm^2 respectively (n=10/300 $p<0.01$). Rat RIC-superfusate caused a significant decrease in the ET-1 induced expression of α-actin (fold-change 8.0±0.4 to 1.7±0.1;

n=4, p<0.01), βMHC (6.5±0.5 to 2.5±0.3; n=4, p<0.01), BNP (1.3±0.3 to 0.4±0.2; n=4, p<0.05) and ms-1 (31.6±2.7 to 13.0±1.4; n=4, p<0.01) determined after 48 hours. Human RIC-serum significantly reduced the ET-1 induced expression of βMHC (7.7±1.0 to 3.9±0.5; n=4, p<0.05) and ms-1 (15.4±2.7 to 7.0±0.7; n=4, p<0.05) after 48 hours.
Conclusion: Our data supports the hypothesis that RIC initiated humoral signalling may also attenuate the deleterious process of cardiac remodelling. The findings identify a new therapeutic approach that may be beneficial in reducing adverse ventricular hypertrophy post-MI.

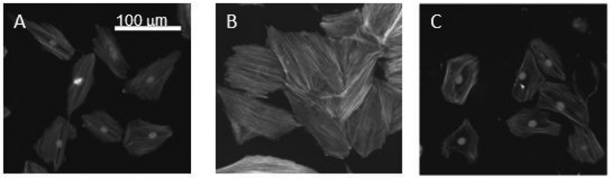

Images of cultured H9c2 cardiomyoblast cells stained with Phalloidin-FITC which binds to actin and Hoechst nuclear stain. A.) Control cells grown in normal media for 48 hours. B.) Cells treated for 48 hours with the hypertrophic chemical stimulus Endothelin-1. C.) Cells pre-treated for 30 minutes with serum from a remotely conditioned (RIC-serum) volunteer prior to treatment for 48 hours with Endothelin-1.

Wei M, Xin P, Li S, Tao J, Li Y, Li J, Liu M, Zhu W & Redington AN. (2011). Repeated remote ischemic postconditioning protects against adverse left ventricular remodeling and improves survival in a rat model of myocardial infarction. Circ Res 108, 1220-1225.

APV holds a studentship from the Leicester Biomedical Research Unit (NIHR)

Where applicable, the authors confirm that the experiments described here conform with The Physiological Society ethical requirements.

PC32

Comparative modulation of rabbit atrioventricular node cell K^+currents by endothelin-1 and phenylephrine

S.C. Choisy, A.F. James and J.C. Hancox

School of Physiology and Pharmacology, University of Bristol, Cardiovascular Research Laboratories, Bristol Heart Institute, Bristol, UK

Both the rapid delayed rectifier K^+ current (I_{Kr}) and muscarinic K^+ current (I_{KACh}) are present in myocytes from the rabbit atrioventricular node (AVN) (Hancox *et al.*, 1993). Recent data indicate that both of these currents can be modulated by activation of G-protein coupled endothelin-A receptors (Choisy *et al.*, 2012a). This study investigated whether or not an alpha-adrenoceptor agonist (phenylephrine), which also works through G-protein coupled receptor signalling pathways (Varma and Deng, 2000) is able to produce similar modulation of I_{Kr} and I_{KACh} to that elicited

by endothelin-1 (ET-1). Adult male New Zealand White rabbits were killed in accordance with UK Home Office legislation and AVN cells were isolated as described previously (Hancox *et al.*, 1993). Whole-cell voltage-clamp was performed at 37 ºC using a standard Tyrode's solution and K^+-based pipette solution (Choisy *et al.*, 2012a,b). Data are presented as means ± S.E.M. and statistical comparisons made using a *t*-test. The amplitude of I_{Kr} tails elicited on repolarisation to -40 mV following 500 ms depolarising voltage commands to +30 mV was reduced from a mean of 2.31 ± 0.14 pA/pF by 31.2 ± 5.3 % ($p<0.01$ versus zero change; n=5). Instantaneous current activated by step hyperpolarisation to -120 mV from -40 mV was transiently increased ~2.5 fold from -4.07 ± 0.83 pA/pF to -10.27 ± 1.15 pA/pF ($p<0.001$; n=14). Repetitive application of a voltage-ramp protocol (Choisy *et al.*, 2012b) showed that this current, which closely resembled I_{KACh} (Choisy *et al.*, 2012a,b) faded with a monoexponential time-course (rate constant of 0.019 ± 0.001 s–1 at -120 mV). Application of 10 μM phenylephrine (applied in the presence of 1 μM of the β_1-adrenoceptor antagonist atenolol) did not produce similar effects to ET-1. Thus, in 8 cells studied, the I_{Kr} tail density elicited on repolarisation to -40 mV from +30 mV in phenylephrine was not significantly different of that in atenolol alone (an insignificant difference of +1.4 ± 8.8 % compared to atenolol alone; $p>0.1$; n=8). Similarly, instantaneous current activated by step hyperpolarisation to -120 mV from -40 mV in phenylephrine was not different from that in atenolol alone (99.0 ± 2.0 % of the value in atenolol alone $p>0.1$; n=8). We conclude that whilst ET-1 and phenylephrine are recognised to activate similar intracellular signalling pathways, under our conditions only ET-1 inhibited AVN I_{Kr} or activated an inwardly rectifying current with properties of I_{KACh}.

Choisy SC, Cheng H, Smith GL, James AF, Hancox JC (2012a). Modulation by endothelin-1 of spontaneous activity and membrane currents of atrioventricular node myocytes from the rabbit heart. PLoS One 7: e33448.

Choisy SC, James AF, Hancox (2012b). Acute desensitization of acetylcholine and endothelin-1 activated inward rectifier K^+ current in myocytes from the cardiac atrioventricular node. Biochem Biophys Res Comm 423: 496-502.

Hancox JC, Levi AJ, Lee CO & Heap P (1993). A method for isolating rabbit atrioventricular node myocytes which retain normal morphology and function. Am J Physiol 265: H755-766.

Varma DR, Deng XF (2000). Cardiovascular alpha-1 adrenoceptor subtypes: functions and signalling. Can J Physiol Pharmacol 78: 267-292.

This work was funded by the British Heart Foundation (PG/08/104 and PG/11/97).

Where applicable, the authors confirm that the experiments described here conform with The Physiological Society ethical requirements.

PC33

Effect of global and local changes of intracellular pH on spontaneous Ca^{2+} waves in rat ventricular myocytes

K.L. Ford[1], E.L. Moorhouse[1], M. Bortolozzi[2] and R.D. Vaughan-Jones[1]

[1]Physiology, Anatomy and Genetics, University of Oxford, Oxford, UK and [2]Department of Physics G.Galilei, University of Padua, Padua, Italy

Acidosis, as found in myocardial ischaemia, potentially triggers arrhythmogenic Ca^{2+} signalling[1], with clinical implications. Here we characterise the effect of reducing pH_i on Ca^{2+} waves in rat isolated ventricular myocytes.

Ca^{2+} waves (induced by raising Ca^{2+}_o from 1 to 5 or 7.5mM) were imaged confocally with AM-loaded fluo-3 (linescan, 37°C). Parallel measurements of pH_i were made in cSNARF-1 AM-loaded cells. pH_i was reduced (up to 0.8 units) by superfusion of 80mM acetate. Results are mean±SEM, *P* values calculated using a paired Student's *t* test unless otherwise stated.

Reducing pH_i first suppressed (16±6% of control after 20s; $P<0.0001$, n=18) then increased (360±62% after 60s; $P=0.0002$, n=18) wave frequency. Inhibiting the sarcolemmal Na^+/H^+ exchanger (NHE; 30μM 5-(N,N-dimethyl)amiloride[2]) attenuated the secondary increase, as after 60s frequency recovered to only 61±22% ($P=0.0023$; n=11). An increase in wave velocity after 60s was seen with (140±3%; $P<0.0001$, n=17) and without (126±6%; $P=0.002$, n=10) NHE activity. These data agree with a previous report[3]. A decrease in pH_i for ≥60s slowed wave relaxation (time constant $\tau_{control}$=87±3ms, $\tau_{acetate}$=97±2ms; $P=0.02$, one-way ANOVA, n=6).

Local effects of pH_i on Ca^{2+} waves were studied by inducing a spatial pH_i gradient in a myocyte (by microperfusing two parallel solution streams perpendicular to the cell using a double-barrelled glass micropipette[4]). One half of the cell was superfused with normal Tyrode, the other with 80mM acetate (both containing 7.5mM Ca^{2+}). This produced a stable longitudinal pH_i gradient (pH_i 6.6 to 7.3). With NHE inhibited, a decrease in wave frequency (31±7% of control; $P<0.05$, n=13) was seen in the acidic microdomain and an increase (164±25%; $P<0.05$, n=13) in the more alkaline microdomain. Conversely, wave velocity was increased (118±5% of control; $P<0.05$, n=6) and decreased (85±4%; $P<0.05$, n=6) in acidic and alkaline microdomains respectively. Thus, wave properties map onto a spatial gradient of pH_i, indicating that pH-dependent control of Ca^{2+} waves is a locally regulated phenomenon.

Computational modelling of Ca^{2+} waves[5] suggests that a slowing of wave decay may reflect SERCA (sarco/endoplasmic reticulum Ca^{2+}-ATPase) inhibition. Although the acute effect of SERCA inhibition is to increase wave velocity (by extending the diffusibility of cytoplasmic Ca^{2+}), at steady-state, however, a decrease in wave velocity is predicted due to a fall in sarcoplasmic reticulum Ca^{2+} content (a factor that affects ryanodine receptor opening probability). This suggests that other H^+-targeted sites may be involved in the observed increase.

We conclude that spatial pH_i heterogeneity elicits multiple localised effects on Ca^{2+} signalling, suggesting that it may contribute to the heterogeneity of Ca^{2+} signalling observed in myocardial ischaemia.

Orchard CH, Houser SR, Kort AA, Bahinski A, Capogrossi MC, Lakatta EG. (1987) *J Gen Physiol* **90**:145-65

Kleyman TR & Cragoe EJ Jr. (1988) *J Membrane Biol* **150**:1-21

Dilworth E, Balnave C, Vaughan-Jones RD. (2003) *J Physiol* **551P**, PC27

Spitzer KW, Ershler PR, Skolnick RL, Vaughan-Jones RD. (2000) *Am J Physiol Heart Circ Physiol* **278**:H1371-H1382

Swietach P, Spitzer KW, Vaughan-Jones RD. (2010) *Front Biosci* **15**:661-680

Funded by the BHF and Wellcome Trust.

Where applicable, the authors confirm that the experiments described here conform with The Physiological Society ethical requirements.

PC34

Atrioventricular nodal dysfunction in the monocrotaline rat model of pulmonary arterial hypertension

I.P. Temple, G.M. Quigley, O. Monfredi, T.T. Yamanushi, V.S. Mahadevan, G. Hart and M.R. Boyett

Medicine, University of Manchester, Manchester, greater manchester, UK

Introduction
Patients with pulmonary arterial hypertension (PAH) have a high incidence of arrhythmias including AV node dysfunction. We investigated the mechanisms of AV node dysfunction in PAH using an animal model.
Hypothesis
We hypothesized that PAH in monocrotaline (MCT) treated rats would result in impairment of AV nodal function as evidenced by changes in Wenckebach cycle length, AV effective refractory period (AVERP) and AV functional refractory period (AVFRP).
Methods
An intraperitoneal injection of MCT (60mg/kg) was given to 200g Wistar rats. The rats were monitored daily and the MCT treated rats were sacrificed if they showed clinical deterioration, or on day 28. Control rats were injected with an equal volume of saline and were sacrificed within 24 hours of the paired MCT treated rats. An ECG was recorded and Echocardiography was performed to record pulmonary artery acceleration time (PAAT), pulmonary artery deceleration (PAD), right ventricle (RV) chamber size and wall thickness immediately prior to sacrifice. The heart was excised and mounted on a Langendorff perfusion column. Baseline ECGs were recorded then the right atrium was stimulated using an S1-S1 protocol to deter-

mine Wenckebach cycle length, and an S1-S2 protocol to determine AVERP and AVFRP.

Results

Echocardiography demonstrated PAH and RV hypertrophy in the MCT treated rats with a decrease in PAAT and an increase in PAD and RV wall thickness. The MCT treated rats had a reduction in AV node function with an increase in AVERP; demonstrating reduced safety of conduction across the AV node, and an increase in AVFRP, demonstrating reduction in the maximum speed of conduction through the AV node (Table 1).

Conclusions

These data suggest that remodelling takes place within the AV node in response to PAH, which may account for conduction disturbances.

Table 1. Echocardiographic and AV node function parameters in control and MCT treated rats. Data were analysed using unpaired Student's t-test

	Control rats (mean ± SD)	MCT treated rats (mean ± SD)
Echocardiographic measurements		
PAAT (ms)	34 ± 3 (n=10)	16 ±2 (n=9)**
PAD (ms-2)	15 ±2 (n=10)	32 ±4 (n=9)**
RV chamber size (systole) (cm)	0.09 ±0.01 (n=10)	0.14 ±0.01 (n=9)**
RV chamber size (diastole) (cm)	0.30 ±0.03 (n=10)	0.35 ±0.04 (n=9)
RV wall thickness (systole) (cm)	0.13 ±0.01 (n=10)	0.16 ±0.01 (n=9)*
RV wall thickness (diastole) (cm)	0.13 ±0.02 (n=10)	0.22 ±0.04 (n=9)*
AV node function		
In vivo PR interval (ms)	45 ±1 (n=16)	47 ±1 (n=16)
Langendorff PR interval (ms)	43 ±1 (n=11)	44 ±1 (n=12)
Wenckebach cycle length (ms)	112 ±2 (N=12)	116 ±3 (n=12)
AVERP (ms)	87±1 (n=12)	94 ±2 (n=11)*
AVFRP (ms)	115 ±2 (n=12)	122 ±2 (n=11)*

PAAT=pulmonary artery acceleration time, PAD=pulmonary artery deceleration, AVERP=atrioventricular effective refractory period, AVFRP=atrioventricular functional refractory period, *p<0.05, ** p<0.005.

Koskenvuo JW et al. (2010). Int J Cardiovasc Imaging 26:509-518.

Where applicable, the authors confirm that the experiments described here conform with The Physiological Society ethical requirements.

PC35

Changes in calcium homeostasis caused by a cardiotoxic drug

F.E. Mason[1], D.A. Eisner[1], M. Morton[2], C. Pollard[2] and A.W. Trafford[1]

[1]Cardiovascular Research, University of Manchester, Manchester, UK and [2]AstraZeneca, Macclesfield, UK

Introduction The movements of intra-cellular calcium (Ca) must be fine-tuned in the heart, in order for it to function normally. Disregulation of Ca handling is well known to underlie arrythmogenic activity and contractile dysfunction. We are investigating changes in cellular calcium homeostasis which occur upon the acute application of cardiotoxic drugs. The anti-psychotic clozapine is being used as a model

of such a drug (previously associated with cases of myocarditis, arrhythmia and sudden cardiac death). Such in vitro analysis may highlight important drug-screening targets for the future.
Methods Rat ventricular myocytes were isolated and stimulated under voltage clamp, inducing systolic Ca transients. Cytosolic calcium was measured using the Ca-sensitive indicator fluo3-AM or FURA-2. Sarcoplasmic reticulum (SR) Ca content was quantified by application of 10 mM caffeine. Rates of decay of calcium transients were used to assess calcium extrusion from the cytosol, by the sarco-endoplasmic reticulum calcium ATP-ase (SERCA) and by sarcolemmal pathways. In order to detect any direct effect of clozapine on ICaL, a step voltage protocol was used to assess changes in the current-voltage (IV) relationship. Phospholamban knockout mice (PLN-KO) were used to ascertain whether effects of the drug on SERCA were phospholamban-dependent.
Results 10 μM clozapine significantly reduces peak ICaL (mean reduction 49.7% S.E.M. 1.8%, $p < 0.001$, one way RM ANOVA, n=20). Ca transient amplitude is also significantly reduced (mean reduction 47.7% S.E.M. 2.5%, $p < 0.001$, one way RM ANOVA, n=19). 10 μM clozapine significantly reduces SR calcium content (mean reduction 14.7% S.E.M. 4.7%, $p < 0.001$, student's t-test, n=11) and SERCA activity (mean reduction 30.5% S.E.M. 2.6%, $p < 0.001$, one way RM ANOVA, n=18). IV results support the findings that 10 μM clozapine significantly and directly affects ICaL. Results from PLN-KO mice show that the effect of clozapine on SERCA is not phospholamban-dependent.
Discussion Overall, clozapine's most noticeable effect is a reduction of peak ICaL, which we speculate could increase the risk of arrhythmogenic activity in the whole heart by introducing refractory heterogeneity. Current work is focusing on the effects of clozapine on calcium spark activity in the quiescent cardiac myocyte.

This work is funded by the Medical Research Council (MRC) and AstraZeneca

Where applicable, the authors confirm that the experiments described here conform with The Physiological Society ethical requirements.

PC36

P21 activated kinase-1 deficiency in cardiomyocytes increases in susceptibility to ventricular arrhythmogenesis in mice

Y. Wang[1], H. Tsui[1], W. Liu[1,2], Y. Shi[3], R. Wang[3], Y. Zhang[1], R. Solaro[4], Y. Ke[4], H. Zhang[5], E. Cartwright[1], X. Wang[2] and M. Lei[1]

[1]Cardiovascular Research Group, School of Biomedicine,, University of Manchester, Manchester, UK, [2]Faculty of Life Sciences & Manchester Academic Health Sciences Centre, University of Manchester, Manchester, UK, [3]Department of Cardiovascular Medicine, Union Hospital, Wuhan, China, [4]Department of Physiology and Biophysics and Centre for Cardiovascular Research,, University of Illinois, Chicago, IL, USA and [5]School of Physics and Astronomy,, University of Manchester, Manchester, UK

Our recent studies indicate a novel role of P21 activated kinase-1 (Pak1) in regulating cardiac electrical and contractile functions. This following-up study thereby aims at further clarify the mechanisms underlying the critical roles of Pak1 in regulating cardiac electrical function and ventricular arrhythmogenesis under stress conditions in mice with genetic modifications of Pak1. Mice carrying a ventricular cardiomyocyte-restricted deletion of Pak1 (Pak1cko) displayed relative high intrinsic heart rate with normal electrocardiography (ECG) parameters including P-R, QRS and QT intervals at baseline condition compared with control Pak1f/f mice. To evaluate ventricular arrhythmic vulnerability, both Pak1cko and Pak1f/f (control) mice were subjected to either acute treatment of isoprenaline (ISO) at in vivo condition in anesthetised mice (1 mg/kg, i.p) with 1.5-2% isoflurane in oxygen, ex vivo heart (10 -50 nM) or chronic treatment by mini-osmotic pumps (Charles river labs, UK) at concentration 100 mg/ml ISO per gram of mouse for the 14 day pump. For in vivo ECG recordings, three-lead limb ECGs were recorded through subcutaneous 27 gauge needle electrodes using a Powerlab 26T system (AD Instruments, Hastings, UK). The resulting digital recordings (16 bit, 2 kHz/channel) were analyzed using the Chart version 5.0 program (AD Instruments) to obtain the signal-averaged ECG. T-wave durations and QT intervals were measured in lead II attached were placed on three of the four limbs. The ex vivo heart studies involve ECG recorded by ECG electrodes (Harvard Apparatus (UK) Ltd, Cambridge, UK) positioned onto atrial and ventricle with Chart version 5.0 program. Two programmed electrical stimulation (PES) protocols were processed to the hearts, 1). Ventricular effective refractory period was determined by S1S2 pacing that begin with a drive cycle of 100 ms with an S2 coupled at 100 ms and bring in S2 by 1 ms until there is loss of ventricular capture. 2). Ventricular burst pacing (S1S1 pacing) deliver ventricular pacing with three trains of 20 S1 at a cycle length of 100 ms with a pause of one second in between trains. Then repeat the protocol with shortened cycle length from 100ms to 30ms by 10ms step. Followed by programmed electrical stimulation (PES), electrocardiographic analysis of both anesthetized and conscious animals revealed a high occurrence of ventricular arrhythmias such as multiple episodes of ventricular tachycardia (VT) or ventricular fibrillation (VF) in Pak1cko

mice but not in control Pak1f/f littermates. Action potentials (APs) recorded from ventricular myocytes isolated from and Pak1cko and Pak1f/f hearts, a delayed afterdepolarization (DAD) type AP and spontaneous APs can be observed from PAK1cko myocytes, but not control Pak1f/f myocytes. Thus our study suggests a crucial role of Pak1 signalling in preventing stress associated ventricular arrhythmogenesis.

Where applicable, the authors confirm that the experiments described here conform with The Physiological Society ethical requirements.

PC37

Endurance training in heterozygous desmoglein-2 mutant mice reveals an arrhythmogenic right ventricular cardiomyopathy-like phenotype

L. Fabritz[1], L. Fortmueller[2], S. Sakhtivel[2], F. Syeda[1], P. Kirchhof[1], R. Leube[3] and C. Krusche[3]

[1]University of Birmingham, Birmingham, UK, [2]University Hospital Muenster, Muenster, Germany and [3]RWTH Aachen University, Aachen, Germany

Arrhythmogenic right ventricular cardiomyopathy (ARVC) is a rare cardiomyopathy but significantly contributes to sudden cardiac death in young otherwise healthy patients, especially endurance athletes. 5-10% of patients with ARVC harbour mutations in the extracellular domains of the desmoglein (DSG) 2 gene. To assess the role of DSG2 in ARVC pathomechanism, mice lacking exons 4-6 of the endogenous DSG2 gene (DSG2mt) were generated. Homozygous DSG2mt/mice developed dilatation of ventricles and pronounced fibrosis. Heterozygous DSG2mt/wt mutants did not show such morphological alterations.
Objective: To study whether physical exercise provokes a cardiac phenotype in DGSwt/mt mice, they were subjected to endurance training and compared with wild-type (WT) littermates.
Methods/Results: Group swimming training sessions were performed 6 times a week, starting with 5 minutes and gradually incrementing to 90 minutes per day for 7 weeks. Echocardiography was performed before and after training, on mice anaesthetised with 2% isoflurane + oxygen, using a small animal ultrasound unit. Right ventricular (RV) diameters were increased in DSG2wt/mt both compared to pre-training, and compared to WT after training. Right ventricular function was also decreased after training compared to pre-training and compared to WT littermates (see table for values, $^{*}p<0.05$, d= diastolic, s= systolic, lav= long axis view, sav= short axis view, FAC= fractional area shortening, HR= heart rate). Neither left ventricular diameters nor function differed between DSG2wt/mt and WT littermates.
Electrophysiological studies in isolated Langendorff DSGwt/mt and Wt hearts from mice terminally anaesthetised with urethane (2mg/kg) showed comparable ventricular action potential duration and effective refractory periods. DSG2 mutation correlated with increased arrhythmia inducibility after endurance training. Ven-

tricular arrhythmias were induced by a single extrastimulus during right ventricular stimulation in 5 of 8 DSG2wt/mt, but in none of the 7 WT hearts (p=0.03).
In conclusion, endurance training reveals an ARVC-like phenotype in otherwise healthy and morphologically inconspicuous DSG2wt/mt mice presenting right ventricular dilation, decreased right ventricular contractility, and increased inducibility of ventricular arrhythmias during right ventricular pacing.

genotype	WT	DSG2 mt/wt
n (females/males)	8 (6/2)	9 (7/2)
HR (bpm)	424±6	435±7
RVlav d (mm^2)	3.67±0.20	4.29±0.28*
RVsav d (mm^2)	4.76±0.28	6.26±0.29*
RVsav s (mm^2)	2.10±0.26	3.50±0.25*
RV FAC (%)	55±4	44±3*
Age (weeks)	21±0.2	21±0.2
Weight (g)	24.3±0.7	25.5±1.6

Where applicable, the authors confirm that the experiments described here conform with The Physiological Society ethical requirements.

PC38

Diminished SR function and adrenergic response co-associate in the ageing sinoatrial node

F.S. Hatch[1], M.K. Lancaster[2] and S.A. Jones[1]

[1]Biological Sciences, University of Hull, Hull, UK and [2]Faculty of Biological Sciences, University of Leeds, Leeds, UK

The Sarcoplasmic Recticulum (SR) plays a vital role in the activity of the sinoatrial node (SAN). Alterations in the expression and/or function of the proteins involved in SR calcium homeostasis with age could affect pacemaking and predispose to arrhythmias. During ageing there is a decline in response to stress partially due to a diminished response to adrenergic stimuli. Our hypothesis was that these age-associated problems may, at least in part, be explained by changes in SR function. Male Wistar rats at the ages of 6 months (young), 12 months (adult) and 24 months (old) (n=5 per group) were sacrificed by anaesthetic overdose via intraperitoneal injection. The SAN region of the heart was removed and intrinsic pacemaker activity recorded in bicarbonate-buffered saline at 37°C, under control conditions and in the presence of 3μM cyclopiazonic acid (CPA) to inhibit the sarcoendoplasmic reticulum ATPase pump (SERCA2a). Incrementing concentrations of isoprenaline (1nm, 10nm, 100nm and 1μm) assessed adrenergic response in the presence and absence of CPA. Western blot and immunocytochemistry measured expression of SERCA2a, phospholamban (PLB) and ryanodine receptors (RYR2). Data are mean±SEM percentages relative to the average young control values, compared by ANOVA with Holm-Sidak post-hoc tests ($P<0.05$).
Isoprenaline (Iso) significantly increased the heart rate (young 100±3.3% vs. 139±4.9% in 1μm Iso: old 78±4.9% vs. 135±7.2% in 1μm Iso; $p<0.05$). The EC50 for

Iso was significantly greater in old animals (24±3nM) than young (10±2nM). CPA caused significant pacemaker slowing (in the young reduction of 49±9bpm), but had a lower effect in the old (25±4bpm; $p<0.05$). In CPA there was no longer a difference in the EC50 for Iso between ages (mean 18±4nM).
An age-associated decrease in conduction velocity was observed with age (young 100±2.2%; old 83±1.8%; $p<0.05$), however CPA had no affect on conduction at any age. Whereas Iso significantly increased conduction (Iso 1μm young 207±9% vs. old 122±1.1%; $p<0.05$). Young animals showed increased conduction velocity in low dose Iso, while only the maximum dose resulted in a significant increase in conduction within the old age group.
SAN protein expression of SERCA2a, PLB and RYR2 was decreased in the old compared with the young (SERCA2a young 100±10.7% vs. old 60±10.4%; $P<0.05$: PLB young 100±10.8% vs. old 64±10.7%; $P<0.05$: RYR2 young 100±10.2% vs. old 68±15.3%; $P<0.05$). Similar decreases in expression of SERCA2a, PLB and RYR2 were observed in the right atria.
In conclusion the expression of SR calcium handling proteins within the SAN exhibit an age-associated decline coupled with an attenuated response to adrenergic stimulation in the old animal.

Where applicable, the authors confirm that the experiments described here conform with The Physiological Society ethical requirements.

PC39

MKK4 dysregulation contributes to age-related atrial structural remodelling and arrhythmias

J. Jin[1], L. Davies[1], V. Christoffels[2], U. Ravens[3], Y. Shi[4], J. Wu[4], E. Cartwright[1], X. Wang[1] and M. Lei[1]

[1]Manchester University, Manchester, UK, [2]University of Amsterdam, Amsterdam, Netherlands, [3]Dresden University of Technology, Dresden, Germany and [4]Huazhong University of Science and Technology, Wuhan, China

Atrial fibrillation (AF) is the most common form of sustained arrhythmia, its incidence increases with age and it is associated with extensive atrial remodelling. The mitogen activated protein kinase cascade (MAPK) is implicated in regulating the pathogenesis of AF. MAPKs regulate fibrosis in the ventricle in aged/hypertrophied hearts. Fibrosis is associated with cardiac arrhythmias, including AF. To establish the role of the MAPK pathway in atrial function in ageing, we have developed an atrial specific conditional knockout (ACKO) mouse model where a central component of this pathway; MKK4, has been specifically deleted from the atria using the Cre-Loxp system.
To determine effect of MKK4 deficiency on atrial electrical function, surface ECG was performed on MKK4f/f and MKK4ACKO mice anesthetized with isoflurane (2.5%) and the recordings were examined. With age, MKK4 atrial-knock outmice (MKK4ACKO) became more susceptible to atrial arrhythmias with characteristic

slow atrial conduction comparing with MKK4F/F mice. In parallel, an increased interstitial fibrosis, up-regulated TGF-β1 signalling and dysregulation of matrix metalloproteinases and their inhibitory enzymes were observed in the atrium of MKK4ACKO mice in contrast to control MKK4F/F mice. Knockdown MKK4 in in-vitro cultured cardiomyocytes led to a more sensitivity to Ang-II stimulation induced TGF-β1 signaling activation, such change in turn enhances paraocrine expression of profibrotic molecules in cultured cardio-fibroblasts, suggesting a cross-talk between two cell types on profibrotic signaling. Further study in AF atrial tissue in human revealed an association of down-regulation of MKK4 and activation profibrotic signalling including a significant increase in expression of col1a1, col3a1, ctgf and downregulation of mmp2. Taken together, our results for the first time have established a critical role of MKK4 in age-related atrial structural remodeling associated with AF. As a negative regulator of TGF-β1 profibrotic signaling pathway, MKK4 is therefore likely to be a new molecular therapeutic target for developing anti-AF drugs.

Where applicable, the authors confirm that the experiments described here conform with The Physiological Society ethical requirements.

PC40

The effects of sympathetic nerve stimulation on cardiac ventricular electrophysiology in long QT syndrome 1 in the innervated guinea pig heart

K.E. Brack, A. Gupta and G. Ng

Cardiovascular Sciences, University of Leicester, Birmingham, Please Select, UK

Introduction: Congenital long QT syndrome 1 (LQTS1) arises from a reduced activity of the slow activating delayed rectifier potassium channel (IKs). Ventricular arrhythmias occur along with increases in sympathetic tone, which can cause sudden cardiac death (SCD). Mechanisms underlying SCD are not understood but may involve changes in ventricular electrophysiology including electrical restitution (RT) – the relationship between action potential duration and diastolic interval. The aim was to develop the innervated heart preparation in the guinea pig and examine the effects of sympathetic nerve stimulation (SNS) on effective refractory period (ERP) and inducibility of ventricular fibrillation (VF) in a pharmacological model of LQTS1. Methods: After anaesthesia (Urethane, 2.5g/kg) was achieved, the decentralised isolated Langendorff perfused innervated heart preparation from adult male guinea pigs (n=6, 450-550g) was prepared. Animals were killed with pentobarbitone (160mg/kg, iv) and the preparation was perfused via the aorta in constant flow. The innervated heart preparation from adult male guinea pigs (n=6, 450-550g) were used. ERP was measured using an extrastimulus protocol whilst the inducibility of VF was assessed with ventricular fibrillation threshold (VFT) during burst pacing. The parameters were measured at baseline (BL) and with SNS (3Hz, 1V) dur-

ing control and in the presence of the IKs blocker HMR1556 to mimic LQTS1. Data are mean±SEM, analysed using paired Student's T-Test.
Results: During control, SNS significantly reduced ERP and VFT (Table, P<0.05 * vs. BL, ~ vs. Control). In the presence of HMR1556, the effects of SNS on ERP and VFT were augmented whilst the effect on RT was abolished.
Conclusion: SNS increases susceptibility to VF which appears to be augmented in this pharmacological LQTS1 model and maybe related to changes in ERP.

	Control			HMR 1556		
	BL	SNS	Change	BL	SNS	Change
ERP (ms)	104 ±5	92 ±5*	-12 ±1	130 ±4	101 ±3*	-29 ±6~
VFT (mA)	4.2 ±1.2	2.9 ±0.9*	-1.42 ±0.5	4.2 ±1.1	1.3 ±0.5*	-3.2 ±1.1~

KEB is supported by a British Heart Foundation Fellowship

Where applicable, the authors confirm that the experiments described here conform with The Physiological Society ethical requirements.

PC41

Sodium-dependent background current in cells from the rabbit atrioventricular node

H. Cheng[1], C.H. Orchard[1], M.R. Boyett[2] and J.C. Hancox[1]

[1]Physiology and Pharmacology, University of Bristol, Bristol, UK and [2]Cardiovascular Medicine, University of Manchester, Manchester, UK

The atrioventricular node (AVN) plays a critical role in normal cardiac conduction and can also take over pacemaking of the ventricles should the sinoatrial node fail. The cellular electrophysiological basis of AVN pacemaking is incompletely understood, although it is likely to involve multiple ionic conductances (Hancox *et al.*, 2003). This study aimed to characterise for the first time sodium-dependent background inward current in rabbit AVN cells. Adult male New Zealand White rabbits were killed in accordance with UK Home Office legislation and AVN cells were isolated as described previously (Hancox *et al.*, 1993). Whole-cell voltage-clamp using step and ramp protocols was used to record the background current, after the Ca^{2+}, K^+, Na^+-K^+ pump and Na^+-Ca^{2+} exchange currents were inhibited by appropriate blockers (Hagiwara *et al.*, 1992). External solutions were as follows: *150mM-Na^+ (mM)*: 150 NaCl, 5 HEPES, 2 CsCl, 2 $NiCl_2$, 1 $BaCl_2$, 1 $MgCl_2$, 0.01 Strophanthidin; *Tris Na^+-free*: Na^+ replaced with equi-molar Tris-hydrochloride. The *pipette solution* contained (mM): 120 CsOH, 20 CsCl, 5 HEPES, 10 EGTA, 5 K_2-creatine phosphate, 5 Mg-ATP, 2 $MgCl_2$, 100 Aspartic acid. Changing the bath solution from Tris Na^+-free to 150 mM-Na^+ induced an inward current, and the slope conductance at -50 mV increased from 0.54±0.03 to 0.91±0.05 nS (mean±S.E.M; n=61 cells). The Na^+-dependent inward background current density obtained by subtracting the current in Tris Na^+-free from that in 150 mM-Na^+ solution was -0.82±0.05 pA/pF at -50 mV (n=61). When a range of external Na^+ concentrations ($[Na^+]_o$) between

30-200 mM was applied, the background current amplitude varied in proportion to $[Na^+]_o$ (n=8). When external Na^+ was replaced with various monovalent cations, the background current (measured at -100 mV) amplitude increased in the order: $Li^+<Na^+<Cs^+<K^+<Rb^+$ (n=7). The Na^+-dependent background current was partially inhibited by cation channel blocker SKF-96365 (10 μM produced ~32.1±5.3% inhibition at -100 mV; n=8, $P<0.01$). We conclude that a Na^+-dependent background inward current exists in rabbit AVN cells and that the channels mediating this current exhibit poor cation selectivity.

Hancox JC, Levi AJ, Lee CO & Heap P (1993). A method for isolating rabbit atrioventricular node myocytes which retain normal morphology and function. *Am J Physiol* 265, H755-766.

Hancox JC, Yuill KH, Mitcheson JS, Convery MK (2003). Progress and gaps in understanding the electrophysiological properties of morphologically normal cells from the cardiac atrioventricular node. *Int J Bifurcation and Chaos* 13, 3675-3691.

Hagiwara N, Irisawa H, Kasanuki H, Hosoda S (1992). Background current in sinoatrial node cells of the rabbit heart. *J Physiol* 448, 53-72.

This work was funded by the British Heart Foundation (PG/11/24).

Where applicable, the authors confirm that the experiments described here conform with The Physiological Society ethical requirements.

PC42

Pro-arrhythmic effects of the electrical coupling between fibroblasts and myocytes in mouse atrium

W. Shen[1], X. Wang[2], M. Lei[3] and H. Zhang[1]

[1]Biological Physics Group, University of Manchester, Manchester, UK, [2]Faculty of Life Sciences, University of Manchester, Manchester, UK and [3]Cardiovascular Research Group, University of Manchester, Manchester, UK

Cardiac fibroblasts are by number the largest component of the non-myocytes, providing structural support for the heart by regulating the synthesis and degradation of extracellular matrix components. Previous experimental studies suggested that there is electrical coupling between fibroblasts and cardiac myocytes (Gaudesius et al. 2003). The aim of this study was to use computational models to investigate the functional impacts of the electrical coupling between fibroblasts and myocytes on mouse atrial tissue vulnerability to the genesis of reentrant excitation waves. Based on extant voltage-clamp data on the kinetics and current densities of mouse atrial membrane ionic channels (I_{Na}, I_{CaL}, I_{NaCa}, I_{to}, I_{K1}, I_{Kur}, I_{Ks}) and intracellular Ca^{2+} dynamics, we developed a novel biophysically detailed mathematical model for simulating the electrical action potential of a mouse atrial cell. The model was validated by its ability to reproduce the experimentally measured physiological characteristics of a mouse atrial myocyte, including the resting potential, action potential amplitude, action potential duration and its rate-dependence). The developed atrial cell model was then coupled to a passive or an active fibroblast model

(MacCannell et al. 2007) with one myocytes being coupled to one to ten fibroblasts. The coupled fibroblast-myocyte single cell model was then incorporated into 1D and 2D multi-cellular tissue models. Our simulation data suggested that at the single cell level, myocyte-fibroblast coupling elevates myocyte resting potential and prolongs its action potential duration (APD), which are monotonically increased with the increased number of fibroblasts. It enhances the supernormal excitability of atrial cells reflected by a larger APD at high pacing rates than at low pacing rates. At the 1D tissue level, the fibroblast-myocyte coupling reduces the conduction velocity of excitation waves, but reduced the width of a time window during which a premature stimulus may evoke unidirectional conductional block. At the 2D tissue level, regions of coupled fibroblast-myocytes disturb the excitation wavefront, leading to formation of re-entrant excitation wave in response to a series of rapid stimulus. In conclusion, the electrical coupling between fibroblast and myocytes disturbs cardiac conduction, facilitating the formation of re-entrant excitation wave that is pro-arrhythmic.

Gaudesius, G., M. Miragoli, et al. (2003). "Coupling of cardiac electrical activity over extended distances by fibroblasts of cardiac origin." Circ Res 93(5): 421-428.

MacCannell, K. A., H. Bazzazi, et al. (2007). "A mathematical model of electrotonic interactions between ventricular myocytes and fibroblasts." Biophys J 92(11): 4121-4132.

Where applicable, the authors confirm that the experiments described here conform with The Physiological Society ethical requirements.

PC43

Ionic mechanisms underlying the difference in the pacemaking action potentials of the rabbit and the murine sinoatrial node cells

R. Wang[1], X. Wang[2], M. Lei[3], M. Boyett[3] and H. Zhang[1]

[1]Biological Physics Group, The University of Manchester, Manchester, UK, [2]Faculty of Life Sciences, The University of Manchester, Manchester, UK and [3]Cardiovascular Research Group, The University of Manchester, Manchester, UK

Previous studies have shown dramatic species-differences in the pacemaking action potentials of the rabbit and murine sinoatrial node (SAN) cells, with the latter having much faster pacemking rate (189 vs 294 beats/min), greater upstroke velocity (2.66 vs 9.21 V/s) but shorter action potential duration (169.60 vs 57.66 ms). However, the ionic mechanisms underlying such species-differences in cardiac pacemaking action potentials are unclear. This study aimed to investigate the ionic basis responsible for the differences in the rabbit and murine pacemaking action potentials by using computer models. The biophysically detailed computer models for the rabbit (Zhang et al., 2000) and murine (Kharch et al., 2011) SAN cells were used to investigate the functional impacts of experimentally observed differences in the kinetics and current densities of individual ionic channels between rabbits and mice on their action potentials. Simulation results suggested that the difference in the

pacemaking action potentials can be attributable to the differences in the I_{Na}, I_{CaL}, I_{CaT}, I_f, and I_{Kr} between the two species. Specifically, the faster pacemaking rate in the murine SAN cells is due to its greater density of I_{Na}, I_{CaT}, and I_f, among which I_{Na} plays a key role. The shorter APD in the murine SAN cells is due to the integral action of its larger I_{CaL} and I_{Kr}. The faster upstroke velocity in the murine SAN action potentials can be accounted for by the integral effect of its larger I_{Na}, I_{CaL}, I_{CaT} and I_f. In conclusion, this study provides mechanistic insights towards understanding the ionic basis underlying the species-difference in the pacemaking action potentials of the rabbit and murine SANs.

Kharche, S., J. Yu, et al. (2011). "A mathematical model of action potentials of mouse sinoatrial node cells with molecular bases." Am J Physiol Heart Circ Physiol 301(3): H945-963.

1) Zhang, H., A. V. Holden, et al. (2000). "Mathematical models of action potentials in the periphery and center of the rabbit sinoatrial node." Am J Physiol Heart Circ Physiol 279(1): H397-421.

Where applicable, the authors confirm that the experiments described here conform with The Physiological Society ethical requirements.

PC44

Development of a one-dimensional whole heart model for rabbit

S.J. Castro[1], J. Higham[1], A.V. Holden[2], M.R. Boyett[1] and H. Zhang[1]

[1]University of Manchester, Manchester, UK and [2]University of Leeds, Leeds, UK

The electrical excitation of the heart is first initiated by the sinoatrial node, and then spreads along the cardiac conduction system and throughout the ventricles. The propagation of electrical activity throughout the heart can be characterised by a one-dimensional (1D) model of the cardiac tissue along its major conduction pathway. This approach offers further insight into cardiac electrical excitation conduction than the standard single cell models, but without the computational demands of a higher dimension anatomical model. In this study, we have developed a 1D computational model for the rabbit whole heart with considerations to the intrinsic electrical heterogeneity of cardiac tissue from the sinoatrial node (SAN) to the left ventricular wall. The 1D whole heart model accounts for the heterogeneous nature of cardiac tissue, incorporating well established single cell models for SAN (Zhang et al. 2000), atrial muscle (Aslanidi et al. 2008), atrio-ventricular node (AVN) (Inada et al. 2009), and Purkinje fibre (PF) and left ventricular tissue (Aslanidi et al. 2010). The cells were coupled together into a single strand using the monodomain equation. The model also considered the fast and slow conduction pathways of the AVN. The choice of gap junctional conductance values for each distinctive region of tissue in the 1D model was validated by reproducing the corresponding conduction velocities of the excitation wave and matching them to experimental data. The developed model was used to simulate the effects of ionic channel blockers, such as TTX, Nifedipine and Ivabradine (blocking I_{Na}, $I_{Ca,L}$, and I_f

respectively) on a simulated ECG. Blocking I_{Na} caused the PP interval, PR interval and QRS duration to increase in a dose-dependent manner, which was accompanied by a slight increase in QT interval (< 5%). 70% block of I_{Na} caused Purkinje-ventricular junction block, subsequently abolishing the QRS complex. Blocking $I_{Ca,L}$ by a low percentage did not alter the PP, RR and QRS intervals; however, a 70% block of $I_{Ca,L}$ caused His-Purkinje fibre block, and higher $I_{Ca,L}$ block caused the leading pacemaker site to shift to the atrio-ventricular node (AVN). QT interval and T wave dispersion both increased with $I_{Ca,L}$ block. For block of I_f, the PP and RR intervals showed a small prolongation (~7 ms / 10% block), and the QT interval was slightly increased (~5 ms at 100% block of I_f), otherwise no significant changes were observed. These simulations were quantitatively comparable to experimental data obtained from Langendorff whole heart preparations with applications of TTX, Nifedipine and Ivabradine. In conclusion, a 1D whole heart model for the rabbit has been developed, providing a time-efficient way of studying cardiac excitation wave conduction and actions of anti-arrhythmic drugs.

Aslanidi OV *et al.* (2008). *Conf Proc IEEE Eng Med Biol Soc* **2008**, 141-4

Aslanidi OV *et al.* (2010). *Biophys J* **98**, 2420–2431

Inada S *et al.* (2009). *Biophys J* **97**, 2117–2127.

Zhang H *et al.* (2000). *Am J Physiol Heart Circ Physiol* **279**, H397–421.

This work is supported by EPSRC.

Where applicable, the authors confirm that the experiments described here conform with The Physiological Society ethical requirements.

PC45

A methodological approach for the study of the cytoarchitecture of the sarcotubular membrane system in cardiac health and disease

C. Pinali, A.W. Trafford and A. Kitmitto

University of Manchester, Manchester, UK

Heart failure (HF) is responsible for the death of over 3.6 million people in Europe each year. HF has a poor prognosis with approximately 40% of patients dying within the first year of diagnosis (www.heartstats.org/) and has an increased prevalence and mortality in the aged. In Western countries it is estimated that by 2050 approximately a quarter of the population will be older than 60 and in some places the elderly may account for nearly 50% of residents (www.globalaging.org/waa2). Disruption of the transverse tubule (TT) membranes and Ca2+-signalling dysfunction are both associated with the development of HF. Our studies involve the application of advanced 3-D electron microscopy methods to investigate the ultrastructural features of cardiac myocytes in particular the dyadic cleft, formed by the TT and junctional sarcoplasmic reticulum (jSR) membranes and map the changes that occur in HF. We have examined tissue from an ovine tachypacing model of

heart failure. Pacemakers were implanted under inhalational anaesthesia (1-3 % isoflurane) and analgesia (0.5 mg/kg meloxicam s/c). Sheep were humanely killed (pentobarbitone (200 mg/kg iv) and left ventricle samples were collected, cut to 2 mm3 size blocks immediately after animal expiration and immersed in primary fixative 2.5% glutaraldehyde 2% paraformaldehyde 2.5mM CaCl2 in 0.1M sodium cacodylate buffer pH 7.2. Blocks were cut to size for mould embedding and left in the primary fixative for 3 hrs followed by 1.5 hrs post fixation in 1% OsO4 and 1.5% K4Fe(CN)6 or 2% OsO4 and 0.75% K4Fe(CN)6. Post fixation was followed by washes with water, dehydration in an ethanol ascending series and embedding in Taab low viscosity resin; 250 nm sections (according to interference colour chart) were cut on a Reichert microtome. To aid alignment and reconstruction 10 nm gold colloid particles (Sigma Aldrich) were added to sections. Single axis tilt series were collected between -70 and +70 degrees in one degree increments using a Polara FEG transmission electron microscope operated at 300 kV. Projections were aligned, reconstructed and segmented with IMOD (1). The nanoscale resolution of the 3-D tomograms permitted delineation of the TTs and SR membranes, including visualization of ryanodine receptor complexes localized to the dyadic cleft. Examination of myocytes from both control sheep and heart failure sheep has allowed morphological features of both health and disease states to be analysed in 3-D. Thus understanding the factors that precipitate HF at the cellular level will be pivotal for the development of new treatment strategies and is clearly a global healthcare priority.

Kremer, J.R., Mastronarde, D.N., McIntosh, J.R., 1996. Computer visualization of three-dimensional image data using IMOD. J. Struct. Biol. 116, 71–76

This work was supported by the British Heart Foundation (RG/11/2/28701).

Where applicable, the authors confirm that the experiments described here conform with The Physiological Society ethical requirements.

PC46

Autonomic regulation in the 3D human atria: insights from the development of a new computational model of the 3D human atria

M.A. Colman, M. Boyett and H. Zhang

University of Manchester, Manchester, UK

Sympathetic and parasympathetic regulation of the sinoatrial node (SAN) and atrial myocardium (AM) are associated with leading pacemaker site shits, rate variability, and changes to the effective refractory period (ERP) and Ca^{2+} transient magnitude, which are potentially linked to the genesis of atrial arrhythmias. In this study we present a realistic and biophysically detailed computer model for simulating the effect of isoprenaline (ISO) and acetylcholine (ACh) on the action potential (AP) and Ca^{2+} transient of newly developed human SAN and AM myocyte models. These are then incorporated into a 3D model of the human atria with realistic atrial

anatomy and SAN complex geometry (Aslanidi et al. 2011). The ISO model incorporates an independent phosphorylation approach (Heijman et al. 2011), which considers individual dose dependencies for each affected substrate. The model accurately reproduced experimental findings at saturating solutions of ISO that the AP in the AM demonstrates a significantly elevated plateau and Ca^{2+} transient, whereas the APD_{90} is not significantly changed. This is primarily due to a balance between increased I_{CaL} and I_{Kur} channels. At non-saturating solutions, there is no longer a balance between the up-regulation of these channels, and the APD is prolonged. It is also shown that the elevated Ca^{2+} transient increases the likelihood of Ca^{2+} and AP alternans. The spontaneous rate of the SAN cell model was increased by ISO. The model of ACh involved a new time dependent formulation of I_{KACh} and a negative shift in I_f. In the SAN, a reduction in I_{CaL} was also modelled as done in a previous study (Zhang et al. 2002). In the AM, ACh resulted in a significant shortening of the APD and reduced Ca^{2+} amplitude. In the SAN, a slowing of the pacing rate was observed. In 3D models, ISO resulted in leading pacemaker site shifts within the SAN and an increased pacing rate. It also increased the vulnerability to reentry when the model was paced at high rates. ACh also resulted in leading pacemaker site shifts and was associated with a slowing of the pacing rate and an increased propensity to SAN exit block at high concentrations: the decreased amplitude of the SAN AP combined with the greater repolarising current due to I_{KACh} in the AM resulted in a reduced ability of the SAN to drive the AM. ISO and ACh combined lead to different complex behaviour, such as a reduced pacing rate but increased ability to drive the surrounding AM. In conclusion, we have presented new and novel models of ISO and ACh in the 3D intact model of the human SAN and AM, providing a useful tool for underpinning the functional effects of sympathetic and parasympathetic regulation on atrial arrhythmia genesis.

Aslanidi *et al.* (2011). Prog Biophys Mol Bio **107**, 156–168.

Heijman *et al.* (2011). J Mol Cell Cardiol **50**, 863–871.

Zhang *et al.* (2002). J Cardiovasc Electrophysiol **13**, 465–474.

This work was supported by the EPSRC.

Where applicable, the authors confirm that the experiments described here conform with The Physiological Society ethical requirements.

PC47

Computational evaluation of heart failure-induced ionic channel remodeling on the transmural heterogeneity in the canine ventricle and Purkinje fibers

C. Li and H. Zhang

Biological Physics Group, The University of Manchester, Manchester, UK

Previous experimental studies have revealed that heart failure (HF) is associated with ionic channel remodelling, which may be pro-arrhythmic. The aim of this study

was to use biophysically detailed computer models of canine ventricular and Purkinje fibres to evaluate the functional impacts of HF-induced ionic channel remodellings on the transmural repolarisation heterogeneity within the ventricle wall and at the junction between ventricle and Purkinje Fibres (PVJ). The single cell models developed by Benson et al. (2008) for canine ventricular myocytes and by Aslanidi et al. (2010) for canine Purkinje fibre cells were used for this study. The two models were modified for simulating HF condition by incorporating extant experimental data on HF-induced remodellings on membrane ionic channels and intracellular Ca^{2+} handling. For ventricular cells, HF was simulated by increasing I_{NaL} by 30% as well as a 34% increase in its inactivation time (Maltsev et al. 2007), reducing I_{Na} by 32% (Maltsev et al. 2002), I_{to1} by 43%(Li et al. 2002), I_{K1} by 41.1% (Li et al. 2002), I_{Ks} by 30% (Li et al. 2002), and $I_{Na/K}$ by 42%. The steady-state activation curve of I_{CaL} was shifted by -7.64 mV, resulted in a 13% reduction in its current density. For the calcium handling mechanisms, I_{NaCa} was increased by 20% in HF cells along with the down regulation of I_{up} by 87.5%, I_{leak} by 34.6% and I_{rel} by 40%. These changes resulted in a ~60% reduction in peak $[Cai^{2+}]_i$, a ~24% increase in $[Cai^{2+}]_i$ resting and a slow diastolic decay of $[Cai^{2+}]_i$ which all matched to experimental observations (O'Rourke et al. 1999). For Purkinje fibre cell model, HF was simulated by reducing I_{Na}, I_{K1}, I_{to1}, I_{Ks}, I_{Kr}, I_{CaL} and I_{CaT} by 30%, 33%, 30%, 10%, 8%, 14.5% and 13% respectively. With the resulting cell models, it was shown that the HF-induced ionic channel remodelling produced a remarkable APD prolongation in the ventricular cells as compared to the control condition. The APD prolongation was heterogeneous across the transmural wall, with a ~30%, ~60% and ~30% APD increase for endocardial, mid-cardial and epi-cardial cells respectively. However, the computed APD from the HF Purkinje cell model remained almost the same as compared to the control condition (CTR: 330.25 ms vs. HF: 328.95 ms). In conclusion, HF-induced ionic channel remodelling enhanced transmural APD dispersion within the ventricle wall, but not the APD difference at the junction between the Purkinje fibre and the ventricle wall.

Li, G. R., C. P. Lau, et al. (2002). "Transmural action potential and ionic current remodeling in ventricles of failing canine hearts." Am J Physiol Heart Circ Physiol 283(3): H1031-1041.

Maltsev, V. A., H. N. Sabbab, et al. (2002). "Down-regulation of sodium current in chronic heart failure: effect of long-term therapy with carvedilol." Cell Mol Life Sci 59(9): 1561-1568.

Maltsev, V. A., N. Silverman, et al. (2007). "Chronic heart failure slows late sodium current in human and canine ventricular myocytes: implications for repolarization variability." Eur J Heart Fail 9(3): 219-227.

O'Rourke, B., D. A. Kass, et al. (1999). "Mechanisms of altered excitation-contraction coupling in canine tachycardia-induced heart failure, I: experimental studies." Circ Res 84(5): 562-570.

Where applicable, the authors confirm that the experiments described here conform with The Physiological Society ethical requirements.

PC48

Ionic mechanisms underlying upright ECG T-wave in a 3D anatomical and electrophysiological model of rabbit ventricles

S.J. Castro[1], J. Higham[1], A.V. Holden[2], M.R. Boyett[1] and H. Zhang[1]

[1]University of Manchester, Manchester, UK and [2]University of Leeds, Leeds, UK

Mechanisms underlying the upright T wave in mammalian hearts are controversial; whilst it is generally agreed that the dispersion of action potential duration (APD) throughout the ventricles lies behind the genesis of the positive T wave, the precise mechanism is still subject to debate. The variation in APD throughout the heart is owing to the heterogeneous distribution of ion channels and varying kinetics. This heterogeneity can broadly be split into three groups: transmural (TM) heterogeneity, apico-basal (AB) heterogeneity and interventricular (IV) heterogeneity (i.e. between left and right ventricles). The aim of this study was to use a biophysically detailed computer model to investigate possible contributions of TM, AB and IV heterogeneities to the positive T-wave. A family of single cell computational models was developed for rabbit ventricular myocytes in a previous study. The kinetics and conductances of the Hodgkin-Huxley equations were modified to create four distinct cell types; Purkinje fibre (PF) and endocardial, midcardial and epicardial cells of the left ventricle (LV), accounting for the transmural heterogeneity of the heart. In the present study, the LV single cell rabbit models were modified based on experimental data (Convery et al., 1998; Suto et al., 2005, 2007) to create a set of RV single cell models. Furthermore, $I_{Ca,L}$, I_{Kr} and I_{Ks} current densities were varied linearly to account for observed differences between apex and base (Cheng et al., 1999; Sims et al., 2008). The single cell models were incorporated into an anatomical model of the ventricles generated by a DT-MRI scan. The monodomain model was used to provide electrotonic coupling between cells, with the diffusion tensor being constructed from DT-MRI data and known conduction velocities. In simulations, the ventricles were activated by stimulating the top end of the PF network with a basic cycle length of 330 ms. The effects of each type of heterogeneity were assessed using five different configurations: 1) completely heterogeneous, 2) completely homogeneous, 3) only AB heterogeneity present, 4) only TM heterogeneity present, 5) AB and TM heterogeneity present. A limb II pseudo-ECG was calculated for each configuration, and the ECG characteristics were compared. In addition, a cross-section from the LV free wall was stimulated from the endocardial surface to simulate a ventricular wedge preparation. Our simulation data suggested that while the TM heterogeneity is sufficient to produce an upright T-wave in the ventricular wedge preparation, it is necessary to have both TM and AB heterogeneity present in order to produce a fully upright T-wave in the whole heart setting. In conclusion, this study provides mechanistic insights towards understanding the ionic basis underlying the positive T-wave in the ECG.

Cheng J *et al.* (1999). *Cardiovasc Res* **43**, 135–147.

Convery MK *et al.* (1998). *Pflugers Arch* **436**, 581–590.

Sims C *et al.* (2008). *Circ Res* **102**, e86–e100.

Suto F *et al.* (2005). *Heart Rhythm* **2**, 293–300.

Suto F *et al.* (2007). *Am J Physiol Heart Circ Physiol* **292**, H1782–1788.

This work is supported by EPSRC

Where applicable, the authors confirm that the experiments described here conform with The Physiological Society ethical requirements.

PC49

Evaluation of autonomic cardiovascular functions in high-altitude natives residing at Jomsom (2800 m) and Muktinath (3400m) of Nepal

B.R. Pokhrel, O. Nepal, S.L. Malik and B.K. Kapoor

Physiology, Kathmandu University School of Medical Sciences, Kavre, Nepal

Different high-altitude native communities may show different autonomic cardiovascular adapting strategies. The present study was undertaken to evaluate and compare the cardiovascular autonomic functions of the high altitude healthy natives residing at two different altitudes of Jomsom, Thini (altitude: 2800 m) and Muktinath, Jharkot (altitude: 3400 m) of South Asian Himalayan Country Nepal. The cross-sectional study included 72 subjects [age=34.19±22.06 years] from Jomsom, 67 subjects [age= 37.55±16.37 years] from Jharkot and 150 subjects [age=41.03±17.91 years] as a Control group from local community Banepa [altitude: 1439 m]. After consent was taken from each participant, responses to Deep Breathing (DB), Orthostatic Tolerance, Valsalva maneuver and Isometric Hand Grip Test (HGT) were studied following standard protocol. One-way ANOVA followed by Tukey's HSD test in SPSS 17 was used to compare pairs of means (mean±SD) between the groups. Age difference within groups was insignificant. High-altitude natives showed higher basal diastolic blood pressure [Jharkot Vs Control; 77.19±6.67 Vs 70.75±6.69 mmHg, $p<0.01$] and heart rate [Jharkot Vs Control; 82.62±5.24 Vs 71.25± 6.84 bpm, $p<0.01$] than local lowlanders. Evaluating Cardio-vagal influence by Deep Breathing Test and Valsalval Maneuver, Deep Breathing Difference (DBD) [Jharkot Vs Control; 31.46± 11.07 Vs 17.42± 13.95 bpm, $p<0.01$], Expiration to Inspiration [Jharkot Vs Thini; 1.54± 0.19 Vs 1.41± 0.17, $p<0.05$] and Valsalva Ratio [Jharkot Vs Control; 1.85± 0.27 Vs 1.37± 0.20, $p<0.01$] were found significantly increased in high-altitude natives. Sympathetic stress assessment by HGT showed higher diastolic blood pressure response (ΔDBP) [Jharkot Vs Control; 24.96± 8.79 Vs 15.74± 13.27 mmHg, $p<0.01$] in high-altitude natives. Finding of the study suggest that although adaptation in high-altitude natives leads to increase sympathetic activity, it enhances cardiovagal tone over resting heart which may increase with increase in the level of altitude.

We are thankful to Dhulikhel Hospital, Kathmandu University School of Medical Sciences, Kavre, Nepal for providing financial assistance to the Department of Physiology for completing the high-altitude research project.

Where applicable, the authors confirm that the experiments described here conform with The Physiological Society ethical requirements.

PC50

Organisation of cardiomyocytes in the rat pulmonary vein studied using a confocal optical mesolens

A. Henry[1], L. Hutchison[1], B. Amos[2], G. McConnell[1], J. Dempster[1], A. Rankin[3], R. Drummond[1] and E. Rowan[1]

[1]SIPBS, University of Strathclyde, Glasgow, UK, [2]MRC, Laboratory of Molecular Biology, Cambridge, UK and [3]School of Medicine, University of Glasgow, Glasgow, UK

Atrial fibrillation is the most common cardiac arrhythmia and is a significant cause of morbidity and mortality. A clinical study by Haissaguerre et al (1998), demonstrated that in 94% of cases of atrial fibrillation, electrical activity originated at ectopic foci in the pulmonary vein It is believed the external sleeve of cardiomyocytes along the pulmonary vein is responsible for its arrhythmogenic propensity, with the veins complex structural orientation providing a substrate for the arrhythmia. This study aimed to characterise the cellular organisation of the rat pulmonary vein using histological techniques and state of the art wide field confocal microscopy. Male Sprague-Dawley rats (250-400g) were euthanised by cervical dislocation, the heart and lungs removed en bloc and sections of the extra- and intrapulmonary veins microdissected. Tissue structure was initially assessed in formalin fixed sections of the pulmonary vein using Masson's Trichrome staining. Transverse sections revealed a thin smooth muscle layer close to the lumen surrounded by the cardiomyocyte sleeve. Longitudinal sections demonstrated a non uniform and complex arrangement of cardiomyocytes that frequently showed abrupt changes in direction and with the cardiomyocytes extending into the intrapulmonary sections. The Confocal Optical Mesolens is the only device of its kind in the world that is capable of producing detailed, high-definition, three dimensional images of sections of living tissue. Using the dye Di4-ANNEPS (1μM), individual cardiomyocytes were visible in transverse and longitudinal directions, consistent with observations from histological studies. The distribution of mitochondria within the pulmonary vein cardiomyocytes was determined with mitotracker green (1μM) or TMRE (1μM) and both indicated that the mitochondria have a regular arrangement within these cells. Nerves were also clearly visible when the pulmonary vein was labelled with these mitochondrial dyes. The pulmonary vein appeared to be highly innervated further supporting the notion that the autonomic nervous system plays an important role in determining its electrical activity. These techniques demonstrated the variable arrangement of cardiomyocytes in the myocardial sleeve of the rat pulmonary vein. Although the histological and epifluorescence techniques created a

clear image of cardiomyocytes arrangement on the pulmonary vein, the Confocal Optical Mesolens provides an opportunity to obtain high resolution three dimensional images, without the need for formalin fixation and serial sectioning of tissues, over a larger field of view with the use of fluorescent dyes to label different structures within the cardiomyocytes. An enhanced insight into the cellular organisation of the pulmonary vein with the use of modern technologies will allow a better understanding of its arrhymogenic properties.

Haissaguerre M, Jais P, C. Shah D, Takahashi A, Hocini M, Quiniou G, Garrigue S, Le Mouroux A, Le Metayer P and Clementy J (1998) Spontaneous Initiation of Atrial Fibrillation By Ectopic Beats Originating In The Pulmonary Veins. N Engl J Med 339: 659-666.

Where applicable, the authors confirm that the experiments described here conform with The Physiological Society ethical requirements.

PC51

The origin of cardiac excitation in zebrafish

K.L. Poon[1,2], J.D. Liu[3], M. Liebling[4], I. Kondrychyn[2], P. Kohl[5,6], T.A. Quinn[5,6], D. Stainier[3], T. Brand[1] and V. Korzh[2]

[1]Developmental Dynamics, NHLI/Imperial College London, London, UK, [2]Institute of Molecular and Cell Biology, Singapore, Singapore, [3]University of California San Francisco, San Francsico, CA, USA, [4]Electrical and Computer Engineering, University of California San Francisco, Santa Barbara, CA, USA, [5]Cardiac Biophysics and Systems Biology, NHLI/Imperial College London, London, UK and [6]Department of Computer Science, University of Oxford, Oxford, UK

Cardiac pacemaker cells residing in the sinoatrial node (SAN), an important component of the cardiac conduction system (CCS), are responsible for setting the pace of the heartbeat and therefore are crucial for maintaining a proper heart rhythm. However, the molecular control of pacemaker development in mammals and especially in zebrafish is unclear. With the increasing popularity of the zebrafish as a model for studies of cardiac physiology and disease, a better characterization of the cardiac pacemaker cells is necessary. By transposon-mediated insertional transgenesis, hundreds of enhancer trap (ET) lines that express EGFP in distinct anatomical localization have been generated. Two of them, termed SA lines, have distinct EGFP expression at the venous pole of the heart, which can be observed from as early as 36 hours post fertilization. These EGFP-positive cells were characterized at different developmental stages and were confirmed by immunostaining and marker gene expression to be cardiac pacemaker cells. The genomic transposon integration site in the SA lines was determined to be on a defined region on chromosome 14. By whole-mount in situ hybridization, the fibroblast growth factor homologous 2 (fhf2) gene was identified to be the gene whose expression pattern was recapitulated by the SA lines. While initially only the sino-atrial junction displayed EGFP expression, a second expression domain in the AV canal became visible in older embryos. Both expression domains were also present in the adult zebrafish heart.

The loss-of-function phenotype of fhf2 was studied by morpholino-mediated knockdown, which resulted in a malfunctioning heart developing pericardial oedema and blood accumulation at the venous pole. In order to test the importance of SAN pacemaker cells in the zebrafish heart, we analysed the electrophysiological phenotype of a mutant which lacked pacemaker cells based on the absence of fhf2 and other pacemaker gene expression. The mutant heart was found to display a severe bradyarrhythmia with extensive pauses indicating the importance of cardiac pacemaker cells in proper heart function. In summary, we describe the first characterization of the cardiac pacemaker cells of the zebrafish and the functional consequences of their absence to the functioning of the heart.

Where applicable, the authors confirm that the experiments described here conform with The Physiological Society ethical requirements.

PC52

Computational evaluation of the pro-arrhythmic effects of KCNH2 channel current-activator in serum in failing human ventricles

C. Li[1], I. Adeniran[1], J. Hancox[2] and H. Zhang[1]

[1]Biological Physics Group, The University of Manchester, Manchester, UK and [2]School of Medical Sciences, The University of Bristol, Bristol, UK

A recent study has reported the presence of a circulating KCNH2 (hERG) current-activating factor in the serum of heart failure (HF) patients with ventricular tachycardia (VT) or fibrillation (VF) (Sugiyama et al., 2011). It was shown that the KCNH2 current-activator enhanced hERG channel macroscopic tail current following depolarising voltage clamp commands, and this was hypothesized to be pro-arrhythmic. The aim of this study was to use computer models to evaluate the functional effects of an augmented I_{Kr} tail current in ventricular cell and tissues models under normal and HF conditions. Two biophysically detailed computer models for human ventricular action potentials developed by ten Tusscher et al. (2006) (TNNP) and O'Hara et al. (2011) (ORD) were implemented in this study. Simulation of HF condition was based on extant experimental data of HF-induced membrane ionic channels including a reduction of the current densities of I_{Na},I_{to1}, I_{Ks}, I_{K1} and I_{NaK} by 57%, 36%, 61.7%, 56.3% and 42% respectively; an increase of I_{NaL} density by 43% and its inactivation time constant by 25%. As experimental data also suggested a 50% reduction in the SERCA protein level in HF, a 50% reduction in SERCA uptake activity was also assumed. In both normal and HF conditions, experimental data of the KCNH2 current-activator on hERG tail current (Sugiyama et al., 2011) was used to modify I_{Kr} incorporated into the two models, together with an assumed reduced (case-1), increased (case-2) or unchanged (case-3) I_{Kr} step current during voltage-clamp. Simulation data suggested that case-1 resulted in a negligible APD increase in the TNNP model (2.5%, 4.4% and 2.1% for endo-, mid- and epi-cells respectively), but a more remarkable APD increase in the ORD (33.1%, 28.8% and 37.5% for endo-, mid- and epi-cells respectively) in normal conditions. In HF condition, it resulted

in a dramatic APD prolongation in the endo- and epi-cells, a non-repolarisation in the mid-cell model. The quantitative differences in APD prolongation in the two models may be attributable to their different ionic channel current densities. Case-2 resulted in a slight APD reduction in both models in the normal condition, but a more dramatic APD reduction in the HF condition. Case-3 resulted in a negligible APD reduction in both models in the control and HF conditions. In conclusion, the presence of circulating KCNH2 current-activating factor can either prolong or shorten ventricular APDs in the HF condition, depending more on the change to the I_{Kr} step current amplitude, than the increased I_{Kr} tail current. Therefore, the hypothesized pro-arrhythmic effect of the circulating I_{Kr} current-activating factor (Sugiyama et al., 2011) in serum from HF patients is likely to depend crucially on overall modulation of I_{Kr} and this warrants further experimental investigation.

O'Hara, T., L. Virag, et al. (2011). "Simulation of the undiseased human cardiac ventricular action potential: model formulation and experimental validation." PLoS Comput Biol 7(5): e1002061.

Sugiyama, H., K. Nakamura, et al. (2011). "Circulating KCNH2 current-activating factor in patients with heart failure and ventricular tachyarrhythmia." PLoS One 6(5): e19897.

ten Tusscher, K. H. and A. V. Panfilov (2006). "Alternans and spiral breakup in a human ventricular tissue model." Am J Physiol Heart Circ Physiol 291(3): H1088-1100.

Where applicable, the authors confirm that the experiments described here conform with The Physiological Society ethical requirements.

PC53

The importance of the sarcoplasmic reticulum for the influence of I(f) carried by hyperpolarization-activated cyclic nucleotide-gated ion channels on pacemaker activity in mouse sino-atrial node

I. Nazarov, T. Thevarajan, R. Bayliss and D.A. Terrar

Pharmacology, University of Oxford, Oxford, UK

The mechanisms underlying pacemaker activity in the sino-atrial (SA) node remain controversial, with some giving greatest prominence to If (1), others emphasising a 'calcium clock' (2), and some favouring membrane currents other than If (3). The aim of the present experiments was to explore the possible dependence of If on cytosolic Ca2+, including that released from the sarcoplasmic reticulum (SR).
All experiments were carried out on mouse spontaneously beating atrial preparations with intact SA node using methods similar to those described in (4). All observations are presented as mean ± SEM, and $P<0.05$ for all reported changes (with Students t test or Analysis of Variance as appropriate).
ZD7288 applied at 1 μM to block If caused a reduction of spontaneous rate from 505 ± 24 to 228 ± 24 bpm (a reduction of 55 ± 4 % expressed as % resting rate). Exposure to ryanodine (3 μM to interfere with SR Ca2+ release) reduced beating rate, and under these conditions the effects of ZD7288 on spontaneous rate were

reduced: ZD7288 reduced rate from 197 ± 40 bpm (ryanodine alone) to 148 ± 40 bpm (ryanodine and ZD7288), a reduction of 27 ± 12%. SR function is also suppressed by cyclopiazonic acid (CPA) to inhibit Ca2+ re-uptake by the SR. CPA (100 μM) reduced spontaneous beating rate, and the effects of ZD7288 were reduced in the presence of CPA: ZD7288 reduced spontaneous rate from 213 ± 13 bpm (CPA alone) to 147 ± 9 bpm (CPA and ZD7288), a reduction of 19 ± 4%. In the presence of ZD7288, the log(concentration)-response curve for effects of isoprenaline on spontaneous rate showed a reduced slope and maximum response. Addition of CPA in the presence of ZD7288, or of ryanodine in the presence of ZD7288 both further reduced the slope and maximum response of the log(concentration)-response curve for isoprenaline.

These observations are consistent with a role for Ca2+ released from the SR in regulating If and therefore the rate of spontaneous beating of mouse SA node. Ca2+ released from the SR may stimulate adenylyl cyclases AC1 and AC8 that are present in SA node (5). The reduced slope and maximum of the log(concentration)-response curve for isoprenaline after ZD7288 is consistent with modulation of If during beta-adrenoceptor stimulation. However, since interference with SR function (with either ryanodine or CPA) caused a further depression of the slope and maximum of the log(concentration)-response curve for isoprenaline even when If was substantially blocked, there appears to be an additional contribution of SR-derived Ca2+ to the effects of β-adrenoceptor stimulation on spontaneous rate that is independent of If.

DiFrancesco D. (2010). Circ Res. 106, 434-46.

Lakatta, EG, Maltsev, VA & Vinogradova, TM (2010) Circ Res. 106, 659-73.

Himeno Y, Toyoda F, Satoh H, Amano A, Cha CY, Matsuura H, Noma A. (2011) Am J Physiol 300, H251-61

Rigg, L., Heath, B.M., Cui, Y. & Terrar, D.A. (2000). Cardiovasc Res 48, 254-264.

Mattick P, Parrington J, Odia E, Simpson A, Collins T, Terrar D.A. (2007) J Physiol. 582, 1195-203

Supported by The British Heart Foundation and The Wellcome Trust

Where applicable, the authors confirm that the experiments described here conform with The Physiological Society ethical requirements.

PC54

Transmural gradients in excitation-contraction coupling in ventricular myocytes isolated from aged failing hearts

E.F. Bode, M.A. Horn, D.A. Eisner and A.W. Trafford

Cardiovascular, University of Manchester, Manchester, UK

Heart failure (HF) is a significant cause of mortality in the aged. Perturbations to calcium (Ca^{2+}) homeostasis in failing ventricular myocytes have been well docu-

mented. However, the transmural variation in Ca^{2+} homeostasis of the failing left ventricle is incompletely understood and data on how this is influenced by ageing is lacking. The aim of this work was to identify any changes in transmural excitation-contraction coupling that may elucidate potential arrhythmogenic mechanisms in the aged failing heart.
HF was induced by tachypacing aged (over 8 years of age) Welsh Mountain sheep anaesthetised using isoflurane (1-3%) and analgesia was provided with meloxicam (0.5mg/kg s/c). Single isolated left ventricular myocytes from either the epicardium or endocardium were voltage clamped using the perforated patch technique at 37 °C. Cells were loaded with the Ca^{2+} sensitive indicator Fluo-5F AM in order to measure changes to intracellular Ca^{2+} concentration. Data are presented as mean ± standard error of the mean (SEM). Differences between groups were determined using a two-way ANOVA.
In HF, Ca^{2+} transient amplitude was decreased in the epicardium (41 ± 17%; n = 12 - 18, p = 0.023), but not in the endocardium when compared to control levels. A reduction in epicardial peak L-type calcium current ($I_{Ca\text{-}L}$) density at +10 mV (37 ± 8%; n = 13 – 17, p < 0.001) was found in the epicardial failing myocytes, along with a decrease in total sarcoplasmic reticulum (SR) Ca^{2+} content (39 ± 9%; n = 11, p = 0.014). However, no changes to either the $I_{Ca\text{-}L}$ density or SR Ca^{2+} content were found in endocardial cells. Threshold SR Ca^{2+} content was determined by using 10 mM Ca^{2+} in external solutions to induce Ca^{2+} waves. Under these conditions, in failing epicardial myocytes only, SR Ca^{2+} content increased by 217 % from 31 ± 3 μmol/l to a threshold level of 100 ± 10 μmol/l (n = 6 – 11, p < 0.001). However, when 100 nM isoprenaline was applied to the failing epicardial cells SR Ca^{2+} content was found to be 83 ± 7 μmol/l and Ca^{2+} waves developed at 121 ± 8 μmol/l which was not different from baseline (n = 4 – 5, p = 0.144).
The smaller Ca^{2+} transient amplitude in failing epicardial cells was the result of a smaller peak $I_{Ca\text{-}L}$ density and reduced SR Ca^{2+} content. Under control conditions, in failing epicardial cells, SR Ca^{2+} content is lower than the threshold at which Ca^{2+} waves develop. However, with the application of isoprenaline SR Ca^{2+} content is similar to threshold levels making these cells under β-adrenergic stimulation more likely to develop spontaneous Ca^{2+} release, potentially resulting in arrhythmias.

Where applicable, the authors confirm that the experiments described here conform with The Physiological Society ethical requirements.

PC55

Role of MKK7 in hypertrophic cardiac diseases

S.K. Chowdhury and X. Wang

Faculty of life sciences, The University of Manchester, Manchester, UK

Maladaptive cardiac hypertrophic remodeling can lead to heart failure and cardiac arrhythmias. Role of mitogen-activated protein (MAP) kinase pathway members in

intracellular signal transduction is important for such remodeling. MAP kinase kinase 7 (MKK7), positioned at a bottleneck of the MAP kinase pathway, is essential for survival in response to pressure overload (1,2).
Ventricular cardiomyocyte specific knockout (MKK7CKO) and littermate wild-type mice were subjected to chronic Angiotensin-II (Ang-II, 0.7μgm/kg/min) or vehicle stimulation for 2 weeks using subcutaneous osmotic pumps inserted under anesthesia (2.5-4% isoflurane, intraperitoneal Buprenorphine 0.1mg/kg analgesia). This resulted in significantly higher heart wt. gain in Ang-II treated MKK7CKO mice compared to similarly treated controls (heart wt/tibia length 6.60 ± 0.17 vs. 5.79 ± 0.10mg/mm, respectively; n=10-12, paired t test, $p<0.001$). Associated similar increase in cardiomyocyte cross-sectional areas (296.22 ± 5.11 vs. 222.41 ± 2.89, n=3, $p<0.0005$) defined this hypertrophy. Rise of average systolic (20-23%) & diastolic (24-31%) blood pressure after Ang-II treatment was alike. In terminally anesthetised (Tribromoethanol, 200mg/kg) mice, trans-thoracic echocardiography showed significant functional impairment of MKK7CKO hearts. Compared to Ang-II treated wild-type mice, similarly treated MKK7CKO hearts had lower ejection fraction (%, 76.39 ± 2.23 vs. 53.5 ± 2.90, n=7-9, $p<0.001$) and fraction shortening (%, 38.73 ± 2.05 vs. 22.8 ± 1.62, n=7-9, $p<0.001$). Alongside, the drug treated MKK7CKO mice had significantly increased QTc interval than the wild-type mice (ms, 85 ± 4.56 vs. 65 ± 3.85, n=8-10, $p<0.005$). Electrical programmed stimulation using S1S2 protocol discovered an increase in mean ventricular effective refractory period (VERP) from about 40ms in vehicle treated mice to 51ms in Ang-II treated wild types. Most (89%) Ang-II treated knockout mice developed ventricular tachycardia (VT) or ventricular premature contractions (VPC) before reaching VERP, obliterating a mean calculation. While S1S2 delay was gradually reduced from 100ms to 40ms, 78% Ang-II treated mutants generated VT/VPCs, compared to 10% similarly treated wild types and none of the untreated controls (n=8-10). Masson's trichrome staining revealed 9.96% interstitial fibrosis in the Ang-II treated knockouts compared to 2.86% in wild types and <0.5% in untreated controls (n=3, $p<0.05$). Although total connexin 43 protein levels were not significantly altered, its distribution in cardiomyocytes was altered as a result of Ang-II treatment in MKK7CKO mice (n=3-4). These data support the essential role of MKK7 for maintenance of functional integrity and rhythmicity of the heart in hypertrophic stress. Subsequent investigations will help unveil the specific role of MKK7 absence in ventricular arrhythmogenesis following different hypertrophic stress.

Wang X, Destrument A, Tournier C. Physiological roles of MKK4 and MKK7: insights from animal models. Biochimica et biophysica acta. 2007 Aug;1773(8):1349–57.

Liu W, Zi M, Chi H, Jin J, Prehar S, Neyses L, et al. Deprivation of MKK7 in cardiomyocytes provokes heart failure in mice when exposed to pressure overload. Journal of molecular and cellular cardiology. Elsevier Ltd.; 2011 Apr;50(4):702–11.

M. Lei, M. Zi, W. Liu, H. Shiels, P. Walker, H. Tsui, S. Ulm, Y. Wang; the Commonwealth Scholarship Commission, UK and the faculty of life sciences of the University of Manchester.

Where applicable, the authors confirm that the experiments described here conform with The Physiological Society ethical requirements.

SA01

Funny channel-based arrhythmias

D. DiFrancesco

Dept Life Sciences, University of Milano, Milano, Italy

Several manifestations of Sinus Node Disease involve improper impulse generation/ propagation and impaired maintenance of normal sinus rhythm. The established role of funny/HCN4 channels in pacemaker activity generation and normal rate control makes them natural candidates in the search for potentially arrhythmogenic ion channel dysfunctions.
Along with the wealth of existing evidence supporting the role of funny/HCN4 channels in the physiological control of rate (for review see DiFrancesco, 2010), experimental data have also been collected showing that a defective funny current can be associated with rhtyhm abnormalities. For example, results from cardiac-specific, Tamoxifen-inducible HCN4 knockout mice show that specific HCN4 deletion in cardiac tissue leads to progressive bradycardia and cardiac arrest after about 5 days; interestingly, death does not occur because of sinus arrest but because of AV block, suggesting a previously unrecognized role of HCN4 channels in AV rhythm and/or AV conduction that requires fuller investigation (Baruscotti et al., 2011).
More direct evidence for the association between funny/HCN4 channels and rate is provided by the HCN blocker ivabradine, the only specific "heart rate-reducing" agent commercially available today and used in the therapy against angina. Heart rate reduction is a therapeutic target in ischemic heart disease and heart failure. By selectively blocking f-channels, ivabradine reduces heart rate and clinical work shows that this occurs without cardiovascular side-effects, highlighting the therapeutic relevance of funny channel-based pacemaking and its pharmacological control. Because of its pure rate-reducing properties, it is to be expected that ivabradine can be useful against tachycardia; indeed, several recent observations indicate that ivabradine can be succesfully used in the treatment of adult and pediatric forms of Inappropriate Sinus Tachycardia (Femenia et al., 2012).
A direct demonstration of the involvement of defective HCN4 channels in cardiac arrhythmias comes from the finding that specific HCN4 mutations leading to loss-of-function defects are associated with arrhythmias and more specifically with bradycardia. Four arrhythmia-related mutations have been described so far in HCN4 channels.
The point mutation S672R in the CNBD of HCN4 channels was found to cause asymptomatic sinus bradycardia in 15 out of 27 members of a large 3-generation family (Milanesi et al., 2006). According to functional studies, S672R is a loss-of-function mutation inducing a negative shift of about 5 mV of the funny current activation curve, when expressed in heterozygous conditions. Therefore, since shifting the funny current activation curve to the negative direction is the typical action of parasympathetic stimulation, in the case of the S672R mutation bradycardia is

caused by a constitutive change of channel properties mimicking cholinergic-induced channel inhibition.
Other arrhythmia-related loss-of-function HCN4 mutations were described in the C-linker, such as L573X, a mutation found in a single patient which generates a truncated protein lacking the CNBD (Schultze-Bahr et al., 2003), and D533N, a point mutation reported to depress membrane trafficking (Ueda et al., 2004). In the first case the patient suffered from bradycardia, chronotropic incompetence and atrial fibrillation; since this patient was investigated individually, no inheritance could however be evaluated. In the second case the report referred to a small family with a complex array of rhythm disturbances including severe bradycardia, syncope, LQT and torsade des pointes; however, a full functional investigation of the correlation between HCN4 mutation and phenotype was not performed.
A fourth mutation associated with familial asymptomatic bradycardia (G480R) was reported in the pore region of the channel (Nof et al., 2007). The mean heart rate of affected family members was lower than 55 bpm, compared with 63 bpm of non-affected individuals. Functional studies revealed that this mutation reduces the size of the diastolic funny current by decreasing channel synthesis and traffiking, and shifts the current activation curve to the negative direction. The mutation modifies the GYG selectivity sequence typical of K+-permeable channels; surprisingly however, the authors did not find a significant change in the Na/K permeability ratio (Nof et al., 2007).
These data suggest the existence of a general mechanism for HCN4-linked arrhythmias and justify the tentative prediction that more HCN4 mutations, yet to be identified, are likely to contribute to different forms of inheritable arrhythmias whose substrate is the sinus node and conduction system.

Baruscotti M, Bucchi A, Viscomi C, Mandelli G, Consalez G, Gnecchi-Rusconi T, Montano N, Casali KR, Micheloni S, Barbuti A, DiFrancesco D. (2011) Deep bradycardia and heart block caused by inducible cardiac-specific knockout of the pacemaker channel gene Hcn4. Proc Natl Acad Sci USA 108(4):1705-1710

DiFrancesco, D. (2010) The role of the funny current in pacemaker activity. Circulation Research 210: 434-446

Femenía F, Baranchuk A, Morillo CA. (2012) Inappropriate sinus tachycardia: current therapeutic options. Cardiol Rev. 20(1):8-14

Milanesi R., Baruscotti M., Gnecchi-Ruscone T. & DiFrancesco D. (2006) Familial sinus bradycardia associated with a mutated cardiac pacemaker channel. New Engl. J. Med. 354(2):151-157

Nof E, Luria D, Brass D, Marek D, Lahat H, Reznik-Wolf H, Pras E, Dascal N, Eldar M, Glikson M. (2007) Point mutation in the HCN4 cardiac ion channel pore affecting synthesis, trafficking, and functional expression is associated with familial asymptomatic sinus bradycardia. Circulation. 116:463-470.

Schulze-Bahr E, Neu A, Friederich P, Kaupp UB, Breithardt G, Pongs O, Isbrandt D. (2003) Pacemaker channel dysfunction in a patient with sinus node disease. J Clin Invest. 111:1537-1545.

Ueda K, Nakamura K, Hayashi T et al (2004) Functional characterization of a trafficking-defective HCN4 mutation, D553N, associated with cardiac arrhythmia. J Biol Chem 279:27194-8

Supported by MIUR grant PRIN 2008ETWBTW.

Where applicable, the authors confirm that the experiments described here conform with The Physiological Society ethical requirements.

SA02

A major actor of the genetic cardiac arrhythmias: *SCN5A*

I. Baró

Inserm, UMR1084, l'institut du thorax, Nantes, France and CNRS, UMR6291, l'institut du thorax, Nantes, France

With their propensity to lead to sudden death, cardiac arrhythmias are a major clinical problem. They also represent an exciting medical challenge which needs gene-to-bedside studies to unravel the underlying arrhythmogenic mechanisms. Although rare, cardiac channelopathies have broadened our understanding of proarrhythmic mechanisms, as demonstrated with *SCN5A*-related arrhythmias.
The *SCN5A* gene encodes the human cardiac voltage-gated sodium channel $Na_v1.5$ (Rook*et al.*, 2012). Representing the vast majority of the cardiac Na^+ channels, $Na_v1.5$ plays a key role in cardiac electrophysiology. $Na_v1.5$ is involved in the initiation and conduction of action potentials. Mutations in $Na_v1.5$ lead to a large spectrum of phenotypes, including long-QT syndrome, Brugada syndrome, isolated progressive cardiac conduction defect (Lenègre disease) and numerous overlap syndromes (Wilde & Brugada, 2011).
For several years now, we have been interested in the study of *SCN5A* mutations trying to decipher the mechanisms linking the protein dysfunction and the disease, in order to unveil the role of $Na_v1.5$ in myocardium electrical activity and structure. Although patch-clamp studies in heterologous expression systems have provided key information to understand the genotype-phenotype relationships of these diseases, they could not clarify how mutations can be responsible for such a large spectrum of diseases, for the late age of onset or the progressiveness of some of them and for the overlapping syndromes. The use of mathematical models of action potentials has provided further information. Genetically modified mouse models turned out to be powerful tools to elucidate the pathophysiological mechanisms of *SCN5A*- and other gene-related arrhythmic diseases and offer the opportunity to investigate the cellular consequences of gene mutations such as the remodelling of other gene expression that might participate to the overall phenotype and explain some of the differences among patients (Derangeon M *et al.*, 2012). Among these genes are those coding for $Na_v1.5$ auxiliary subunits. Dozens of $Na_v1.5$ auxiliary proteins have been described (Abriel, 2010). We identified and studied the function and potential role of one of them, 14-3-3 (Allouis *et al.*, 2006). We are currently investigating its involvement in the regulation of $Na_v1.5$ expression by the ubiquitin ligase Nedd4-2. Most recently, we linked a new pathological entity that we named MEPPC for multifocal ectopic Purkinje-related premature contractions, to a single *SCN5A* mutation (Laurent *et al.*, 2012).

Abriel H (2010). *J Mol Cell Cardiol* **48**, 2-11

Allouis M *et al.* (2006). *Circ Res* **98**,1538-1546

Derangeon M *et al.* (2012). *Front Physiol* **3**, 210

Laurent G *et al.* (2012). *J Am Coll Cardiol* **60**, 144-156

Rook MB *et al.* (2012). *Cardiovasc Res* **93**, 12-23

Wilde AA & Brugada R (2011). *Circ Res* **108**, 884-897

The Agence Nationale de la Recherche (ANR COD/A05045GS and ANR-09-GENO-003-01), the Association Française contre les Myopathies (n°14120), and the Fondation pour la Recherche Médicale (DVC20070409253) financially supported parts of this work. The research leading to some of these results has also received funding from the European Community's Seventh Framework Programme FP7/2007-2013 under grant agreement n° FP7-HEALTH-2009-single-stage 241526.

Where applicable, the authors confirm that the experiments described here conform with The Physiological Society ethical requirements.

SA03

Genetic variants causing lone atrial fibrillation in young patients

S.P. Olesen, M. Olesen, B. Liang, N. Schmitt, L. Yuan, T. Jespersen, I. Christophersen, A. Holst, J. Nielsen, J. Svendsen and S. Haunsø

BIomedicine, University of Copenhagen, Copenhagen, Denmark

Atrial fibrillation (AF) is the most common type of cardiac arrhythmia affecting about 1% of the general population, and the incidence increases strongly with age. A number of diseases such as hypertension, ischemic heart disease and metabolic diseases predispose to AF, and patients devoid of confounding diseases are said to have lone AF. We assume that genetic factors may be specifically important in young AF patients and investigated a cohort of 197 patients developing lone AF before the age of 40. The average age of onset was 31 years.
In this young lone AF cohort, 10 variants of Nav1.5 were found distributed widely over the length of the protein. Nine out of 10 variants had compromised peak current, and 5 out of 5 that were studied for effects on the sustained Na current had a 3-8 fold increase. Interestingly, 7 of the probands carried a mutation previously associated with Long QT syndrome type 3, and these were also the patients showing the longest QT intervals in our study. The overlap between the diseases could indicate an increased tendency to early afterdepolarization in both atria and ventricles.
The young patients further showed a number of mutations in Kv7.1 conducting the cardiac Iks current and in Kv1.5 conducting the atrial Ikur current. In Kv7.1 four mutations were found (3 gain- and 1 loss-of-function), and in Kv1.5 six mutations were detected (3 gain- and 3 loss-of-function). Gain-of-function mutations in Kv1.5 have not been described before as cause of AF. The Kv1.5 loss-of-function variants

were caused by decreased surface expression. None of the above variants were present in 307 healthy control individuals.
In conclusion, patients with the onset of AF at young age exhibit a high prevalence of Nav and Kv variants. The Nav variants are dominated by a decreased peak current and an increases late current, whereas both loss- and gain-of-function of the Kv channels are seen to enhance AF susceptibility.

Where applicable, the authors confirm that the experiments described here conform with The Physiological Society ethical requirements.

SA04

Session: Ion channel abnormalities and arrhythmias Presentation title: LQTS, beyond the causal mutation

A. Wilde

Academic Medical Centre, Amsterdam, Netherlands

In all primary arrhythmia syndromes, and more general, in probably all inherited diseases, it is well known that disease penetrance and expressivity is markedly variable between individuals hosting identical mutations. It has been established that a number of clinical variables impact on disease penetrance. These variables include gender, age and external factors like concomitant disease, drug use etc. In addition, genetic factors are also most likely to contribute.
In the Long QT Syndrome (LQTS) known genetic factors include pathogenic variants in other LQT-related genes and modifying single nucleotide polymorphisms (SNP's) in LQT-related and other genes. Indeed, it is well known that patients with double mutations have a more severe phenotype. SNP's seem to impact, in gross terms, on repolarization reserve by several mechanisms including an effect on the ion currents involved. Several of these SNP's have been identified in the general population (with impact on the QTc interval). Among others, functional SNP's have been identified in KCNH2 for example and in NOS1AP.
The LQT phenotype can also be influenced by altered transcriptional regulation, for example by genetic variants (SNP's) in the promotor elements or by SNP's in the 3' untranslated region (3'UTR). The latter mechanism has been shown to be very robust for LQT1. The effect depends on the KCNQ1 allele on which they reside. QTc intervals are almost normal when the SNPs are on the allele that contains the mutation. Oppositely, when they reside on the healthy allele (i.e. the allel without the LQT1-causing mutation), QTc intervals are longer and symptoms more frequent. The allele-specific effects of these 3'UTR SNPs on disease severity strongly suggest that they are functional variants that directly alter the expression of the allele on which they reside. As such, the balance between proteins stemming from either
the normal or the mutant KCNQ1 allele is disturbed.
In conclusion, phenotypic heterogeneity is arrhythmia syndromes is well known and we are starting to the understand the underlying causes. These include a num-

ber of clinical and genetic factors, among which genetic variants that alter protein expression.

Amin AS, Giudicessi JR, Tijsen AJ, Spanjaart AM, Reckman YJ, Klemens CA, Tanck MW, Kapplinger JD, Hofman N, Sinner MF, Müller M, Wijnen WJ, Tan HL, Bezzina CR, Creemers EE, Wilde AAM*, Ackerman MJ*, Pinto YM*. Variants in the 3' Untranslated Region of the KCNQ1-Encoded Kv7.1 Potassium Channel Modify Disease Severity in Patients with Type 1 Long QT Syndrome in an allele-specific manner.

Eur Heart J 2012;33:714-723.

Dr AS Amin, Heart Failure Research Centre, Amsterdam, The Netherlands.

Dr Y Pinto, Heart Failure Research Centre, Amsterdam, The Netherlands.

Where applicable, the authors confirm that the experiments described here conform with The Physiological Society ethical requirements.

SA05

Ventricular arrhythmogenesis in Nav1.5-haploinsufficient murine hearts

C. Huang

Physiological Laboratory, Cambridge University, Cambridge, Cambs, UK

Ventricular arrhythmogenesis leading to sudden cardiac death is a major cause of clinical mortality. Brugada Syndrome (BrS) is one important cause of sudden cardiac death from fast polymorphic ventricular tachycardia (VT) or ventricular fibrillation in middle age. It is typified by electrocardiographic right bundle branch block and right precordial ST elevation, often unmasked by flecainide challenge. Previously used canine wedge model preparations required application of potentially non-specific pharmacological agents to replicate the BrS phenotype. However, 30% of BrS patients show a loss of Na^+ channel function associated with *SCN5A* gene mutations. A *Scn5a*+/- mouse, a heterozygous knock-out for the cardiac voltage-gated Na^+ channel, might then help model its physiological arrhythmogenic mechanisms [1]. These had been variously suggested to involve loss of the epicardial cardiac action potential dome increasing vulnerability to early, phase II re-entry from the endocardium or conduction delays particularly in the right ventricular outflow tract (RVOT).

The murine model reproduces clinical arrhythmic and electrocardiographic features of BrS: intact anaesthetized animals show ventricular tachycardia (VT) as well as ST elevation, conduction abnormalities detected as increased PR intervals and AV block, and repolarization abnormalities appearing as increased QT dispersion, all exacerbated or unmasked by flecainide but relieved by quinidine [2]. RT-PCR and Western blots demonstrated that *Scn5a*+/- hearts show reduced Nav1.5 expression relative to wild-type (WT), and reduced right (RV) relative to left ventricular (LV) Nav1.5 expression. Both *Scn5a*+/- and WT show increased RV relative to LV Kv1.4 and KCHIP2 expression. *Scn5a*+/- ventricular myocytes show correspondingly

reduced transient and persistent Na^+ currents (I_{Na} and I_{pNa}) relative to WT, and reduced I_{Na} in RV relative to LV. Both *Scn5a*+/- and WT showed similarly increased RV relative to LV maximum transient outward currents (I_{to}). *Scn5a*+/- correspondingly showed reduced maximum rates of both LV and RV action potential increase (dV/dt_{max}) compared to WT, and greater RV compared to LV dV/dt_{max}. Similarly, action potential durations at 90% recovery (APD_{90}s) were lower in *Scn5a*+/- than WT in the RV, similar between the two variants in the LV, and therefore lower in the RV than the LV in *Scn5a*+/- but not WT [3].

Arrhythmogenecity might then arise from abnormalities in either or both depolarization and repolarization in RVs of *Scn5a*+/- hearts. Monophasic action potential and bipolar electrogram studies in intact Langendorff-perfused *Scn5a*+/- hearts indeed demonstrated increased spatial and temporal heterogeneities in activation latencies, repolarization times, refractory periods and electrogram fractionation, and discordant alternans specifically involving their RVs [4]. Thus, *Scn5a*+/- showed shorter APDs than WT. Their shorter RV than LV epicardial but similar RV and LV endocardial APDs, gave strongly positive transmural APD gradients particularly in the RV further accentuated by flecainide and reduced by quinidine [5]. However, although epicardial ventricular effective refractory periods (VERPs) were *shorter* in the RV than the LV in *both* variants, they were *greater* in *Scn5a*+/- in *all* cardiac regions studied. Furthermore they were *increased* by *both* flecainide and quinidine in *both* variants in *all* regions. This gave constant VERP/APD ratios through all regions in both variants, *larger* in *Scn5a*+/- reflecting their larger VERPs but smaller APD70, *reducing* the likelihood of early re-entry events [6].

Furthermore, multi-electrode mapping array explorations in spontaneously beating flecainide-treated hearts implicated lines of functional conduction block arising in the RV, leading to reentrant circuits, in their VT. Activation epicardial propagation maps showed single planar intra-epicardial wavefronts proceeding from apex to base during sinus activity but with greater activation time differences and crowded isochronal lines, in both the RV and LV of *Scn5a*+/- than WT. These were increased by flecainide, but not quinidine, particularly in the *Scn5a*+/- RV. Superimposed premature beats then produced a line of block with impulse propagation flowing around it in the RV, with subsequent beats in the resulting VT showing different lines of block creating a non-stationary vortex, and polymorphic arrhythmia [7].

Papadatos GA et al. (2002) Proc Natl Acad Sci U S A. 99, 6210-6215.

Martin CA et al. (2010). J Electrocardiol 43, 433-439.

Martin CA et al. (2011). Open Biol. 2, 120072.

Martin CA et al. (2011). Am J Physiol Heart Circ Physiol. 300, H605-616.

Martin CA et al. (2010). J Cardiovasc Electrophysiol. 21, 1153-1159.

Martin CA et al. (2011). Pflugers Arch 462, 495-504.

Martin CA et al. (2011). Am J Physiol Heart Circ Physiol. 300: H1853-1862

We thank the Medical Research Council, Wellcome Trust, British Heart Foundation and the Sackler Foundation for generous support.

Where applicable, the authors confirm that the experiments described here conform with The Physiological Society ethical requirements.

SA06

Translating computational modelling to the heart of the clinic

N.P. Smith

Biomedical Engineering, Kings College London, London, UK

The significance of heart disease has motivated the application of state of the art clinical imaging techniques to aid diagnosis and clinical planning. However to exploit the full value of such imaging technologies, and the combined information content they produce, requires the ability to integrate multiple types of functional data into a consistent framework. An exciting and highly promising strategy for underpinning this integration is the assimilation of multiple image sets into personalised and biophysically consistent mathematical models. The development of these models provides the ability to capture the multi-factorial cause and effect relationships which link the underlying pathophysiological mechanisms. Applying this approach I will present the development and application of a computational cardiac framework representing the cardiac electrical, mechanical and fluid systems and related functions. Through the development of these computational models, I will show results quantifying the importance of each of these coupling effects and discuss their significance for interpreting measurement data and for predicting cardiac function. I will outline future planned developments for integrating these three systems together in the heart, and the common features and tools of relevant for developing other organ system models.

Where applicable, the authors confirm that the experiments described here conform with The Physiological Society ethical requirements.

SA07

SR Ca^{2+} release, reduced repolarization reserve and arrhythmias: possible role of Ca^{2+} window and Na/Ca exchange currents

G. Antoons

Cardiology, Medical University of Graz, Graz, Austria

Ventricular arrhythmias often occur in a setting of abnormal repolarization, and an increase in adrenergic drive is a common triggering event. In diseased hearts that are prone to arrhythmias, repolarization is intrinsically less stable, showing larger variability in the duration of the QT interval or action potential (AP) on a beat-to-beat basis, which then further destabilizes upon an arrhythmogenic challenge. This beat-to-beat variability of repolarization (BVR) is thought to reflect a

reduced repolarization reserve due to a loss of repolarizing, or a gain of inward currents. In the predisposed heart, also β-adrenergic stimulation causes beat-to-beat instability[1]. One mechanism is a blunted response of I_{KS} to β-agonists which prevents accumulation of repolarizing current and compromises repolarization reserve[2].

One other possible mechanism is increased SR Ca^{2+} release as a consequence of β-adrenergic stimulation. In single cardiomyocytes, beat-to-beat variability increases with AP duration, and at long durations there is also variability in the duration of the global Ca^{2+} transient. This is because changes in voltage and Ca^{2+} are interrelated through Ca^{2+}–dependent membrane currents. At shorter AP durations, there is no variability in global Ca^{2+} duration and amplitude, but AP variability remains. However, inhibition of SR Ca^{2+} release (caffeine, thapsigargin) reduces BVR while increasing SR Ca^{2+} release (BayK) promotes BVR. There might be variability in SR Ca^{2+} release at the subcellular level which is not reflected in the global Ca^{2+} transient. Variability in local Ca^{2+} release must then be translated in AP variability through Ca^{2+}–dependent currents in close proximity of release sites. The most likely candidates are the L-Type Ca^{2+} channel (LTCC) and Na/Ca exchanger (NCX).

LTTC is located near RyR release sites and senses local Ca^{2+} release through feedback by Ca^{2+}-dependent inactivation. When Ca^{2+} declines, a fraction of channels recovers from release-dependent inactivation. When SR Ca^{2+} release is large, there is more inactivation, but also more recovery of Ca^{2+} channels, producing a larger Ca^{2+} window current facilitating the development of early afterdepolarizations (EADs)[3].

A fraction of NCX also senses local Ca^{2+} near release sites[4]. SR Ca^{2+} release activates inward NCX current which superimposes on the inactivating Ca^{2+} current and precedes reactivation of the Ca^{2+} window current. Blocking NCX reduces the recovery of Ca^{2+} window current, probably by slower removal of Ca^{2+} from the LTTC microdomain. In a well-established canine model of repolarization-dependent arrhythmias, the dog with chronic atrioventricular block, partial block of NCX with SEA-0400 stabilized dofetilide-induced BVR and suppressed TdP arrhythmias, at the cellular level and during in vivo experiments. Selective LTCC block was also effective, but unlike SEA-0400, caused negative inotropic effects.

In conclusion, under β-adrenergic stimulation, NCX may reduce repolarization reserve by producing inward current during the AP plateau, and possibly indirectly, by modulating the Ca^{2+} microdomain near LTCC. Partial NCX block stabilizes repolarization and is an effective antiarrhythmic strategy against repolarization-dependent arrhythmias.

Stengl M, Ramakers C, Donker DW, Nabar A, Rybin AV, Spätjens RL, van der Nagel T, Wodzig WK, Sipido KR, Antoons G, Moorman AF, Vos MA, Volders PG (2006). *Cardiovasc Res* **72**, 90-100.

Volders PG, Stengl M, van Opstal JM, Gerlach U, Spatjens RL, Beekman JD, Sipido KR, Vos MA (2003). *Circulation* **107**, 2753-2760.

Antoons G, Volders PG, Stankovicova T, Bito V, Stengl M, Vos MA, Sipido KR (2007). *J Physiol* **579**, 147-160.

Acsai K, Antoons G, Livshitz L, Rudy Y, Sipido KR (2011). *J Physiol* **589**, 2569-2583.

Where applicable, the authors confirm that the experiments described here conform with The Physiological Society ethical requirements.

SA08

The possible role of NCX in the generation of cardiac arrhythmias

A. Varro

Department of Pharmacology and Pharmacotherapy, University of Szeged, Szeged, Hungary

The disturbance of normal Ca2+ homeostasis is cardiac muscle can enhance the risk of life threatening arrhythmias. The Na+/Ca2+ exchanger (NCX) has an essential role in maintaining cardiac Ca2+ homeostasis and is considered as the main pathway for Ca2+ extrusion from the cardiomyocytes. Therefore, NCX can be assumed to play an important role in arrhythmogenesis under certain conditions such as heart failure and calcium overload. In these situations, i.e during Ca2+ overload enhanced function of NCX is associated with early (EAD) and delayed (DAD) afterdepolarizations which represent important trigger mechanisms in the generation of arrhythmias. Therefore, both selective and non-selective NCX inhibition may represent possible options for the treatment of cardiac arrhythmias. In addition, since NCX function critically depends on intra/extracellular Ca2+ concentrations and membrane potential -both dynamically changing during the action potential- NCX inhibition can also influence cardiac repolarization and dispersion of repolarization that represent substrates for arrhythmogenesis. Until very recently it was not possible to address this question directly due to the lack of specific NCX inhibitors.

Supported by the Hungarian National Office for Research and Technology (NCXINHIB, OMFB-00337/2010) and Hungarian National Development Agency (TÁMOP 4.2.2/B-10/1-2010-0012).

Where applicable, the authors confirm that the experiments described here conform with The Physiological Society ethical requirements.

SA09

Cardiac sodium channelopathy: electrophysiology and beyond

C. Remme

Academic Medical Center, Amsterdam, Netherlands

Sodium channel dysfunction causes cardiac conduction disturbances, ventricular arrhythmias, and sudden death, both during common pathological conditions such as myocardial ischemia and heart failure, and in the setting of inherited mutations in the SCN5A gene encoding the cardiac sodium channel. Mutations in SCN5A are

associated with a broad spectrum of cardiac rhythm disorders (1). Gain-of-function mutations prolong cardiomyocyte repolarization and cause the Long-QT syndrome (type 3, LQT3), which manifests with QT-interval prolongation on the ECG. Loss-of-function mutations reduce the action potential upstroke velocity and cause Cardiac Conduction Disease (CCD), associated with prolonged conduction indices (PR interval, QRS duration) on the ECG, occurring either in isolation or in combination with ST-segment elevation in the right precordial ECG leads (Brugada syndrome, BrS). In some instances, SCN5A mutations are associated with multiple sodium channel biophysical defects and lead to clinical manifestations of both gain (LQT3) as well as loss (CCD, BrS) of sodium channel function. The first such "overlap" mutation, SCN5A-1795insD, was described by our group in a large Dutch family with clinical manifestations of LQT3, BrS and CCD occurring either in isolation or in combinations thereof (2). Knock-in mice (Scn5a1798insD/+) carrying the mouse homolog of this mutation recapitulated the diverse clinical features observed in patients and provided insight into the distinct sodium channel biophysical defects underlying the different disease manifestations (3).
More recently, sodium channelopathies have also been associated with the development of cardiac fibrosis, dilatation and hypertrophy, conditions which may further contribute to arrhythmogenesis (4). These observations have led to the re-evaluation of the initial view that mutations in a cardiac ion channel would only lead to pure electrical dysfunction and imply a functional role as signal transducer for the sodium channel, regulating myocyte structural integrity and viability. However, the underlying mechanisms involved are not completely known, and it remains unclear how the sodium channel regulates cardiomyocyte integrity and viability.
Sodium channelopathies are also characterized by reduced penetrance and variable disease expression, with extensive variability in clinical manifestations often observed even among family members carrying an identical ion channel gene mutation. We have demonstrated a greater severity of conduction and repolarization disease in Scn5a1798insD/+ mice of the 129P2 inbred strain, as compared to the FVB/N inbred genetic background, attesting to the important role for genetic background in modulation of disease severity in cardiac sodium channelopathy (5,6). However, genetic modifiers of phenotypic variability in patients with arrhythmia syndromes remain largely unknown. Identification of these modifiers represents an exciting next major step in research related to cardiac sodium channel disease, ultimately enabling improved diagnosis, risk stratification, and treatment strategies.

Remme CA, Wilde AA, Bezzina CR. Cardiac sodium channel overlap syndromes: different faces of SCN5A mutations. Trends Cardiovasc Med 2008;18:78-87

Bezzina C, Veldkamp MW, van den Berg MP, et al. A single Na(+) channel mutation causing both long-QT and Brugada syndromes. Circ Res.1999;85:1206-13.

Remme CA, Verkerk AO, Nuyens D, van Ginneken AC, van Brunschot S, Belterman CN, Wilders R, van Roon MA, Tan HL, Wilde AA, Carmeliet P, de Bakker JM, Veldkamp MW, Bezzina CR. Overlap syndrome of cardiac sodium channel disease in mice carrying the equivalent mutation of human SCN5A-1795insD. Circulation 2006;114:2584-2594

Coronel R, Casini S, Koopmann TT, Wilms-Schopman FJ, Verkerk AO, de Groot JR, Bhuiyan Z, Bezzina CR, Veldkamp MW, Linnenbank AC, van der Wal AC, Tan HL, Brugada P, Wilde AA, de Bakker JM. Right ventricular fibrosis and conduction delay in a patient with clinical signs of Brugada syndrome: a combined electrophysiological, genetic, histopathologic, and computational study. Circulation. 2005;112(18):2769-77.

Remme CA, Scicluna BP, Verkerk AO, Amin AS, van Brunschot S, Beekman L, Deneer VHM, Chevalier C, Oyama F, Miyazaki H, Nukina N, Escande D, Houlgatte R, Wilde AAM, Tan HL, Veldkamp MW, de Bakker JMT, Bezzina CR. Genetically determined differences in sodium current characteristics modulate conduction disease severity in mice with cardiac sodium channelopathy. Circ Res 2009;104(11):1283-92.

Scicluna BP, Tanck MW, Remme CA, Beekman L, Coronel R, Wilde AA, Bezzina CR. Quantitative trait loci for electrocardiographic parameters and arrhythmia in the mouse. J Mol Cell Cardiol 2011;50(3):380-9

Where applicable, the authors confirm that the experiments described here conform with The Physiological Society ethical requirements.

SA10

Spatial Ca^{2+}/H^+ ion coupling in the myocardium: a key substrate for arrhythmia?

R. Vaughan-Jones

Department of Physiology, Anatomy and Genetics, Burdon Sanderson Cardiac Science Centre, Oxford, UK

A pH-driven compromise of intracellular Ca^{2+} signalling in cardiac myocytes can underpin arrhythmogenesis, particularly during myocardial ischaemia, a clinical condition associated with low pH_i. Myocardial pH_i (normally kept at ~7.20) is spatially regulated via H^+-ion chemoreceptors on Cx43 (connexin) protein channels expressed at gap junctions. These receptors acutely regulate Cx-channel opening and closure, resulting in a biphasic dependence of junctional permeability on pH_i (maximal permeability at pH_i 6.95). High concentrations (10-20mM) of cytoplasmic mobile molecules that reversibly bind H^+ ions mediate passive cell-to-cell H^+ flux through open Cx channels, in response to local pH_i non-uniformity. Cx channels thus regulate spatial variations in myocardial pH_i.
H^+ ions are universal end-products of metabolism. They modulate Ca^{2+} signalling, electrical rhythm and contractility in the heart. The spatial control of myocardial pH_i via Cx channels thus spatially modulates Ca^{2+}i. Key pH_i /Ca^{2+}i coupling is mediated by common binding sites on small intracellular molecules, such as carnosine and ATP, as well as via a functional coupling between sarcolemmal Na/Ca and Na/H exchangers. As a result, low pH_i triggers a rise of Ca^{2+}i. Furthermore, spatial gradients of pH_i, when they occur within cells or in groups of cells, induce local gradients of both diastolic and systolic Ca^{2+}. Depending on the activity of local Na/H exchangers, pH_i gradients can also stimulate or suppress spontaneous Ca^{2+} waves and their local propagation. Ca^{2+} waves, particularly at border zones, are a common feature of regional myocardial ischaemia. It is likely that a spatial disordering

of pH_i in the heart provides a key substrate for this Ca^{2+} heterogeneity, which, in turn, is an important substrate for arrhythmia. When mapping out the clinical causes of arrhythmogenesis, it is therefore necessary to consider the integrated control of both Ca^{2+} *and* pH.

Where applicable, the authors confirm that the experiments described here conform with The Physiological Society ethical requirements.

SA11

Do t-tubules play a role in arrhythmogenesis in cardiac myocytes?

C. Orchard

University of Bristol, Bristol, UK

Contraction of a mammalian cardiac ventricular myocyte is normally initiated by an action potential, which causes a rapid increase of intracellular [Ca] (the Ca transient) by triggering Ca release from the sarcoplasmic reticulum (SR) via Ca-induced Ca release (CICR). The Ca transient is temporally and spatially synchronised within the cell because of the presence of transverse (t-) tubules, invaginations of the cell membrane that form a complex network which carries excitation into the cell. The function of many of the proteins involved in excitation-contraction coupling and its regulation appears to be located predominantly at the t-tubules, including ~80% of L-type Ca current (I_{Ca}) and ~65% of Na/Ca exchange current (I_{NCX}; for review see Orchard *et al.*, 2009). Synchronous release of Ca from the SR is ensured by the proximity of L-type Ca channels in the t-tubule membrane to ryanodine receptors clustered in the SR membrane at the dyad.

Spontaneous Ca release can also occur, particularly in conditions of Ca overload. Such Ca release can occur either as localised release from a cluster of ryanodine receptors (Ca spark) or as waves of Ca propagated within the cell by CICR, either between, or independent of, normal Ca transients. Such Ca release can cause arrhythmias by activating Ca-dependent inward currents, such as I_{NCX}. Since t-tubules are the main site of SR Ca release and the location of the majority of NCX activity in normal ventricular myocytes it is likely that they play an important role in the genesis of such arrhythmias.

Disruption of t-tubule structure, and an accompanying decrease in Ca transient synchrony, has been reported in pathological conditions, such as heart failure (HF; e.g. Louch *et al.*, 2006). It is unclear whether localised changes in protein function also occur; for example, basal protein kinase A (PKA) activity is involved in localisation of I_{Ca} and I_{NCX} at the t-tubules (e.g. Chase *et al.*, 2010), so that changes of PKA activity during HF may cause local changes in protein, and thus t-tubule, function. However, loss of t-tubules results in loss of action potential propagation into the cell. In consequence, Ca release is initiated at the cell surface and propagates towards the centre of the cell, rather than arising as a rapid and synchronous Ca transient. There is also a decrease in the frequency of Ca sparks, which occur predominantly

at the peripheral cell membrane rather than throughout the cell as in intact myocytes (Brette *et al.*, 2005).

Such changes may alter the propensity to arrhythmias due to spontaneous Ca release. Loss of synchronous Ca release and decreased Ca extrusion into the t-tubules could provide a substrate for altered Ca propagation (Li *et al.*, 2012) and thus regenerating waves of intracellular Ca, although the associated decrease in Ca spark frequency will decrease the probability of such waves occurring. In addition, loss of t-tubules may alter the probability of spontaneous Ca release causing arrhythmias, because:

(i) I_{NCX} normally occurs predominantly at the t-tubules (i.e. at the site of SR Ca release); thus, following loss of t-tubules, there may be insufficient activation of I_{NCX} by spontaneous Ca release to cause arrhythmias, unless NCX increases in remaining cell membrane and/or its activity is increased, for example by PKA; interestingly, an increase in NCX activity has been reported in HF.

(ii) The density of I_{Ca} and neuronal-type Na channels is greater in the t-tubules than in the peripheral membrane, whereas the density of I_{TO}, I_K and I_{K1} is the same at the two sites, and cardiac-type Na channels are located predominantly in the peripheral membrane. Changes in each of these currents associated with loss of t-tubules will alter excitability, but the net effect is difficult to predict. However, detubulation has little effect on resting membrane potential but decreases action potential duration (APD; Brette *et al.*, 2006), implying that membrane currents in the t-tubules prolong APD. Computer models incorporating a t-tubule compartment and experimentally-determined distributions of membrane currents suggest that the decrease in APD is due predominantly to loss of I_{Ca} and I_{NCX} (Pasek *et al.*, 2008). Shortening of APD, and thus of the refractory period, may increase susceptibility to arrhythmias generated by spontaneous Ca release.

(iii) Computer modelling also suggests an activity-dependent increase of K, and decrease of Ca, in the t-tubule lumen which may alter susceptibility to arrhythmias caused by Ca overload (Pasek *et al.*, 2008).

Thus in normal myocytes the t-tubules may play an important role in the genesis of arrhythmias. However, the net effect of altered t-tubule morphology in conditions such as HF is unknown, and will depend on changes in the expression, distribution and activity of proteins normally located at the t-tubules.

Brette F *et al.* (2005). *J Mol Cell Cardiol* **39**, 804-812.

Brette F *et al.* (2006). *Biophys J* **90**, 381-389.

Chase A *et al.* (2010). *J Mol Cell Cardiol* **49**, 121-131.

Li Q *et al.* (2012). *Biophys J* **102**,1471-82.

Louch WE *et al.* (2006). *J Physiol* **574**,519-33.

Orchard CH *et al.* (2009). *Exp Physiol* **94**,509-519.

Pásek M *et al.* (2008). *Prog Biophys Mol Biol* **96**, 226–243.

This work was supported by the British Heart Foundation

Where applicable, the authors confirm that the experiments described here conform with The Physiological Society ethical requirements.

SA12

Intracellular Na^+ and its role in the initiation and propagation of potentially arrhythmogenic SR Ca^{2+} release events

K. MacLeod

NHLI, Imperial College, London, UK

Heart failure is a disorder with diverse aetiology and increasing prevalence. 50% of deaths related to this condition are due to sudden ventricular arrhythmias. Although the changes in cellular Ca^{2+} regulation that occur in failing hearts are now more recognized and better understood than in the past, the links between such alterations and the occurrence of arrhythmias remain uncertain.

Ca^{2+} waves are thought to underlie some forms of ventricular tachyarrhythmia and are considered to be associated with increased spontaneous sarcoplasmic reticulum (SR) Ca^{2+}release for a given SR Ca^{2+} content. The spontaneous release events appear to result from a change in (1) the control of cytoplasmic $[Ca^{2+}]$ by the SR Ca^{2+}ATPase (SERCA2a) and the sarcolemmal Na^+/Ca^{2+} exchange (NCX) and (2) certain regulatory elements of the SR Ca^{2+} release channel (the ryanodine receptor – RyR2). There is also complex interplay between intracellular Na^+ and Ca^{2+} regulation, so altered levels of intracellular Na^+ concentration ($[Na^+]_i$) could be expected to have profound effects on the Ca^{2+} transient and, via NCX, the membrane potential and consequently arrhythmogenesis. The experiments that will be described focus (1) on the changes that may take place to the regulation of $[Na^+]_i$ in heart failure and (2) provide evidence that suggests sub-sarcolemmal $[Na^+]$ has an important role to play in the initiation and propagation of potentially arrhythmogenic SR Ca^{2+} release events.

The former were conducted on a well characterised model of cardiac hypertrophy and heart failure in the guinea-pig induced by constriction of the ascending aorta (AC). Voltage clamp experiments were used to assess Na^+/K^+ ATPase current in ventricular myocytes enzymatically isolated from 30, 60 and 150 days sham and AC hearts. The size of the current recorded in cells isolated from hearts 30 days after AC is not different from cells isolated from sham operated hearts. However, the size of the current recorded from cells isolated from hearts 60 and 150 days after AC is reduced by about half compared with sham operated hearts. These data indicate that there are alterations to the regulation of $[Na^+]_i$ in the failing heart.

The latter experiments were conducted on ventricular myocytes isolated from normal healthy rat hearts. The main finding was that reducing Na^+ current (either pharmacologically or by voltage clamping the cells at different holding potentials) decreases the frequency of Ca^{2+} sparks and the frequency and velocity of Ca^{2+} waves. Together these findings suggest that changes to intracellular $[Na^+]$ maybe a reason for the increased predisposition of the failing heart to arrhythmia.

The support of the BHF and Wellcome Trust is gratefully acknowledged.

Where applicable, the authors confirm that the experiments described here conform with The Physiological Society ethical requirements.

SA13

Atrial selectivity of antiarrhythmic drug action

U. Ravens

Department of Pharmacology and Toxicology, Dresden University of Technology, Dresden, Germany

Antiarrhythmic agents exhibit a narrow therapeutic window due to their limited efficacy and high incidence of cardiac and extracardiac side effects. In particular, antiarrhythmic drugs that directly modify cellular electrophysiological properties may cause proarrhythmic effects. Suppression of excitability by Na^+ channel block, for instance, will effectively suppress extrasystoles or slow down pacemaker activity but can also enhance reentry arrhythmias by slowing of conduction. Prolongation of action potential duration and effective refractory period by block of K^+ channels may cause early after-depolarisations that can initiate torsades de pointes arrhythmia and lead to sudden cardiac death. Proarrhythmic events may afflict all cardiac chambers, however, they are life threatening only when affecting the ventricles. Therefore the concept of "atrial selectivity" has emerged for antiarrhythmic drugs directed against supraventricular tachy-arrhythmias. These drugs target atrial-specific mechanisms of abnormal impulse formation or block ion channels only expressed in the atria in order to avoid ventricular proarrhythmic events.
In atrial fibrillation (AF), frequency-dependent Na^+ channel blockers exhibit functional atrial selectivity due to their larger effect at high atrial than at slow ventricular excitation rates. The ultraslow outward rectifier K^+ current I_{Kur} is conducted via Kv1.5 channel that are almost completely absent in human ventricles. This particular channel is targeted by numerous newly developed agents, some of which are truly selective for Kv1.5, however clinical efficacy of these compounds to convert AF into sinus rhythm or preventing recurrence of AF remains to be demonstrated in clinical trials. The acetylcholine-activated inward rectifier K^+ channel Kir3.1/3.4 is predominantly expressed in atria, becomes constitutively active during remodelling in persistent AF, and hence may be yet another target for atrial-selective antiarrhythmic drugs. Moreover, several other K+ channels, in particular Ca^{2+}-activated, small conductance K^+ (SK) channels are being scrutinized for their contribution to background K^+ conductance in human atria and whether they may serve as putative atrial-selective drug targets.

Where applicable, the authors confirm that the experiments described here conform with The Physiological Society ethical requirements.

SA14

Calcium and β–αδρενεργιχ μισμαναγεμεντ ιν ηεαρτ φαιλυρε; α δουβλε ωηαμμψ οφ δψσφυνχτιον?

A.W. Trafford

University of Manchester, Manchester, UK

Even in the face of improving therapeutic approaches, heart disease remains a major cause of premature death and morbidity. The two main causes of death in diseases such as heart failure are arrhythmias and deteriorating contractile performance. This presentation will introduce both recently published (e.g. Briston *et al* 2011) and unpublished work from our laboratory demonstrating a pivotal role for changes in intracellular calcium handling and β-adrenergic signalling as contributors to the occurrence of contractile dysfunction and arrhythmias using an ovine model of heart failure.

All experiments were conducted on enzymatically dissociated single myocytes isolated from the hearts of either control (non-failing) sheep or sheep in which heart failure had been induced by right ventricular tachypacing (pacemaker insertion under 1-3 % isoflurane inhalational anaesthesia with 0.5 mg/kg meloxicam analgesia s/c). The tachypacing model produces a dilated cardiomyopathy with substantial atrial and ventricular dilatation and contractile dysfunction. Once symptoms of heart failure were present (lethargy, dyspnoea) animals were humanely killed (pentobarbitone 200 mg/kg i/v) and cells isolated. Changes in intracellular calcium concentration were measured with fluorescent indicators using either confocal microscopy or standard epifluorescence techniques. Cells were also voltage clamped at 37 °C using either the whole cell or perforated patch techniques as appropriate for the experiment being conducted.

Under baseline conditions, heart failure resulted in a reduction in the amplitude of the systolic calcium transient which was entirely attributable to a reduction in the L-type calcium current. Moreover, during β-adrenergic stimulation with the mixed agonist isoprenaline the systolic calcium transient remained reduced in the heart failure cells compared to non-failing cells. However, under these circumstances the reduction in calcium transient amplitude was due to the combined effects of a smaller L-type calcium current *and* a smaller sarcoplasmic reticulum (SR) calcium content.

To determine the mechanism as to why SR calcium content failed to increase appropriately in heart failure we undertook protein expression analysis using Western blotting which revealed a reduced phosphorylation of phospholamban at both the serine16 and threonine17 sites. There was also an increase in protein phosphatase and G-protein receptor kinase (GRK-2) protein expression and a reduction in protein kinase A (PKA) activity.

Given the requirement for a threshold SR calcium content to be reached for the occurrence of arrhythmogenic diastolic calcium waves (Venetucci *et al*, 2007) we then sought to determine if changes in the threshold SR calcium content were

involved in the increased propensity for arrhythmias in heart failure. Diastolic calcium waves were produced by raising the extracellular calcium concentration to 10 mM. In both control conditions and following β-adrenergic stimulation with isoprenaline the threshold SR calcium content was reduced in heart failure cells compared to non-failing cells. Importantly, in non-failing cells the threshold SR calcium content was greater than the SR calcium content *before* arrhythmogenic diastolic calcium waves occurred. However, in heart failure cells during β-adrenergic stimulation the threshold SR calcium content was no different to the cells SR calcium content *before* calcium waves occurred.

We conclude therefore that changes to intracellular calcium homeostasis and β-adrenergic signalling both contribute to the pathophysiology of heart failure. Specifically, in this particular model of heart failure, an important role exists for the smaller L-type calcium current, enhanced protein phosphatase and GRK-2 expression and reduced PKA activity in contributing to the reduced calcium transient amplitude. Furthermore, we suggest that in heart failure the similarity between the cells 'operating' SR calcium content and threshold SR calcium content for arrhythmogenic diastolic calcium release during β-adrenergic stimulation provides a possible mechanism for the increased prevalence of arrhythmias in patients with heart failure particularly following an increase in catecholamine production.

Briston SJ, Caldwell JL, Horn MA, Clarke JD, Richards MA, Greensmith DJ, Graham HK, Hall MC, Eisner DA, Dibb KM, Trafford AW. Impaired β-adrenergic responsiveness accentuates dysfunctional excitation contraction coupling in an ovine model of tachypacing induced heart failure. J Physiol. 2011;589:1367-1382.

Venetucci LA, Trafford AW, Eisner DA. Increasing ryanodine receptor open probability alone does not produce arrhythmogenic calcium waves: threshold sarcoplasmic reticulum calcium content is required. Circ Res. 2007;100:105-111.

This work was supported by The British Heart Foundation

Where applicable, the authors confirm that the experiments described here conform with The Physiological Society ethical requirements.

SA15

The electrophysiological basis of T-wave alternans and the induction of arrhythmias in rabbits with MI-induced left ventricular dysfunction

G. Smith, R. Myles, F. Burton and S. Cobbe

Institute of Cardiovascular and Medical Sciences, University of Glasgow, Glasgow, UK

T-wave alternans is thought to predict the occurrence of ventricular arrhythmias in patients with left ventricular dysfunction and may be the basis of a clinical test for arrhythmia predisposition. Experimental work has associated T-wave alternans to alternating epicardial action potential duration and regions of discordant repolarization alternans has been linked to the induction of re-entry. The occurrence of transmural repolarization alternans was investigated using optical techniques to

investigate the link between alternans and ventricular arrhythmia in rabbits with left ventricular dysfunction following myocardial infarction. Optical mapping using the voltage sensitive dye RH237 was used to record action potentials from the transmural surface of left ventricular wedge preparations from normal and post-infarction hearts during a progressive reduction in pacing cycle length at normal (37 °C) and hypothermic temperatures (30 °C). There were no significant differences in baseline transmural electrophysiology between the groups. Post-infarction hearts had a lower threshold for both repolarization alternans (286 vs. 333 bpm, $p < 0.05$) and ventricular arrhythmias (79 vs. 19%, $p < 0.01$) during rapid pacing, which was not accounted for by increased transmural discordant alternans. In VF-prone hearts, alternans in optical action potential amplitude was observed and increased until 2:1 block occurred. The degree of optical action potential amplitude alternans but not APD90 alternans was associated with VF inducibility during rapid pacing. Post-infarction hearts are more vulnerable to transmural alternans and ventricular arrhythmias at rapid rates. In some preparations, alternans in optical action potential amplitude was associated with conduction block and VF. The data suggest that changes in optical action potential amplitude and regional block may underlie a mechanism for alternans-associated ventricular arrhythmia in left ventricular dysfunction.

Where applicable, the authors confirm that the experiments described here conform with The Physiological Society ethical requirements.

SA16

The molecular pathophysiology of atrial fibrillation: mechanistic insights and therapeutic innovation

S. Nattel

Montreal Heart Institute, Montreal, QC, Canada

Research into the pathophysiology of AF has produced enormous advances in our understanding of the arrhythmia. These include insights into the basis of ectopic activity, determinants of atrial reentry, atrial remodeling, and genetic determinants. Atrial ectopic activity is enhanced by AF-related remodeling, with the principal underlying mechanism being Ca^{2+}-handling abnormalities leading to abnormal diastolic Ca^{2+}-releases from the sarcoplasmic reticulum (SR). A central feature is dysfunction of the SR ryanodine-receptor (RyR) Ca^{2+}-release channel, due primarily to calcium/calmodulin-dependent kinase II (CaMKII) hyperphosphorylation. Reentry substrate-generation may result from refractory-period abbreviation due to reduced inward L-type Ca^{2+} current (I_{CaL}) or enhanced outward K^+ current. The rapid atrial activation-rates during AF reduce I_{CaL} and increase inward-rectifier K^+-currents (background I_{K1} and constitutive acetylcholine-dependent K^+-current I_{KACh}). A common mediator is cellular Ca^{2+}loading and consequent signaling, particularly via the Ca^{2+}/calcineurin-NFAT system. Another contributor to reentry substrates is structural remodeling, like changes in atrial tissue-composition (fibrosis), loss/dys-

localization of cell-coupling connexin-channels and atrial dilation. Autonomic dysfunction is also an important contributor. Genetic /molecular-pathophysiology studies have provided insights by revealing the basis of monogenic familial AF and clarifying the complex predisposing heritable factors in the population.
These new findings have resulted in the development of novel therapeutic options. Novel drug-therapies target atrial-selective ion-channels (like I_{KACh}, I_{Kur} and I_{SK}) and the mechanisms involved in ectopic-activity generation, like RyR-release abnormalities and CaMKII-signaling. Insights into the molecular basis of atrial remodeling has led to "upstream therapy", which has shown promise in improving the natural history of AF. Mechanism-based ablation-approaches include targeting cardiac innervation and AF-maintaining rotors. Agents being developed include classical small-molecule drugs, along with newer approaches like modulation of microRNA-pathways and gene/cell-therapy. Finally, studies of genetic associations and biomarkers promise new inroads into risk prediction and stratification, and ultimately personalized individual-patient based treatment.

Where applicable, the authors confirm that the experiments described here conform with The Physiological Society ethical requirements.

SA17

Nonlinear physics of pacemaking and propagation in the mammalian heart – bifurcations, stability and arrhythmias

A.V. Holden

School of Biomedical Sciences, University of Leeds, Leeds, UK

Electrophysiological cardiac virtual tissues are computational implementations of excitation propagation in a heterogeneous anisotropic and orthotropic tissue architecture. They are compact, simplified representations of quantitative experimental data and have been constructed, for pacemaking and conducting systems, atria and ventricles of various mammalian species. Numerical solutions provide quantitative predictions of the normal tissue activity, and how it is altered by changes in cell behaviour and intercellular coupling produced by pharmacological agents, changes in expression, or in pathologies. These predictions can be tested by further experiments, that lead to model refinement in an experiment – model- prediction closed loop. The models are generally stiff, high order, nonlinear systems of differential or partial differential equations (Benson et al., 2008)
Pacemaking has been ascribed to membrane dynamics, or to an intracellular calcium clock. In a cell these are coupled, and the cell model is a dynamical system, with parameters (e.g. channel densities), and variables (e.g. membrane potential, ionic concentrations, gating variables), and can have stable/unstable solutions. The stability of a solution changes at a bifurcation, where a qualitatively new behaviour emerges, e.g. periodic solutions from an equilibrium. Bifurcation analysis determines the parameter value at which the bifurcation occurs, and the nature of the bifurcation. At a Hopf bifurcation periodic solutions emerge at a defined frequency

i.e. are switched on by a change in the parameter. At a homoclinic bifurcation the period at the bifurcation is infinite, and reduces logarithmically with further changes in parameter. Both kinds of bifurcation have been found in cardiac membrane excitation systems as maximal ionic conductances/channel densities are varied (Benson et al., 2006).
In a paced excitable cell model, a high rate can lead to a period doubling bifurcation, with alternating short and long action potential durations. (Aslanidi et al., 2012). Electrical alternans is pro-arrhythmogenic.
Cardiac myocytes are electrically coupled and propagation can be modelled by a continuous partial differential equation, where the electrotonic/diffusive spread of voltage is represented by a the diffusion tensor D, a diagonal matrix of the diffusion coefficients for voltage in three orthogonal directions. Propagation velocity in cardiac tissue is anisotropic and orthotropic, appears smooth and is fastest along the local myofibre orientation. High resolution magnetic resonance and micro-computed tomographic imaging shows a fractured ventricular architecture, with local cleavage planes between local layers of cells. Propagation in this fractured geometry can be simulated by a continuous, anisotropic and orthotropic D. (Benson et al, 2011)
Numerical solutions within atrial or ventricular architecture and geometries can model re-entrant arrhythmias, and their breakdown into electrical fibrillation.

Aslanidi OV et al. (2012) Eur J. Pharm Sci 46 209-221

Benson AP et al (2006) Phil Trans Roy Soc A 364 1313-1327

Benson AP et al. (2008) Prog Biophys Mol Biol 96 187-208

Benson AP et al (2011) Interface Focus 1 101-116

Where applicable, the authors confirm that the experiments described here conform with The Physiological Society ethical requirements.

SA18

Arrhythmias and the cardiac conduction system

M.R. Boyett, G. Hart and H. Dobrzynski

Cardiovascular Medicine, University of Manchester, Manchester, Lancashire, UK

The cardiac conduction system (CCS) includes the sinus node, atrioventricular (AV) node and His-Purkinje system (Boyett, 2009). The CCS is associated with a wide range of arrhythmias: dysfunction of the sinus node results in sinus bradyarrhythmias and tachyarrhythmias; the AV node is the substrate of AV nodal reentrant tachycardia (AVNRT) and dysfunction of the AV node results in heart block; the His-Purkinje system is prone to afterdepolarizations and torsades de pointes and it can be the substrate of reentrant arrhythmias and dysfunction of the system results in bundle branch block. However, the CCS also includes lesser-known tissues, including paranodal tissue running alongside the sinus node, AV ring tissues running around the AV valves and nodal-like tissue in the ventricular outflow

tract. Like the main components of the CCS, the additional components arise from 'primary myocardium' (as distinct from 'working myocardium') in the embryo. These extra tissues are also likely to be involved in arrhythmogenesis. The paranodal tissue is potentially responsible for the 'cristal tachycardias' (a class of atrial tachycardias) and the AV ring tissues are known to be responsible for other atrial tachycardias (the right AV ring especially constitutes 'a ring of fire'). We hypothesise that the nodal-like tissues in the ventricular outflow tract are responsible for the highly arrhythmogenic nature of the right ventricular outflow tract in general and the ventricular outflow tract ventricular tachycardias in particular.

In general, the arrhythmogenic nature of the CCS is largely the consequence of the unique electrophysiological phenotype of the CCS and its well known propensity for pacemaking. This in turn is a consequence of the unique pattern of expression of ion channels, Ca^{2+}-handling proteins and gap junction channels in the CCS. We have shown that the expression profiles of the sinus node, AV node, Purkinje fibres, paranodal tissue, AV ring tissues and nodal-like tissue in the ventricular outflow tract have features in common and which are distinct from those of the working myocardium (e.g. Chandler et al., 2009). For example, many of them express the pacemaker ion channel, HCN4, and all show poor expression of the inward rectifier K^+ channel, Kir2.1, and all the nodal and nodal-like tissues lack expression of the Na^+ channel, Nav1.5, and the gap junction channel, Cx43. In part, it is the expression of HCN4 and/or poor expression of Kir2.1 that is responsible for the propensity for pacemaking. It is the lack of expression of Nav1.5 and Cx43 at the AV node that is in part responsible for AVNRT. However, AVNRT is also the result of the highly complex three-dimensional structure of the CCS at the AV junction – at this point, there is an intersection of the AV ring tissues, AV node and bundle of His. We are generating detailed three-dimensional anatomical models of all parts of the CCS (e.g. Li et al., 2008). Computer simulation has confirmed that it is possible to explain AVNRT based on the combination of the complex structure of the CCS at the AV junction together with the equally complex pattern of expression of ion channels and gap junction channels at the AV junction (Li et al., 2008; Inada et al., 2009).

Dysfunction of the CCS can be hereditary, but it is primarily a disease of ageing – the incidence of sinus bradycardia, heart block and bundle branch block all increase with ageing. This is why electronic pacemakers are primarily fitted to the elderly. In addition, we and others have associated dysfunction of the CCS with heart failure, myocardial infarction, pulmonary hypertension, atrial fibrillation, diabetes, possibly obesity and, surprisingly, athletic training. For example, former professional cyclists show a higher incidence of sick sinus syndrome and pacemaker implantation (Baldesberger et al., 2008). Previously, the dysfunction of the CCS has been explained by 'fibrosis' and, as an example, there is well documented fibrosis in the sinus node of the ageing mouse (Hao et al., 2011). However, in many instances, there is no evidence of fibrosis, for example in the sinus node of the ageing human (Alings et al., 1995). Furthermore, even in cases in which fibrosis is documented, the importance of the fibrosis is questionable. This is because in all investigated instances (ageing, heart failure, myocardial infarction, pulmonary hypertension, atrial fibrillation and athletic training) there is a widespread remodelling of ion channels, Ca^{2+}-handling proteins and gap junction channels. For exam-

ple, in many instances, there is a downregulation of HCN4. Computer simulation has shown that the remodelling can explain the dysfunction of the CCS (e.g. Hao et al., 2011).

In summary, mapping of ion channels, Ca^{2+}-handling proteins and gap junction channels throughout the CCS in health and disease (as well as mapping of anatomy), often in combination with computer simulation, is shedding new light on CCS-related arrhythmias.

Alings AM et al. (1995). European Heart Journal 16, 1655-1667.

Baldesberger S et al. (2008). European Heart Journal 29, 71-78.

Boyett MR (2009). Experimental Physiology 94, 1035-1049.

Chandler NJ et al. (2009). Circulation 119, 1562-1575.

Hao X et al. (2011) Circulation: Arrhythmia and Electrophysiology 4, 397-406.

Inada S et al. (2009). Biophysical Journal 97, 2117-2127.

Li J et al. (2008). Circulation Research 102, 975-985.

Where applicable, the authors confirm that the experiments described here conform with The Physiological Society ethical requirements.

SA19

In silico pursuit of K^+ channel-linked short QT syndrome

J.C. Hancox[1], I. Adeniran[2] and H. Zhang[2]

[1]School of Physiology and Pharmacology, University of Bristol, Bristol, UK and [2]School of Physics and Astronomy, University of Manchester, Manchester, UK

The short QT syndrome (SQTS) is a rare but dangerous condition that is associated with accelerated ventricular repolarisation and that carries a risk of potentially fatal ventricular arrhythmias (Patel *et al*., 2010). The SQT1-SQT3 variants of the syndrome are associated with mutations to *KCNH2* (*hERG*), *KCNQ1* (*KvLQT1*) and *KCNJ2* that lead to increased repolarising ionic currents through channels responsible, respectively, for I_{Kr}, I_{Ks} and I_{K1} (Patel *et al*, 2010). At present there are no animal models of SQT1-SQT3 that incorporate the precise ion channel current alterations that have been identified through the in vitro study of recombinant SQTS mutant K^+ channels. Consequently, we have adopted a computer simulation approach in order to investigate electrophysiological changes that may increase arrhythmia susceptibility in the SQTS (Zhang *et al*., 2008; Adeniran *et al*., 2011; Adeniran *et al*., 2012). The properties of each of I_{Kr}, I_{Ks} and I_{K1} in human ventricular cell models were in turn altered, to recapitulate changes observed in in vitro studies of SQT1-3 mutant channels (respectively N588K-hERG, V307L-KCNQ1, D172N-Kir2.1). The resulting cell models were then incorporated into one-, two- and three-dimensional ventricular tissue models that considered ventricular transmural electrical heterogeneity of endocardial, midmyocardial and epicardial cell regions. The intact tissue model recapitulated QT interval shortening with each SQT mutant, confirming

that the current alterations arising from these gain-of-function mutations are causally linked to QT interval shortening (Zhang *et al*., 2008; Adeniran *et al*., 2011; Adeniran et al*., 2012). Effective refractory period (ERP) shortening was observed for each SQTS variant and in tissue simulations alterations to transmural dispersion of repolarization were also observed (Zhang* et al*., 2008; Adeniran* et al*., 2011; Adeniran* et al*., 2012). Tissue vulnerability to genesis of re-entry was increased and the lifespan of re-entrant spiral waves was also increased in the SQT variant simulation conditions (Zhang* et al*., 2008; Adeniran* et al*., 2011; Adeniran* et al*., 2012). Thus, the changes to repolarising K^+ currents resulting from SQT1-3 linked channel defects increase susceptibility to the genesis and maintenance of re-entrant arrhythmia.*

Adeniran I, El Harchi A, Hancox JC, Zhang H (2012) Proarrhythmia in KCNJ2-linked short QT syndrome: insights from modelling Cardiovasc Res **94**: 66-76.

Adeniran I, McPate MJ, Witchel HJ, Hancox JC, Zhang H (2011) Increased vulnerability of human ventricle to re-entrant excitation in hERG linked variant-1 short QT syndrome. PLoS Comput Biol **7**: e1002313.

Patel C, Yan GX, Antzelevitch C (2010) Short QT Syndrome: from bench to bedside. Circ Arrhythm Electrophysiol **3**: 401-408.

Zhang H, Kharche S, Holden AV, Hancox JC (2008) Repolarisation and vulnerability to re-entry in the human heart with short QT syndrome resulting from KCNQ1 mutation – a simulation study. Prog Biophys Mol Biol **96**: 112-131.

The authors thank the British Heart Foundation and EPSRC for funding

Where applicable, the authors confirm that the experiments described here conform with The Physiological Society ethical requirements.

SA20

MKK4 and Pak1 signalling in the heart, intriguing candidate targets for upstream therapy of cardiac arrhythmias

M. Lei[1], X. Wang[1], Y. Ke[2], E. Cartwright[2] and R. Solaro[2]

[1]Institute for Cardiovascular Sciences, University of Manchester, Manchester, UK and [2]4Department of Physiology and Biophysics and Centre for Cardiovascular Research, University of Illinois at Chicagor, Chicago, IL, USA

50% of mortalities attributable to cardiac causes are accounted for by cardiac arrhythmias occurring either independently or as a result of other underlying heart diseases. Classic pharmacological antiarrhythmic approaches suffer from poor efficacy and risk of serious complications. Recently, the notion of "upstream therapy", targeting the processes involved in the development of arrhythmic substrates, has increasingly become the focus of attention. This talk will overview our recent research by using genetically modified mouse models to investigate the potential roles of several intracellular signalling proteins, particularly, mitogen-activated protein kinase kinse 4 (MKK4) and P21-activated kinase1 (Pak1), in atrial and ventricular arrhythmias associated with ageing and stress. For example, in our newly devel-

oped mouse model with atrial cardiomyocyte-specific deletion of mkk4 (MKK4ACKO), with age, MKK4ACKO mice became more susceptible to atrial arrhythmias with characteristic slow atrial conduction comparing with control MKK4F/F mice. In parallel, an increased interstitial fibrosis, up-regulated TGF-β1 signalling and dysregulation of matrix metalloproteinases and their inhibitory enzymes were observed in the atrium of MKK4ACKO mice in contrast to control mice. The results for the first time have determined a critical role of MKK4 in age-related atrial structural remodelling associated with atrial fibrillation. In summary, our research provides new insights into exploring upstream therapeutic targets for treating cardiac arrhythmias.
Where applicable, the authors confirm that the experiments described here conform with The Physiological Society ethical requirements.

The research was supported by BHF, MRC and the Wellcome Trust.

Where applicable, the authors confirm that the experiments described here conform with The Physiological Society ethical requirements.

SA21

Multi-physical computer model of the human atria and torso: a platform for the study of atrial fibrillation

H. Zhang[1], M. Colman[1], C. Garratt[2], H. Dobrzynski[3] and M. Boyett[3]

[1]Biological Physics Group, The University of Manchester, Manchester, UK, [2]Manchester Heart Centre, The University of Manchester, Manchester, UK and [3]Cardiovascular Research Group, The University of Manchester, Manchester, UK

Atrial arrhythmias, including atrial fibrillation (AF), are characterised by irregular and rapid electrical activation of the atria. The mechanisms underlying the initiation and maintenance of AF, however, are incompletely understood. It is believed that the electrical heterogeneity and structural anisotropy of the atria play an important role in generating and sustaining AF. In the past few years, we have developed a 3D anatomical model of the human atria and torso to investigate the underlying mechanisms of AF (Kharche et al., 2008; Colman et al., 2011; Aslanidi et al., 2011). The model considered a new family of cellular models for describing the regional differences in the electrical properties of the atria that include the sinoatrial node (SAN), left and right atrial appendage, atrial septum, pectinate muscle, crista terminalis, Bachmann bundles, pulmonary vein, atrioventricular ring, coronary sinus and atrioventricular node. It also considered the 3D anatomical structures that were constructed from visible human project. A recently reconstructed anatomical structure for the human SAN geometry and fibre structure (Chandler et al., 2011) was incorporated into the 3D atrial model. The atria model was then integrated into a torso geometry mesh and the forward problem was solved in order to simulate realistic ECG P-waves (Aslanidi et al., 2011). The developed model was validated by quantitatively comparing the simulated atrial activation patterns

to experimental data in both normal and abnormal conditions (Lemery et al., 2007; Kistler et al., 2006), and comparing the simulated body surface potential (BSP) to experimental BSP maps (Mirvis, 1980) and ECG P-waves under normal conditions. The model was then used to investigate the role of atrial electrical heterogeneity and anisotropy in initiation and maintenance of re-entrant excitation wave induced by the standard S1-S2 stimulus protocol. It was shown that while the electrical heterogeneity plays an important role for initiating re-entrant excitation waves, the structural anisotropy is the key for sustaining these re-entrant wavelets (Aslanidi et al., 2011). In conclusion, a validated multi-scale biophysically detailed model of the human atria and torso has been developed, providing a powerful platform for studying AF mechanisms.

Aslanidi OV, Colman MA, Stott J, Dobrzynski H, Boyett MR, Holden AV, Zhang H (2011). 3D virtual human atria: A computational platform for studying clinical atrial fibrillation. Prog Biophys Mol Biol. 107(1):156-68.

Chandler N, Aslanidi O, Buckley D, Inada S, Birchall S, Atkinson A, et al. (2011). Computer three-dimensional anatomical reconstruction of the human sinus node and a novel paranodal area. Anat Rec (Hoboken). 294(6):970–9.

Colman MA, Aslanidi OV, Stott J, Holden AV, Zhang H (2011). Correlation between P-wave morphology and origin of atrial focal tachycardia—insights from realistic models of the human atria and torso. IEEE Trans Biomed Eng. 58(10):2952–5.

Kharche S, Garratt CJ, Boyett MR, Inada S, Holden AV, Hancox JC, Zhang H (2008). Atrial proarrhythmia due to increased inward rectifier current (I(K1)) arising from KCNJ2 mutation—a simulation study. Prog Biophys Mol Biol. 98(2-3):186-97.

Kistler PM, Roberts-Thomson KC, Haqqani HM, Fynn SP, Singarayar S, Vohra JK, et al. (2006). P-wave morphology in focal atrial tachycardia: development of an algorithm to predict the anatomic site of origin. J. Am. Coll. Cardiol. 48(5):1010–7.

Lemery R, Birnie D, Tang ASL, Green M, Gollob M, Hendry M, et al. (2007). Normal atrial activation and voltage during sinus rhythm in the human heart: an endocardial and epicardial mapping study in patients with a history of atrial fibrillation. J. Cardiovasc. Electrophysiol. 18(4):402–8.

Mirvis DM (1980). Body surface distribution of electrical potential during atrial depolarization and repolarization. Circulation. 62(1):167–73.

This work was supported by EPSRC.

Where applicable, the authors confirm that the experiments described here conform with The Physiological Society ethical requirements.

J

K

L

M

N

O

P